Black Hole Singularities in the Framework of Gauge/String Duality

by

Guido Nicola Innocenzo Festuccia

Submitted to the Department of Physics
in partial fulfillment of the requirements for the degree of

Doctor of Philosophy

at the

MASSACHUSETTS INSTITUTE OF TECHNOLOGY

May 2007

Author ...
Department of Physics
May 18, 2007

Certified by..
Hong Liu
Assistant Professor
Thesis Supervisor

Accepted by .....
Thomas Greytak
Professor and Associate Department Head for Education

Black Hole Singularities in the Framework of Gauge/String Duality

by

Guido Nicola Innocenzo Festuccia

Submitted to the Department of Physics
on May 18, 2007, in partial fulfillment of the
requirements for the degree of
Doctor of Philosophy

Abstract

In this dissertation black hole singularities are studied using the AdS/CFT correspondence. These singularities show up in the CFT in the behavior of finite-temperature correlation functions. A direct relation is established between space-like geodesics in the bulk and momentum space Wightman functions of CFT operators of large dimensions. This allows to probe the regions inside the horizon and near the singularity using the CFT. Information about the black hole singularity is encoded in the exponential falloff of finite-temperature correlators at large imaginary frequency. We also find a UV/UV connection that governs physics inside the horizon. For the case the bulk theory lives in 5 dimensions the dual theory is an $SU(N)$ Yang-Mills theory on a sphere, a bounded many-body system. The signatures of the singularity we found are only present as $N \to \infty$. To elucidate the emergence of the singularity in the gauge theory we further study the large N limit. We argue that in the high temperature phase the theory is intrinsically non-perturbative in the large N limit. At any nonzero value of the 't Hooft coupling λ, an exponentially large (in N^2) number of free theory states of wide energy range (or order N) mix under the interaction. As a result the planar perturbation theory breaks down. We argue that an arrow of time emerges in the gauge theory and the dual string configuration should be interpreted as a stringy black hole.

Thesis Supervisor: Hong Liu
Title: Assistant Professor

Acknowledgments

It is with deep gratitude that I thank my advisor Hong Liu for his unwavering support. The many discussions held with him in the last four years constitute an important part of my education as a physicist. I will look at his unprejudiced, open attitude toward research and his relentless aim to understand completely all the facets of a problem as a source of inspiration in my future work.

Many thanks also go to my friend Mauro Brigante with whom I had the privilege of collaborating on many projects. My dearest friends Antonello Scardicchio and Alexander Boxer have been a constant source of support as has been Qudsia Jabeen Ejaz. The discussions I had with all of them provided both entertainment and occasions to learn new physics or to get a clearer understanding of many issues. I also want to thank all my fellow students and in particular Sergio Benvenuti, Brian Fore, Claudio Marcantonini, Rishi Sharma and Leonardo Senatore. Finally I want to congratulate the staff and faculty of CTP for providing an incredible learning environment and in particular professors Amihay Hanany, and Daniel Freedman for being good teachers and answering many questions of mine.

Contents

List of Figures

Chapter 1

Introduction

The classical theory of general relativity predicts that reasonable initial matter distributions will evolve generically into spacetime singularities[47, 77, 46]. In the resulting space-time there are geodesics that cannot be extended for an arbitrary proper time either in the past or in the future[1]. An observer traveling along such a geodesic will hit in a finite time a singularity after which the theory of general relativity is not predictive. Many solutions of great physical relevance are singular such as the Schwarzschild metric for a black hole and the Big Bang in the Friedmann-Robertson-Walker spacetime which should describe our universe. Therefore singularities arise in many situations of physical interest and their understanding is essential both in cosmology and as a necessary step towards the clarification of the structure of the theory itself. In this introduction we will review known facts about the physics of singularities, motivate the direction of the research described in later chapters and summarize its main results.

The theorems implying the generic formation of singularities typically involve three classes of assumptions:

- First an energy condition on the matter distribution is assumed. An example usually referred to as the "weak energy condition" is that the energy density of the matter is non negative in any frame. Classically matter coming from any

[1]That is the spacetime is geodetically incomplete

reasonable source satisfies this condition[2]

- Also some global structure on the spacetime is imposed like the absence of closed time-like curves.

- The final requirement is that gravity must be strong enough to trap a region as happens if a spatial cross section of space-time is closed.

The singularity resulting from the evolution of a nonsingular matter distribution satisfying the assumptions can be of different kinds.

- It can be possible for timelike observers to see the singularity before hitting it. In this case there is a region of spacetime lying in the future of the singularity. The evolution of spacetime in this region depends in principle on what happens at the singularity and therefore general relativity is not predictive there. The surface separating the future of such a singularity from the rest of spacetime is called a Cauchy horizon and the singularity itself is denoted as timelike.

- If no observer can see the singularity before hitting it we are in the presence of a spacelike[3] singularity. This kind of singularity constitutes a genuine boundary of spacetime as the evolution of a timelike observer could in principle follow the laws of general relativity up to the singularity. The ensemble of all the world-lines of timelike observers which do not intersect the singularity is separated from the rest of spacetime by a surface called an event horizon. By its definition it is possible for an observer outside the event horizon not to fall into the singularity indefinitely while observers inside the horizon will hit it in a finite proper time.

Cosmic censorship hypothesis have been put forward asserting in their weak form that any observer who has observed a singularity is destined to fall into it eventually. Nature should abhor naked singularities and any Cauchy horizon should be chastely cloaked by an event horizon. This at least would make the theory of general relativity

[2]Quantum fluctuations of the energy momentum tensor however can modify this picture
[3]or null

predictive for any observer outside the event horizon of the singularity[76, 33]. In order to understand the fate of observers falling inside the horizon a theory beyond general relativity is required. It has to be noticed in this respect that many spacelike singularities like for example the Schwarzschild black hole or the Big Bang singularity are such that the curvature of spacetime blows up in their neighborhood. Then as the radius of curvature is of the order of the Planck length quantum effects should become important and a quantum mechanical theory would be necessary to describe the evolution of the system.

The fact that quantum mechanical effects have to be taken into consideration to understand the physics of a black hole singularity can also be ascertained in a different way. The mass M of a black hole solution is simply related to the area A of its event horizon by the following relation[4]:

$$dM = \frac{\kappa}{8\pi G} dA \tag{1.1}$$

The area of the event horizon moreover can be proven to increase in any physical process under quite general assumptions [15]. The two facts above are strikingly similar to the first and second law of thermodynamics $dE = TdS, \quad dS > 0$ and indicate that one should associate to the black hole a finite entropy proportional to the area of its event horizon. This idea finds an astounding confirmation in the realization by Hawking that quantum mechanical effects are responsible for radiation to be emitted from the horizon [42]. At the level of his semiclassical analysis this radiation has a thermal nature with temperature

$$T_{BH} = \frac{\hbar \kappa}{2\pi}. \tag{1.2}$$

Classically the black hole horizon absorbs anything which crosses it, the consideration of quantum mechanical effects albeit only at the semi-classical level shows that it also emits thermal radiation. The requirement of consistency with the first law of

[4]other parameters describing the solution being kept fixed

thermodynamics then implies that the entropy of the black hole should be given by

$$S = \frac{A}{4\hbar G}. \tag{1.3}$$

The assignment of a nonzero entropy to a particular solution to the theory [43, 15, 16] however is a perplexing concept and seems to point out to the fact that the black hole spacetime is the effective macroscopic description of a system with many microstates. A more fundamental theory incorporating quantum mechanics consistently should be able to recognize what these microstates are and to count them matching the entropy S of the event horizon.

The association to a black hole of a finite entropy which is proportional to the area of its event horizon has other interesting ramifications. Consider for example some system occupying a spherical region of area A having entropy S_1. We can now collapse some spherical distribution of matter in such a way to form a black hole whose horizon is exactly the boundary of the sphere we started with. This black hole will have an entropy $S_{BH} = \frac{A}{4G\hbar}$ which must be greater than S_1. We therefore obtain a bound on the entropy of a system proportional to the area of the surface enclosing the system itself [17]. This is quite peculiar as we would expect the entropy to scale as the volume of the system as happens for example for any local quantum field. It appears that a local quantum field theory has no hope of describing a theory of quantum gravity unless such description is holographic in nature, that is the field theory lives in one less dimension than the gravity theory.

The fundamental inconsistency of the picture obtained above with our usual understanding of a quantum mechanical system is made even clearer by the following consideration: The time evolution of the state describing some mass distribution undergoing a gravitational collapse has to be unitary but this is at odds with the fact that, after the evaporation of the black hole, what remains is radiation described by a density matrix! The resolution of this "information paradox" [44] has to come from a more refined analysis of the quantum gravitational effects, an analysis for which, presumably, a complete consistent theory is required.

If the full theory of quantum gravity is unitary we expect that all the information about the state collapsing to form a black hole must be found in the radiation emitted by the horizon before the black hole evaporates. This information would then be stored in long time correlations in the emitted radiation and its recovery would be possible only over a period comparable to the evaporation time of the black hole. This description is acceptable for an observer outside the black hole for whom a lump of matter falling into the horizon will never quite reach its surface[5] and will somehow thermalize there, all information remaining trapped just above the horizon. However the description seems to be completely inconsistent from the point of view of an observer falling with the lump of matter into the black hole for whom the crossing of the horizon, where spacetime is smooth, will not be registered in a particular way and all the information will cross the horizon. The principle of black hole complementarity [89] states that such a difference in the description of the localization of information for the two classes of observers is not contradictory.

String theory is the leading candidate for a theory of quantum gravity[6] and should provide a consistent framework in which to study the physics of spacelike singularities. The theory has already been proved to resolve many time-like singularities [7]. Unfortunately the high curvature of the geometry near a black hole singularity makes the theory strongly coupled. Nevertheless we will see how string theory can provide a microscopic description of the microstates of a black hole and how it makes plausible the principle of black hole complementarity. Moreover we will see that it allows for an holographic description of the degrees of freedom of a quantum gravity theory.

A fundamental object in any string theory are closed strings. These can be visualized as small loops with length$\sim l_s$ propagating in time, sweeping a $1+1$ dimensional world sheet. The strings can interact by splitting and joining and the strength of the interaction is governed by a string coupling constant g which is determined dynamically. Each string has several oscillation modes which, for an observer who cannot

[5] In fact signals sent from the black hole horizon will reach an external observer only after an infinite time

[6] Introductory treatises about string theory are for example [79, 35]

[7] see for example [26, 54, 36]

distinguish the finite size of the string, propagate as particles of different masses. The growth of the number of these particles with their mass is exponential $N(m) \sim e^{ml_s}$. There are always massless modes corresponding to the propagation of a particle which can be associated with the graviton. The low energy limit of a consistent string theory is therefore a theory of gravity. This low energy limit is valid as long as the curvature radius of spacetime is much bigger than the string scale l_s. For definitiveness we will consider type II string theory whose low energy limit is type II supergravity in 10 dimensions. 6 of these dimensions can then be compactified to get to a low energy effective theory in 4 dimensions with gravitational constant $G \sim g^2 l_s^2$.

Consider a black hole solution of this low energy theory with fixed entropy[8] S. As G is proportional to g^2 the area of the event horizon goes like g^2 because of 1.3. Decreasing g the radius of the horizon decreases and the curvature radius reaches l_s at some point. At this point the low energy description is invalid and one has to describe the solution as some collection of stringy excitations. For a Schwarzschild black hole in four dimensions, with the radius of the horizon being r_o, the entropy and mass scale as $M = \frac{r_o}{2G}$ and $S \sim \frac{r_o^2}{G}$. The Newton constant in four dimension is related to the string length and the string coupling as $G = g^2 l_s^2$. Therefore at $r_o = l_s$ we have $M \sim \frac{1}{2g^2 l_s}$, $S \sim \frac{1}{g^2}$. Around this point we should switch to a stringy description of the black hole. The degeneracy of string excitations with mass m is given by e^{ml_s}. Setting the entropy to be equal at $r_0 = l_s$ therefore implies $m = \frac{1}{g^2 l_s} = 2M$ which differs from the mass of the Schwarzschild solution by a factor of order $O(1)$. The fact that this factor is not one reflects our lack of precise knowledge about the region of parameters where we match the two descriptions but we nevertheless realize that string theory has the ability to give a microscopic account of the entropy of a black hole[50]. In fact by exploiting the fact that some protected quantities can be computed reliably at weak coupling string theory has very successfully described the microscopic degrees of freedom providing the entropy of certain extremal supersymmetric black holes [87, 23].

Consider now an observer falling through the horizon of a black hole and at a small

[8] and charges Q if present

distance d from it, then because of the red-shift effect a timescale Δt measured by the in-falling observer will be seen as a timescale $\frac{\Delta t}{d}$ by an external observer. Therefore if an external observer looks at a string falling into the horizon with a time resolution of order one this corresponds to a proper time resolution of order $O(d)$. A general property of string theory is that the size of a string grows when looked with better and better time resolution Δt. The growth of the volume occupied by the string is logarithmic in Δt while the total length of the string[9] grows like $(\Delta t)^{-1}$. Therefore as the string approaches the horizon an external observer will see it grow in size and become denser never quite reaching the horizon but spreading and thermalizing over it instead. An observer falling with the string however will always look at it at the same time-scale and therefore will not see any difference in the string as it falls through the horizon. String theory gives therefore an intuitive explanation of the complementarity principle plausibility which relies on its qualitative difference with respect to a theory of point-like particles [89].

Finally AdS/CFT [64] provides us with a non-perturbative holographic description of string theory. According to the strongest form of the correspondence it is conjectured that $\mathcal{N} = 4$ $SU(N)$ super Yang-Mills theory gives a nonperturbative description of type IIB superstring theory in $AdS_5 \times S_5$. In the following we will often refer to the string theory as the bulk theory and to the gauge theory as the boundary theory. The next section gives a brief review of the terms of the correspondence, with special attention to the limit in which the bulk theory reduces to classical supergravity, before describing how we can use it to learn more about the quantum theory of black holes.

1.1 Parametric relations in AdS/CFT

$\mathcal{N} = 4$ $SU(N)$ super Yang-Mills theory, is a conformally invariant theory with two parameters: the rank of the gauge group N and the 't Hooft coupling $\lambda = g^2_{\rm YM}N$. From the operator-state correspondence, physical states of the theory on S^3 can be

[9] this picture neglects the effect of interactions which can split and join the string

obtained by acting with gauge invariant operators on the vacuum and their energies are given by the conformal dimensions of the corresponding operators. As S^3 is compact the spectrum of the gauge theory is gapped and discrete for any finite N. Below any energy E we only find a finite number of states, in this respect the theory is similar to a quantum mechanical system with a finite number of degrees of freedom.

The AdS string theory also has two parameters: the ratio between string length l_s and the curvature radius R of AdS, and the ratio between the (10d) planck length l_p and R. These ratios respectively characterize classical stringy corrections and quantum gravitational corrections beyond classical supergravity. For small l_s/R and l_p/R, the parameters of the SYM theory and of the bulk string theory are related by[10] [64]

$$\frac{\alpha'}{R^2} = \frac{1}{\sqrt{\lambda}}, \qquad \frac{G_N}{R^8} = \frac{1}{N^2}, \qquad G_N = l_p^8 \sim g_s^2 \alpha'^4 \,. \tag{1.4}$$

The above relations indicate that the classical supergravity limit is given by the large N and large λ limit of the SYM theory. In particular, a departure from the large N limit of the Yang-Mills theory corresponds to turning on *quantum* gravitational corrections in the AdS spacetime, while a departure from the large λ limit (with $N = \infty$) corresponds to turning on *classical* stringy corrections.

AdS/CFT implies an isomorphism between the Hilbert space of the two theories. In particular, any bulk configuration with asymptotic AdS_5 boundary conditions can be associated with a state (either pure or a density matrix) of the Yang-Mills theory. The mass M of the bulk configuration is related to the energy E in the YM theory as [39, 96]

$$E \sim MR \,. \tag{1.5}$$

Depending on how E scales with N in the large N limit, states of Yang-Mills theory are related to different objects in string theory in AdS. For example those whose E do not scale with N (i.e. of order $O(N^0)$) should correspond to fundamental string

[10] We omit order one numerical constants.

states. An object in AdS with a classical mass M satisfies

$$G_N M = \text{fixed}, \qquad G_N/R^8 \to 0 \tag{1.6}$$

From 1.4 and 1.5 the corresponding state in YM theory should have $E \sim O(N^2)$.

1.2 Black holes in AdS/CFT

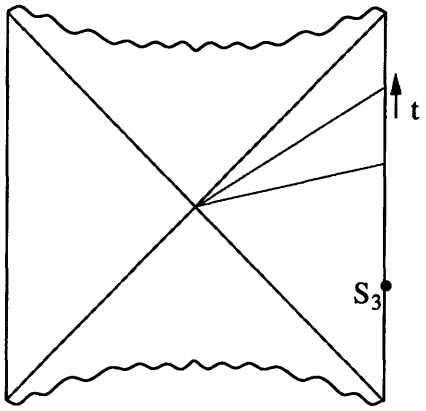

Figure 1-1: Penrose diagram for the AdS_5 Schwarzschild black hole. Each point in the diagram represents a three sphere S^3. The radius of this sphere shrinks to zero at the past or future curvature singularities which are represented by wavy lines. The diagram is separated in four regions by the red lines representing the horizon. Near the two vertical boundaries the spacetime is asymptotic to AdS_5. The Schwarzschild time coordinate maps the region outside the horizon on the right to the real line and is constant on the blue lines. The region on the left of the diagram can be associated with a Schwarzschild time having an imaginary part equal to $\pm T_{BH}^{-1}$ and flowing from up to down. This geometry is considered in detail in chapter 2.1

The classical supergravity equations admit a solution describing a Schwarzschild black hole embedded in AdS_5 [11]. This solution describes an eternal black hole, there are past and future spacelike singularities separated by horizons from an asymptotic observer. For large enough mass the black hole has positive specific heat and is in equilibrium with its own Hawking radiation[12].

[11] in this introduction we will always refer to this five dimensional background even if most of the results of the main text are valid in a different number of dimensions.

[12] The AdS boundaries providing an effective "box" for the system

One can define a canonical ensemble for semi-classical quantum gravity in an AdS. background [45]. The system undergoes a first order phase transition at a temperature T_{HP}, for $T > T_{HP}$, the ensemble is dominated by the contribution of the stable black hole with $T_{BH} = T$. The AdS-CFT correspondence then dictates that the boundary theory in the state corresponding to a thermal density matrix at temperature $T > T_{HP}$ must be dual to the stable black hole bulk configuration with the same temperature[13]. Time evolution in the boundary theory is identified with the bulk Schwarzschild time. The symmetries under time translation and $SO(4)$ rotations in the internal S^3 for the gauge boundary theory extend to isometries of the bulk black hole spacetime. This leads to the following two sets of questions:

- 1 Does the finite temperature boundary gauge theory encode information about the spacetime region inside the horizon of the black hole? If yes in the strongly coupled large N limit the gauge theory should correspond to a classically singular field configuration; how is the singularity encoded in the boundary theory?

- 2 In case we are able to pinpoint the manifestations of the black hole singularity in the gauge theory we can study how these are affected by going to finite N, corresponding to the consideration of the quantum theory in the bulk, or by going to finite coupling λ which corresponds to giving strings a finite size.

To study the first set of questions we must consider the physical observables in the boundary theory which are finite temperature correlation functions of gauge invariant operators. The possibility that these can be used to probe the region inside the horizon is complicated by the fact that the conformal field theory evolves through the bulk Schwarzschild time. This time coordinate, appropriate to describe physics as seen from an asymptotic external observer maps the region outside the horizon to the complete real line and therefore does not probe directly the region beyond the horizon. If time evolution inside the horizon of a black hole is to be described by the boundary theory, time has to be generated holographically. While challenging

[13]This correspondence established at the Euclidean level extends to real time [64, 4]. At temperature $T = T_{HP}$ the gauge theory also undergoes a first order deconfinement phase transition in the large N limit [97, 96]. See chapter 2.3 for further details

this opens the possibility to describe holographically time evolution in the regions containing the past and future singularities which can be viewed as Big Bang or Big Crunch cosmologies.

The notion of an horizon is intrinsically non-local as, for example, the future horizon corresponds to the boundary of the past of the future infinity and therefore the determination of its location involves the knowledge of the future evolution of spacetime. If gauge theory correlators were to encode only the region of the spacetime outside the horizon this would entail that the Ads-CFT correspondence is very non local in time. Considerations of this nature led to imagine some gedanken-experiment to disprove this possibility. For example by assuming the existence of precursors (non-local operators encoding the bulk "instantaneously") in the gauge theory [80, 29] it would be possible to recover information about an event P in the bulk before the collapse of some matter distribution would form a black hole whose horizon encompasses P [51].

The quest for understanding if and how the region beyond the horizon is encoded in the boundary conformal theory was undertaken by many. In particular the authors of [28] were able to pinpoint an interesting albeit subtle manifestation of the singularity in the gauge theory correlation functions. We now describe in more detail their work as it plays an important place in the results described below.

The starting point is the consideration of the following finite temperature two point function for a gauge invariant scalar operator $O(t)$ in the boundary theory:

$$G_{12}(2t) = \left\langle O\left(t + \frac{i}{2}\beta\right) O\left(-t\right) \right\rangle_{\beta} \tag{1.7}$$

where $\langle\rangle_{\beta}$ represents the expectation value on the canonical ensemble at temperature $T = \frac{1}{\beta}$. The possibility that this quantity could encode the geometry inside the horizon had already been suggested in [64]. The operator $O(t)$ is dual to a scalar field propagating in the bulk black hole geometry. The mass of the field being proportional to the conformal dimension of O. The two point function $G_{1,2}(2t)$ in the large N limit at strong coupling λ can be computed by solving in the supergravity limit for the

propagation of the scalar field in the black hole background with point-like sources positioned on the boundary at times $t + \frac{i}{2}\beta$ and $-t$ respectively. As the mass m of the scalar field becomes large the correlator can be evaluated in the semi-classical geodesic approximation and is given by

$$G_{12}(2t) = e^{-m\mathcal{L}(t)}$$

where $\mathcal{L}$ is the proper length of the spacelike geodesic joining the boundary points[14].

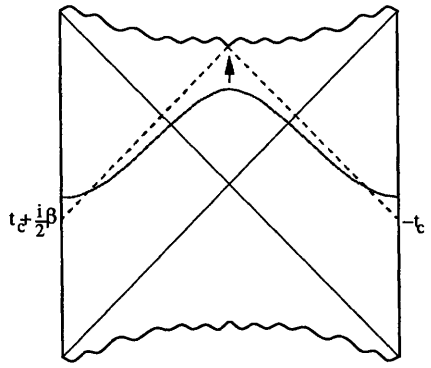

Figure 1-2: Spacelike geodesics connecting $t + \frac{i}{2}\beta$ and $-t$ at the boundary. As $t \to t_c$ (black arrow) the geodesics becomes null and approaches the singularity. The extremal geodesic is dashed in figure.

As can be seen from the figure the geodesic passes through spacetime regions inside the horizon. There exists a particular time t_c beyond which there are no geodesics connecting the two boundaries. Moreover as $t \to t_c^-$ the length of the geodesic diverges as $L(t) \sim \log(t_c - t)$. This corresponds to a light-cone singularity in the field theory, since the geodesics are becoming almost null and would imply the following singular behaviour for the correlator:

$$G_{12}(t) \sim \frac{1}{(t_c - t)^m}$$

[14]this length has to be regularized by subtracting the length of the geodesic corresponding to $t = 0$

However such a divergence is excluded by the following simple spectral consideration:

$$|G_+(t+i\frac{\beta}{2})| = |Z(\beta)^{-1}\sum_{n,m} e^{-\frac{1}{2}\beta(E_n+E_m)-it(E_n-E_m)}|\,\langle m|O(0)|n\rangle\,|^2| \leq$$
$$\leq |Z(\beta)^{-1}\sum_{n,m} e^{-\frac{1}{2}\beta(E_n+E_m)}|\,\langle m|O(0)|n\rangle\,|^2| = |G_+(0)| \qquad (1.8)$$

where the sums run over all the states in the theory, the E_n are their energies and $Z(\beta) = \sum_n \exp(-\beta E_n)$.

The source of the problem lies in the assumption that it is the bouncing geodesic we have drawn in figure that has to be considered in evaluating the correlation function. By a careful consideration of the analytic continuation of the correlation function from Euclidean time to real time the authors of [28] conclude that, on the contrary, for any real value of t the correlator is dominated by the contribution of two geodesics in the complexified spacetime which do not approach the singularity. The correlator however turns out to be a multivalued analytic function of t (in the large m limit) and the contribution of the singular geodesic can still be obtained by a subtle continuation of the two point function on a different Riemann sheet.

This suggestive result provided a starting point for our investigation which is described in detail in chapters 3 and 4. We considered a scalar operator $O(t,\hat{x})$ in the gauge theory ($\hat{x}$ being the position on the S^3 the boundary theory lives on) and its finite temperature two point Wightman function $G_+(t,\hat{x}) = \langle O(t,\hat{x})O(0)\rangle_\beta$. As the theory is invariant under time translations and rotations in the S^3 directions it is convenient to perform a Fourier transform in time and consider a decomposition in spherical harmonics in the $\hat{x}$ directions:

$$G_+(\omega,l) = \int_{-\infty}^{\infty} dt e^{-i\omega t}\int_{S^3} d\Omega_3 Y_l^*(\hat{x})G_+(t,\hat{x})$$

where l is a set of $SO(4)$ quantum numbers.

We obtain the following results about the structure of $G_+(\omega,l)$ in the $N=\infty$ and $\lambda\to\infty$ limit:

- (Ch 2.3) $G_+(\omega)$ has a continuous spectrum whose origin can be traced back to

the presence of the horizon in the dual bulk theory. All the singularities of the correlation function are away from the real axis which implies an exponential decay in time of its Fourier transform back into coordinate space.

- (Ch 3) The analytic structure of the correlation function is such that the complex ω plane can be divided into several asymptotic regions. In two of these regions $\omega \to \pm\infty$ while in the remaining two $\omega \to \pm i\infty$. The asymptotic expansion of the function $G_+(\omega)$ for large ω in each of these sectors cannot be obtained by analytic continuation from the one valid in another sector.

- (Ch 3.2) Let the conformal dimension of O be $\Delta = 2 + \nu$ then asymptotically for $\nu \to \infty$ we have the following WKB expansion for the two point function:

$$G_+(\omega = \nu u, l = \nu k) \sim 2\nu e^{\nu Z(u,k)}(1 + O(\nu^{-1}))$$

  The function $Z(u,k)$ can be determined by studying spacelike geodesics in the black hole background. These are labeled by the value of the integral of motion E coming from the isometry under Schwarzschild time translations and p coming from the isometry under $SO(4)$ rotations. For each geodesic we can evaluate its length[15] which will depend on E and p. The Legendre transform of this function in the (E,p) variables is $Z(iE,ip)$.

- Ch (3.2.3) For each (ω,l) we determine the geodesic which has to be considered in computing $G_+(\nu u,\nu k)$ in the large ν limit. For $\omega \to \pm\infty$ this geodesic approaches the boundary of the spacetime. For $\omega \to \pm i\infty$ the geodesic is the one represented in the previous figure, it enters the region beyond the horizon and comes closer and closer to the singularity. The turning point of the geodesic scans the black hole spacetime as we change (ω,l), in particular the timelike coordinate inside the horizon is holographically generated and encoded in the behaviour of gauge theory correlation functions for imaginary ω. The different asymptotic sectors of $G_+(\omega)$ for large ω correspond to the geodesic approaching

[15] boundary to boundary proper length regularized as in footnote 7

the boundary or the singularity.

- (Ch 4.3) We identify two manifestations of the presence of the singularity in the asymptotic behaviour of $G_+(\omega, l)$ for $\omega \to \pm i\infty$ along the imaginary ω axis.The first manifestation is that $G_+(\omega)$ decays exponentially along the imaginary axis. This asymptotic behavior is due to the fact that light-like geodesics reach the singularity in a finite time. By various different methods we prove that this exponential decay survives in the case O has a finite conformal dimension and is controlled by a simple parameter encoding the geometry of the black hole in the region inside the horizon. The second manifestation is given by the divergent behaviour of the k derivatives of $Z(u, k)$ as $u \to i\infty$:

$$\frac{d^{2n}}{dk^{2n}} Z(iu, k) \mid_{k=0} \sim u^{2n} \qquad u \to \infty$$

  This divergence is due to the shrinking of the radius of curvature as we approach the singularity.

- (Ch 4.4) At any finite N the boundary theory has a discrete spectrum being a bounded quantum mechanical system. We can then write a spectral decomposition of $G_+(\omega, l)$

$$G_+(\omega, l) = 2\pi \sum_{m,n} e^{-\beta E_m} \rho_{mn} \delta(\omega - E_n + E_m)$$

  where the sum is over all the states in the system. The correlator is a sum of delta functions on the real axis and cannot be analytically continued for imaginary ω. In particular the signatures of the singularity we found in the large N limit at strong coupling disappear indicating that quantum effects should resolve the singularity. This still leaves open the possibility that stringy effects (small coupling) could resolve the singularity already at the classical (large N) level.

We see that a first step towards the understanding of the resolution of spacelike singularities is the study of the appearance of a continuous spectrum in the large N

limit of the boundary theory. So far we know that in the $N \to \infty$ limit $G_+(\omega, l)$ develops a continuous spectrum. For any finite N it is quasi-periodic in time but it decays exponentially in the $N \to \infty$ $\lambda \to \infty$ limit. The emergence of a continuous spectrum and time decay in the gauge theory is connected with some of the deepest features of the physics of spacelike singularities and the resolution of the information paradox.

1.3 Time arrow and space-like singularities

The equations of general relativity are time symmetric, but in presence of spacelike singularities an intrinsic arrow of time can be generated. This happens in both the examples of FRW cosmologies and the formation of a black hole in a gravitational collapse. We have stated that a black hole behaves like a thermodynamical system, thus in the case of a gravitational collapse, the direction of time appears to have thermodynamical nature. It has also been speculated that the thermodynamic arrow of time observed in nature may be related to the big bang singularity [76].

With the tools provided by the AdS/CFT correspondence we can try to achieve a microscopic understanding of the emergence of thermodynamic behavior in a gravitational collapse in an anti-de Sitter spacetime.

The classical gravity limit of the AdS string theory corresponds to the large N and large 't Hooft coupling limit of the boundary theory. As we have described, a matter distribution of classical mass M in AdS can be identified with an excited state of energy $E = \mu N^2$ in the SYM theory with μ a constant independent of N. This mass distribution[16] can collapse to form a black hole which we can identify with a thermal density matrix in the gauge theory [97, 64]. Then the gravitational collapse of the matter distribution should be identified with the thermalization of the corresponding state in SYM theory. We can speculate that the appearance of a spacelike singularity at the end point of a collapse should be related to certain

[16] Assume M is sufficiently big that a big black hole in AdS is formed, which also implies that μ should be sufficiently big.

universal aspects of thermalization in the SYM theory[17]

In the boundary theory consider the following correlator of an arbitrary gauge invariant operator $\mathcal{O}$ which when acting on the vacuum creates a state of finite energy of order $O(N^0)$.

$$G_i(t) = \langle i|\mathcal{O}(t)\mathcal{O}(0)|i\rangle - \langle i|\mathcal{O}(0)|i\rangle^2 \tag{1.9}$$

where $|i\rangle$ is a generic energy eigenstate in the high energy sector $E \sim N^2$. Thermalization occurs and an arrow of time is generated, if for all such operators $\mathcal{O}$ and generic states $|i\rangle$ with energy big enough that their dual field configuration can collapse in a stable black hole, we have

$$G_i(t) \to 0, \qquad t \to \infty \tag{1.10}$$

In particular, 1.10 implies that information is lost as one cannot distinguish different initial states from their long time behavior.

A crucial element for the emergence of thermalization in the boundary theory is the large N limit. $\mathcal{N} = 4$ SYM theory on S^3 is a closed, bounded quantum mechanical system with a discrete energy spectrum. At any finite N, no matter how large, such a theory is time reversible and never really thermalizes. However, to match the picture of a gravitational collapse in classical gravity, an arrow of time should emerge in the large N limit for the SYM theory in a generic state of energy $E = \mu N^2$ with sufficiently large μ. At finite N, the theory is unitary and there is no information loss. But in the large N limit, the information is lost, since one cannot recover the initial state from the final thermal equilibrium. Thus the information loss in a gravitational collapse is clearly a consequence of the classical approximation (large N limit), but not a property of the full quantum theory. AdS/CFT implies that the time evolution of the quantum gravity theory is unitary and therefore in principle resolves the information loss paradox[18].

[17]Some interesting ideas regarding spacelike singularities and thermalization have also been discussed recently in [8].

[18]To our knowledge this connection was first pointed out in the context of AdS/CFT in [64]. It

In order to reconcile the unitary time evolution at finite N with the emergence of an arrow of time and thermalization implied by the bulk theory in its classical limit we have to accept that these are effects of the large N limit in the gauge theory. Then we are challenged to answer the following questions:

- 1. What is the underlying physical mechanism for the emergence of an arrow of time and thermalization in the boundary gauge theory?
- 2. We know such a mechanism must involve the large N limit. Is the large 't Hooft coupling limit also needed? It could be that an arrow of time emerges only for a certain range of λ therefore implying the presence of a large N phase transition as the coupling is decreased from ∞ to 0.
- 3. If an arrow of time also emerges at finite 't Hooft coupling λ, what would be the bulk string theory interpretation of the SYM theory in a state of high energy which thermalizes? A stringy black hole? Is a singularity present in such a black hole?

It would be very desirable to have a clear physical understanding of the questions above as it could shed light on how spacelike singularities appear in the classical limit of a quantum gravity theory and lead to an understanding of their resolution in a quantum theory.

In Chapter 5 we suggest a simple mechanism for the emergence of an arrow of time in the gauge theory in the large N limit and initiate a statistical approach to understanding the quantum dynamics of a Yang-Mills theory in highly excited states. We avoid the complications of working with correlation functions on specific highly excited states and take into consideration correlation functions computed in the canonical ensemble. The temperature must be such that the average energy of the states in the ensemble is of order μN^2. For the case of a $SU(N)$ Yang Mills theory compactified on S^3 it has been proven [1, 97] both at small coupling and at large coupling that this is the case for $T > T_{dec}$ where T_{dec} is a function of λ of order

remains a puzzle whether one can recover the lost information using a semi-classical reasoning; see e.g. [64, 12, 11, 10, 57, 49, 67, 62, 6] for recent discussions.

N^0 [19]. As a second simplification we consider a simpler quantum mechanical system (see Chapter 5.2) with far less degrees of freedom than $\mathcal{N} = 4$ SYM on S^3 but which shares with it many features like the existence of a finite T_{dec} in the large N limit.

We obtain the following results:

- 1 We first prove that in the large N limit at any finite order in perturbation theory the boundary theory does not thermalize.
- 2 We prove that for high enough temperature (such that the system probes states of energy of order N^2) the large N perturbation theory does not converge for any value of λ.
- 3 We interpret this as due to the fact that the high energy states $E \sim N^2$ in the free theory are exponentially degenerate e^{N^2} in N^2. We show that the introduction of a tiny perturbation $\lambda \neq 0$ would strongly mix an exponentially large (in N^2) number of free states which span an energy interval of order λN. Thus for any finite λ the theory is nonperturbative in the large N limit in the high energy sector. As a consequence the small λ and the long time limits do not commute at infinite N.
- 4 We finally develop a statistical method for studying the dynamics of the theories in highly excited states, which indicates that time irreversibility occurs for any nonzero 't Hooft coupling λ.

In particular, we argue that the perturbative planar expansions breaks down for real-time correlation functions and that there is a large N "phase transition" at zero 't Hooft coupling[20]. We also argue that time irreversibility occurs for any nonzero value of the 't Hooft coupling in the large N limit therefore answering some of the questions we posed.

[19] for $T < T_{dec}$ the average energy computed in the canonical ensemble is $O(N^0)$. In the large N limit we therefore have a phase transition which was identified as due to the deconfinement of the theory at large temperature.

[20] See [61, 32, 41] for some earlier discussion of a possible large N phase transition in λ.

Chapter 2

AdS Black Holes and AdS/CFT at Finite Temperature

This chapter sets the stage for our investigations. We describe how to compute real time thermal boundary correlation functions from gravity. In the first two sections we first introduce the AdS Schwarzschild black hole geometry and then review some of the properties of real time correlation functions in finite temperature field theory. In the last section we describe how to compute them using AdS/CFT.

2.1 Black hole geometry

In this section we briefly review the classical geometry for a Schwarzschild black hole in an AdS_{d+1} ($d \geq 3$) spacetime. The metric can be written as

$$ds^2 = -f(r)dt^2 + f(r)^{-1}dr^2 + r^2 d\Omega_{d-1}^2 \tag{2.1}$$

with

$$f(r) = r^2 + 1 - \frac{\mu}{r^{d-2}}, \tag{2.2}$$

where μ is proportional to the mass of the black hole and $d\Omega_{d-1}^2$ denotes the metric on a unit $(d-1)$-sphere. We have set the curvature radius of AdS to be unity, as we will do throughout the thesis. As $r \to \infty$, the metric goes over to that of global AdS with t identified as the boundary Yang-Mills theory time. The fully extended black hole spacetime has two disconnected time-like boundaries, each of topology $S^{d-1} \times \mathbb{R}$ (see Fig. 1 for the Penrose diagram).

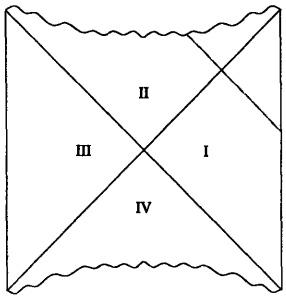

Figure 2-1: Penrose diagram for the AdS black hole. A null geodesic going from the boundary to the singularity is indicated in the figure.

The event horizon radius r_0 is given by the unique positive root of the equation

$$r^2 + 1 - \frac{\mu}{r^{d-2}} = 0$$

and the inverse Hawking temperature is given by

$$\beta = \frac{4\pi}{f'(r_0)} = \frac{4\pi r_0}{dr_0^2 + (d-2)} \,. \tag{2.3}$$

In the limit that the mass of the black hole goes to infinity, i.e. $\mu \to \infty$ and thus $r_0 \to \infty$, after a scaling of the coordinates

$$r \to r_0 r, \qquad t \to t/r_0, \qquad r_0^2 d\Omega_{d-1}^2 = dx_i^2 \tag{2.4}$$

the metric becomes

$$ds^2 = -f dt^2 + \frac{1}{f} dr^2 + r^2 dx_i^2 \tag{2.5}$$

with

$$f = r^2 - \frac{1}{r^{d-2}} \tag{2.6}$$

In the above dx_i^2 denotes the metric for a flat $(d-1)$-dimensional Euclidean space. After the rescaling, the horizon is located at $r_0 = 1$ and the inverse Hawking temperature is

$$\beta = \frac{4\pi}{d} \,. \tag{2.7}$$

The boundary manifold now consists of two copies of $\mathbb{R}^{d,1}$.

The black hole singularities are located at $r = 0$ in region II and IV respectively, at which f blows up and the radius of the three sphere in 2.1 or the overall size of $\mathbb{R}^3$ in 2.5 goes to zero.

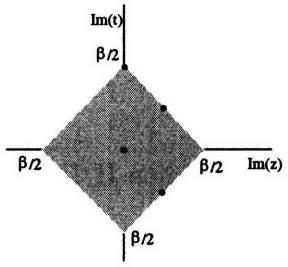

Figure 2-2: A choice of fundamental domain in the $\mathrm{Im}\, z - \mathrm{Im}\, t$ plane is indicated. The red dots belong to the real Lorentzian section of the geometry. The dot at the origin corresponds to region I in 2-1. The dots with $\mathrm{Im}\, z = \frac{\beta}{4}$ correspond to regions II/IV and the dot at $\mathrm{Im}\, t = \frac{\beta}{2}$ corresponds to region III.

To describe the black hole geometry it is often convenient to use the tortoise coordinate

$$z(r) = \int_r^\infty \frac{dr}{f(r)} = -\sum_{i=0}^{d-1} \frac{1}{f'(r_i)} \log(r - r_i) \tag{2.8}$$

where r_i are zeros of f with r_0 being the horizon.

The region outside the horizon (region I) corresponds to $z \in (0, +\infty)$. At the

boundary $r \to \infty$, we have $z \approx \frac{1}{r} \to 0$. At the horizon $r \to r_0$, we have

$$z \approx -\frac{\beta}{4\pi} \log(r - r_0) \to +\infty \ .$$

In region I of the Penrose diagram 2-1, the Kruskal coordinates can be written in terms of z and t as

$$U = -e^{-\frac{2\pi}{\beta}(t+z)}, \qquad V = e^{\frac{2\pi}{\beta}(t-z)} \tag{2.9}$$

and therefore $U < 0, \ \ V > 0$. General real values of U, V cover the full Lorentzian section of the spacetime with the horizon at $UV = 0$, the boundaries at $UV = -1$, and the singularities at $UV = e^{-\pi\frac{\tilde{\beta}}{\beta}}$ with $\tilde{\beta}$ a constant to be introduced below. We will extend 2.9 to the fully complexified Kruskal spacetime in which both z, t and U, V take general complex values. Values of z and t which lead to the same values of U, V are identified, i.e.

$$t \sim t + i\frac{m+n}{2}\beta, \qquad z \sim z + i\frac{m-n}{2}\beta, \quad m, n \in \mathbf{Z} \ . \tag{2.10}$$

In terms of complex z and t, in region II/IV we have $\mathrm{Im}\, t = \pm\frac{\beta}{4}$, $\mathrm{Im}\, z = \frac{\beta}{4}$ and in region III $\mathrm{Im}\, t = \frac{\beta}{2}$, $z \in R_+$. A choice of fundamental domain in the $\mathrm{Im}\, z - \mathrm{Im}\, t$ plane is shown in 2-2, where we also indicate points which correspond to the real Lorentzian section of the complexified spacetime.

In the fully complexified spacetime the boundary has complex codimension-one and is located at $z = 0$. The black hole singularity is a complex codimension-one singularity located at (up to the identifications 2.10)

$$z_0 = z(r = 0) = \int_0^\infty \frac{dr}{f(r)} = \frac{1}{4}(\tilde{\beta} + i\beta) \ . \tag{2.11}$$

The imaginary part of z_0, which is one quarter of the inverse Hawking temperature β, arises by going around the pole at $r = r_0$ (location of the horizon) in the complex

r-plane. $\tilde{\beta}$ is a positive real number[1] obtainable from the roots of equation $f(r) = 0$. Note that 2.11 is also the complex Schwarzschild time that it takes for a radial null geodesic to go from the boundary to the singularity. A nonzero $\tilde{\beta}$ implies that the Penrose diagram for the black hole is not a square, as was first pointed out in [28]. In function of $\tilde{\beta}$ the range of $\mathrm{Re}\, z$ in regions II/IV is $\mathrm{Re}\, z > \frac{\tilde{\beta}}{4}$.

For our future discussion, it is convenient to introduce a complex quantity

$$\mathcal{B} = \tilde{\beta} + i\beta = |\mathcal{B}| e^{i\theta_{\mathcal{B}}} \ . \tag{2.12}$$

For example, for the metric 2.5,

$$\tilde{\beta} = \frac{4\pi}{d} \cot \frac{\pi}{d}, \qquad \mathcal{B} = \frac{4\pi}{d \sin \frac{\pi}{d}} e^{i\frac{\pi}{d}}, \qquad \theta_{\mathcal{B}} = \frac{\pi}{d} \ . \tag{2.13}$$

For a finite mass black hole 2.1-2.2 in AdS_5 ($d = 4$),

$$\tilde{\beta} = \frac{2\pi r_1}{r_0^2 + r_1^2}, \qquad \mathcal{B} = \frac{2\pi(r_1 + i r_0)}{r_0^2 + r_1^2} = \frac{2\pi}{r_1 - i r_0}, \qquad \theta_{\mathcal{B}} < \frac{\pi}{4} \tag{2.14}$$

where

$$r_1^2 = r_0^2 + 1, \qquad \mu = r_0^2 r_1^2$$

The explicit expressions of $\mathcal{B}$ for a finite mass black hole for other dimensions are more complicated.

To conclude this section we note that in equation 2.3 β has a maximum at $\beta_0 = \frac{2\pi}{\sqrt{d(d-2)}}$ above which there is no black hole solution. For a given $\beta < \beta_0$ there are two solutions for r_0, the larger of which describes a stable black hole (the so-called big black hole) with a positive specific heat. The one with smaller r_0 is called a small black hole and has a negative specific heat. The Euclidean action of the big black hole is always smaller than that of the small black hole and becomes negative for $\beta < \beta_{HP} = \frac{2\pi}{d-1}$ [45, 97]. One can define a canonical ensemble for semi-classical quantum gravity in AdS background and when $\beta < \beta_{HP}$, the ensemble is dominated

[1]The analogous quantity for a flat space Schwarzschild black hole is infinite.

by the contribution of the big black hole [45]. We will focus on the big black hole.

Note that one can invert 2.8 to find $r(z)$. In particular, for $\mathrm{Re}z > \frac{\beta}{4}$, r is a one-to-one periodic function of z with period $i\frac{\beta}{2}$. This property will be important later.

2.2 Finite temperature correlation functions in boundary theories

Since the main purpose of this chapter is to compute thermal boundary correlation functions from gravity, in this section we review general properties of various real-time correlation functions at finite temperature. We will consider that the boundary theory lives either on $\mathbb{R} \times S^{d-1}$ or $\mathbb{R}^{1,d-1}$.

Consider a gauge invariant operator $\mathcal{O}$ in the boundary theory of conformal dimension Δ. For simplicity we will take $\mathcal{O}$ to be a Lorentz scalar. The real-time thermal Wightman functions are defined by

$$\begin{aligned} G_+(x) &= \tfrac{1}{Z}\mathrm{tr}\left(e^{-\beta H}\mathcal{O}(x)\mathcal{O}(0)\right), \\ G_-(x) &= \tfrac{1}{Z}\mathrm{tr}\left(e^{-\beta H}\mathcal{O}(0)\mathcal{O}(x)\right) \end{aligned} \tag{2.15}$$

where H is the Hamiltonian of the boundary theory, tr denotes the sum over all states in the Hilbert space, $Z = \mathrm{tr}e^{-\beta H}$ is the partition function, $x = (t, \vec{x})$ with $\vec{x}$ denoting the spatial coordinates. The Feynman, retarded and advanced propagators are given by

$$\begin{aligned} G_F(x) &= \theta(t)G_+(x) + \theta(-t)G_-(x), \\ G_R(x) &= \frac{i}{Z}\theta(t)\mathrm{tr}\left(e^{-\beta H}[\mathcal{O}(x), \mathcal{O}(0)]\right), \\ G_A(x) &= -\frac{i}{Z}\theta(-t)\mathrm{tr}\left(e^{-\beta H}[\mathcal{O}(x), \mathcal{O}(0)]\right) . \end{aligned} \tag{2.16}$$

Since spatial coordinates do not play an active role in our discussion below, we will suppress them for the rest of the section for notational simplicity. We will also be

interested in correlators with the following complex time separation[2]

$$G_{12}(t) = \frac{1}{Z}\mathrm{tr}\left[e^{-\beta H}\mathcal{O}(t - i\beta/2)\mathcal{O}(0)\right] = G_+(t - i\beta/2) \tag{2.17}$$

which can be obtained from $G_+(t)$ by an analytic continuation.

By inserting complete sets of states in 2.15, $G_+(t)$ can be written as

$$G_+(t) = \frac{1}{Z}\sum_{m,n} e^{-iE_n t}e^{iE_m(t+i\beta)}\,\rho_{mn} \tag{2.18}$$

where m, n sum over the physical states of the theory[3] and $\rho_{mn} = |\langle m|\mathcal{O}(0)|n\rangle|^2$. Assuming the convergence of the sums is controlled by the exponentials, it follows from 2.18 that $G_+(t)$ is analytic in t within the range[4] $-\beta < \mathrm{Im}\, t < 0$. Similarly $G_-(t)$ is analytic for $0 < \mathrm{Im}\, t < \beta$ and $G_{12}(t)$ for $-\frac{\beta}{2} < \mathrm{Im}t < \frac{\beta}{2}$.

Going to frequency space one finds that

$$\begin{aligned} G_+(\omega) &= \int_{-\infty}^{\infty} dt\, e^{i\omega t}G_+(t) \\ &= \frac{1}{1 - e^{-\beta\omega}}\rho(\omega) \end{aligned} \tag{2.19}$$

where we have introduced the spectral density function

$$\rho(\omega) = \frac{1}{Z}(1 - e^{-\beta\omega})\sum_{m,n}(2\pi)\delta(\omega - E_n + E_m)e^{-\beta E_m}\rho_{mn}\ . \tag{2.20}$$

We will use the same letter for functions in frequency and coordinate spaces and distinguish them only by the arguments of the function.

In terms of ρ, other correlators in frequency space can be written as

$$\begin{aligned} G_-(\omega) &= e^{-\beta\omega}G_+(\omega) \\ G_{12}(\omega) &= e^{-\frac{1}{2}\beta\omega}G_+(\omega) = \frac{1}{2\sinh\frac{\beta\omega}{2}}\rho(\omega) \end{aligned}$$

[2]In the thermal field formulation, $G_{12}(t)$ corresponds to having $\mathcal{O}(0)$ acting on the first Hilbert space while $\mathcal{O}(t)$ acting on the second Hilbert space.

[3]When the theory has a continuous spectrum like the boundary theory on $\mathbb{R}^{1,d-1}$, one should replace the sums by appropriate integrals.

[4]This is the minimal range. The actual range can be bigger.

$$
\begin{aligned}
G_R(\omega) &= -\int_{-\infty}^{\infty} \frac{d\omega'}{2\pi} \frac{\rho(\omega')}{\omega - \omega' + i\epsilon} \\
G_A(\omega) &= -\int_{-\infty}^{\infty} \frac{d\omega'}{2\pi} \frac{\rho(\omega')}{\omega - \omega' - i\epsilon} \\
iG_F(\omega) &= G_R(\omega) + iG_-(\omega)
\end{aligned} \tag{2.21}
$$

From 2.21 we also have

$$
\rho(\omega) = -i(G_R(\omega) - G_A(\omega)) \tag{2.22}
$$

We also note that the Euclidean correlation function in momentum space can be obtained from $G_{R,A}(\omega)$ evaluated at discrete frequencies

$$
G_E(\omega_l) = \begin{cases} G_R(i\omega_l) & l \geq 0 \\ \\ G_A(i\omega_l) & l < 0 \end{cases}, \qquad \omega_l = \frac{2\pi l}{\beta}, \quad l \in \mathbf{Z} \tag{2.23}
$$

Thus Lorentzian correlation functions in frequency space have a much richer analytic structure than the Euclidean one.

Some further remarks:

- 1. From 2.20–2.21,

$$
\rho(-\omega) = -\rho(\omega), \qquad G_{12}(-\omega) = G_{12}(\omega), \qquad G_R(-\omega) = G_A(\omega)\ . \tag{2.24}
$$

- 2. For a theory with a discrete spectrum, from 2.20, the spectral function $\rho(\omega)$ and $G_+(\omega)$ are given by a sum of discrete delta functions supported on the real axis, while $G_R(\omega)$ is given by a discrete sum of poles along the real axis.

- 3. For a theory with a continuous spectrum, the analytic behaviors of various propagators in the complex ω plane give important information about the theory. From 2.21 one finds that for generic complex ω

$$
G_{12}^*(\omega) = G_{12}(\omega^*), \qquad G_R^*(\omega) = G_R(-\omega^*) = G_A(\omega^*)\ . \tag{2.25}
$$

$G_R(\omega)$ is analytic in the upper half plane, while $G_A(\omega)$ is analytic in the lower half plane. From 2.25 the singularities of $G_A(\omega)$ in the upper half plane are simply the reflection with respect to the real axis of those of $G_R(\omega)$ in the lower half plane. Furthermore the singularities of $G_R(\omega)$ and $G_A(\omega)$ are symmetric with respect to the imaginary ω-axis. Equation 2.22 implies that $G_{12}(\omega)$ (and $G_+(\omega)$) have singularities in both the upper and the lower half plane, given by those of $G_A(\omega)$ and $G_R(\omega)$ respectively.

2.3 AdS/CFT correspondence in the black hole background

The thermodynamic aspects of quantum gravity in AdS spacetime were discussed long ago by Hawking and Page [45], using the semi-classical Euclidean path integral formalism. They realized that it is possible to define a canonical ensemble for quantum gravity in a Schwarzschild black hole background in AdS. They also found that in the semi-classical limit, the system undergoes a first order phase transition at a temperature T_{HP} of the order of the inverse curvature radius of the spacetime. Below T_{HP}, the system is described by a thermal gas in AdS, while above T_{HP} it is described by a big black hole. With the discovery of the AdS/CFT correspondence [63, 39, 96], the results of Hawking and Page were given a natural interpretation in terms of the boundary Yang-Mills theory [96, 97]. The thermal AdS and the Euclidean big black hole in AdS_{d+1} correspond to a confined and to a deconfined phase of the boundary theory on S^{d-1} respectively, and the Hawking-Page transition corresponds to a large N deconfinement transition [93]. The boundary theory at finite temperature on $\mathbb{R}^{d-1}$, which is dual to 2.5 and corresponds to the high temperature limit of the theory on S^{d-1}, is always in the deconfined phase.

The correspondence can be extended to Lorentzian signature [64, 4] with the Hartle-Hawking vacuum [40] of the black hole background identified with the thermal density matrix of the boundary theory. The choice of the Hartle-Hawking vacuum is

natural since it describes the black hole in thermal equilibrium. The Lorentzian black hole background has two asymptotic regions with disconnected boundaries. The bulk Hilbert space can be written as a product of two identical copies, each accessed by a single asymptotic region. The Hartle-Hawking vacuum is the maximally entangled state between the two copies and tracing over one copy in the product produces the thermal ensemble accessible to the other asymptotic observer [53]. This is in complete parallel with the thermal field formulation of the boundary theory at finite temperature, with identical copies of the boundary theory Hilbert space associated with each disconnected component of the boundary.

Now consider a scalar operator $\mathcal{O}$ in the boundary theory corresponding to a bulk scalar field ϕ of mass m. In the supergravity limit, the conformal dimension of $\mathcal{O}$ is given by [39, 96]

$$\Delta = \frac{d}{2} + \nu, \qquad \nu = \sqrt{\frac{d^2}{4} + m^2}\ , \tag{2.26}$$

and thermal boundary two-point functions of $\mathcal{O}$ can be obtained from free bulk Green functions in the Hartle-Hawking vacuum by taking the arguments of ϕ to the boundary.[5] For example, the boundary Wightman function 2.15 is obtained by

$$G_+(x,x') = \lim_{r,r'\to\infty} (2\nu r^{\Delta})(2\nu r'^{\Delta})\mathcal{G}_+(x,r;x',r') \tag{2.27}$$

where $x = (t,\vec{x})$ denotes a boundary point and $\mathcal{G}_+$ is the bulk Wightman function for ϕ in the Hartle-Hawking vacuum

$$\mathcal{G}_+(x,r;x',r') = \langle 0|\phi(r,x)\phi(r',x')|0\rangle_{HH}\ . \tag{2.28}$$

A Fourier transform of 2.27 in the t and $\vec{x}$ directions leads to the relation in momentum

[5] Obtaining boundary correlation functions by taking the boundary limit of the bulk ones was discussed, for example, in [9, 34, 58]. For other discussion of boundary Lorentzian correlation functions in the supergravity approximation, see also [3, 84, 48, 66, 60].

space

$$G_+(\omega,\vec{p}) = \lim_{r,r'\to\infty}(2\nu r^{\Delta})(2\nu r'^{\Delta})\mathcal{G}_+(\omega,\vec{p};r,r') \ . \tag{2.29}$$

For boundary theories on S^{d-1}, $\vec{p}$ in the above equation should be interpreted as the angular momentum on S^{d-1}.

The bulk retarded (Feynman) propagator for ϕ leads to the retarded (Feynman) propagator for $\mathcal{O}$ in the boundary theory by the same procedure. For example,

$$G_R(\omega,\vec{p}) = \lim_{r,r'\to\infty}(2\nu r^{\Delta})(2\nu r'^{\Delta})\mathcal{G}_R(\omega,\vec{p};r,r') \ . \tag{2.30}$$

Note that the $r, r' \to \infty$ limits for $\mathcal{G}_R$ on the right hand side of 2.30 contains also a divergent term proportional to $r^{2\nu}$. The divergent term is analytic in $\omega, \vec{p}$ and should be discarded. When Fourier transformed to the coordinate space, such a term gives rise to an irrelevant contact term.

Since the extended black hole background has two asymptotic boundaries, we can also take r and r' to different boundaries. It follows from the thermal field interpretation of the Hartle-Hawking vacuum that this procedure gives rise to G_{12} introduced in 2.17

$$G_{12}(x,x') = \lim_{r,r'\to\text{different boundaries}}(2\nu r^{\Delta})(2\nu r'^{\Delta})\mathcal{G}_+(x,r;x',r') \ . \tag{2.31}$$

Equation 2.31 can also be derived directly from the explicit expressions of the bulk propagators in the Hartle-Hawking vacuum reviewed in Appendix A1.

We now look in some detail at the analytic properties of the boundary real-time correlation functions using 2.27–2.31.

2.3.1 Bulk propagators

Consider a free scalar field[6]

$$S = -\frac{1}{2}\int dr d^d x \sqrt{-g}\left[(\partial\phi)^2 + m^2\phi^2\right] \tag{2.32}$$

in the background of 2.1 or 2.5. For 2.5 let

$$\phi = e^{-i\omega t}e^{i\vec{p}\cdot\vec{x}}r^{-\frac{d-1}{2}}\psi(\omega, p; r), \tag{2.33}$$

the Laplace equation for ϕ can then be written in terms of the tortoise coordinate z 2.8 as

$$\left(-\partial_z^2 + V_p(z) - \omega^2\right)\psi = 0, \tag{2.34}$$

where V_p is an implicit function of z (below $p^2 = \vec{p}\cdot\vec{p}$)

$$V_p(z) = f(r)\left[\frac{p^2}{r^2} + \nu^2 - \frac{1}{4} + \frac{(d-1)^2}{4r^d}\right] . \tag{2.35}$$

For 2.1 one replaces the plane wave in the $\vec{x}$ directions in 2.33 by spherical harmonics on S^3 and get 2.34 with now the potential given by

$$V_l(z) = f(r)\left(\frac{(2l+d-2)^2 - 1}{4r^2} + \nu^2 - \frac{1}{4} + \frac{\mu(d-1)^2}{4r^d}\right) \tag{2.36}$$

where l is the angular momentum on S^3.

As discussed below 2.8, the region outside the horizon corresponds to $z \in (0, +\infty)$ with $z = 0$ at the boundary and $z \to +\infty$ at the horizon. Both 2.35 and 2.36 behave near the boundary as

$$V_p \approx \frac{\nu^2 - \frac{1}{4}}{z^2}, \qquad z \to 0 , \tag{2.37}$$

[6]Since the background Ricci scalar is a constant, the m^2 term below should be considered as the sum of the standard mass term and the coupling to the background curvature.

and near the horizon

$$V_p \propto e^{-\frac{4\pi}{\beta}z} \to 0, \qquad z \to +\infty \ . \tag{2.38}$$

The fact that for $\mathrm{Re}z \gg 1$, r is a one-to one periodic function of z with a period $i\frac{\beta}{2}$ implies that $V_p(z)$ can be expanded for large real z as

$$V_p(z) = \sum_{n=1}^{\infty} a_n e^{-\frac{4\pi n}{\beta}z} \ . \tag{2.39}$$

This property will be important in our discussion below.

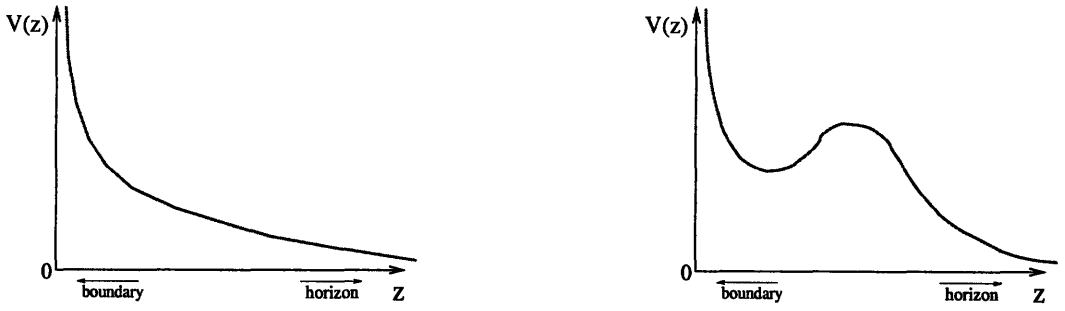

Figure 2-3: Schematic plots of the potential 2.35 or 2.36 for $l < l_c$ (left) and $l > l_c$ (right).

Note that the potential 2.35 is positive definite and monotonic in $z \in (0, +\infty)$ for $\nu^2 > \frac{1}{4}$ and any $p^2 > 0$ (see 2-3). The potential 2.36 is monotonic as in 2-3 for l smaller than a critical value l_c, while for $l > l_c$ the potential develops a well as 2-3 . l_c can be found by solving $V'(r) = V''(r) = 0$. Its explicit value is rather complicated and we do not give it here. An implicit expression in the large ν limit will be given in sec 3.3.2. The potential well reflects that when the angular momentum is sufficiently large there exist stable orbits for a particle moving outside the horizon. We will see later this has interesting consequences for correlation functions of the boundary theory.

In our discussions below, we will use the notation appropriate for 2.5. The discussions apply to both 2.5 and 2.1 unless mentioned explicitly.

For any given real ω, the Schrodinger equation 2.34 has a unique normalizable

mode $\psi_{\omega p}$, which we will take to be real. We normalize it at the horizon as (δ_ω is a phase shift)

$$\psi_{\omega p}(z) \approx -e^{-i\omega z - i\delta_\omega} + e^{i\omega z + i\delta_\omega}, \qquad z \to +\infty \ . \tag{2.40}$$

As $z \to 0$, $\psi_{\omega p}$ has the form

$$\psi_{\omega p} \approx C(\omega, p) z^{\frac{1}{2}+\nu} + \cdots, \qquad z \to 0 \tag{2.41}$$

where the constant C is fixed by the normalization of 2.40.

The bulk Wightman propagator $\mathcal{G}_+$ 2.16 and the retarded propagator G_R in momentum space can be written in terms of $\psi_{\omega p}$ as (see Appendix A1 for a derivation)

$$\begin{aligned} \mathcal{G}_+(\omega, p; z, z') &= \frac{e^{\beta\omega}}{e^{\beta\omega}-1} \tilde{\rho}(\omega, p; z, z') \\ \mathcal{G}_R(\omega, p; z, z') &= -\int_{-\infty}^{\infty} \frac{d\omega'}{2\pi} \frac{\tilde{\rho}(\omega', p; z, z')}{\omega - \omega' + i\epsilon} \end{aligned} \tag{2.42}$$

with the spectral density function

$$\tilde{\rho}(\omega, p; z, z') = \frac{1}{2\omega} (rr')^{-\frac{d-1}{2}} \psi_{\omega p}(z) \psi_{\omega p}(z'), \tag{2.43}$$

Going to the boundary using 2.29 and 2.30, we find that

$$\begin{aligned} G_+(\omega, \vec{p}) &= \frac{e^{\beta\omega}}{e^{\beta\omega}-1} \rho(\omega, \vec{p}) \\ G_R(\omega, p) &= -\int_{-\infty}^{\infty} \frac{d\omega'}{2\pi} \frac{\rho(\omega', p)}{\omega - \omega' + i\epsilon} \end{aligned} \tag{2.44}$$

with the boundary spectral density

$$\rho(\omega, p) = \frac{(2\nu)^2}{2\omega} C^2(\omega, p) \ . \tag{2.45}$$

2.3.2 An alternative expression

Equations 2.40–2.45 reduces the task of finding real-time boundary correlation functions to solving a non-relativistic scattering problem in the potential 2.35. Using standard techniques of scattering theory one can in fact deduce many analytic properties of those correlation functions without solving the Schrodinger equation 2.34 explicitly. For this purpose, we will first write 2.44 in a different form.

We introduce the following solutions to equation 2.34 specified by different boundary conditions:

$$\begin{aligned} g(\omega,p;z) &\approx z^{\frac{1}{2}+\nu}, \qquad z\to 0_+ \\ \tilde{g}(\omega,p;z) &\approx z^{\frac{1}{2}-\nu}, \qquad z\to 0_+ \\ h_R(\omega,p;z) &\approx e^{i\omega z}, \qquad z\to\infty \\ h_A(\omega,p;z) &\approx e^{-i\omega z}, \qquad z\to\infty\ . \end{aligned} \tag{2.46}$$

Note that by construction,

$$h_A(\omega,p;z)=h_R(-\omega,p;z), \qquad g(\omega,p;z)=g(-\omega,p;z), \qquad \tilde{g}(\omega,p;z)=\tilde{g}(-\omega,p;z)$$

The function $g(z)$ can be written as a linear superposition of h_R, h_A

$$g(\omega,p;z)=\frac{1}{2i\omega}\left(-f(\omega,p)h_A(\omega,p;z)+f(-\omega,p)h_R(\omega,p;z)\right) \tag{2.47}$$

which defines the Jost function $f(\omega,p)$. Similarly h_R (h_A) can be written as a linear superposition of g and $\tilde{g}$

$$h_R(\omega,p;z)=\frac{1}{2\nu}\left[f(\omega,p)\tilde{g}(\omega,p;z)+K(\omega,p)g(\omega,p;z)\right]\ . \tag{2.48}$$

That $f(\omega,p)$ also appears in the coefficient of the first term on the right hand side of 2.48 can be seen from the Wronskian, which can be worked out from 2.46–2.48

$$W[h_R,g] \;=\; h_R\partial_z g-g\partial_z h_R=f(\omega,p)$$

$$W[h_R, \tilde{g}] = h_R \partial_z \tilde{g} - \tilde{g} \partial_z h_R = -K(\omega, p) \ . \tag{2.49}$$

The phase shift in 2.40 can be written in terms of the Jost function $f(\omega, p)$ by

$$e^{2i\delta_\omega} = \frac{f(-\omega, p)}{f(\omega, p)} \tag{2.50}$$

and the normalization factor in 2.41 is

$$C^2(\omega, p) = \frac{4\omega^2}{f(\omega, p) f(-\omega, p)} \ . \tag{2.51}$$

From 2.44 we thus find that

$$\begin{aligned} G_+(\omega, p) &= (2\nu)^2 \frac{e^{\beta\omega}}{e^{\beta\omega} - 1} \frac{2\omega}{f(\omega, p) f(-\omega, p)} \\ \rho(\omega, p) &= (2\nu)^2 \frac{2\omega}{f(\omega, p) f(-\omega, p)} \end{aligned} \tag{2.52}$$

The bulk retarded propagator (second line of 2.42) can also be written as

$$\mathcal{G}_R(\omega, p; z, z') = (rr')^{-\frac{d-1}{2}} \frac{1}{f(\omega, p)} g(\omega, p; z_<) h_R(\omega, p; z_>) \tag{2.53}$$

where $z_<$ ($z_>$) denotes the smaller (bigger) between the z, z'. Taking z, z' to the boundary and extracting the normalizable term one finds that

$$G_R(\omega, p) = 2\nu \frac{K(\omega, p)}{f(\omega, p)} = -\int_{-\infty}^{\infty} \frac{d\omega'}{2\pi} \frac{1 - e^{-\beta\omega'}}{\omega - \omega' + i\epsilon} G_+(\omega', p) \ . \tag{2.54}$$

The first line of 2.54 reproduces the results [84, 48] which were derived using different methods. All expressions 2.50–2.54 can be extended to complex ω and p.

As a consistency check, note that by plugging 2.48 into 2.47 we find that

$$f(-\omega, p) K(\omega, p) - f(\omega, p) K(-\omega, p) = (2\nu)(2i\omega) \tag{2.55}$$

which leads to

$$\frac{K(\omega,p)}{f(\omega,p)} - \frac{K(-\omega,p)}{f(-\omega,p)} = \frac{(2\nu)(2i\omega)}{f(\omega,p)f(-\omega,p)} \ . \tag{2.56}$$

Equation 2.56, together with 2.52 and 2.54, leads to

$$\rho(\omega,p) = -i(G_R(\omega,p) - G_R(-\omega,p))$$

which is equation 2.22 upon using $G_R(-\omega) = G_A(\omega)$.

2.3.3 Analytic properties

In this subsection we discuss analytic properties of the boundary $G_+(\omega,p)$ and $G_R(\omega,p)$ in the complex ω- and p-planes using 2.52 and 2.54.

From 2.46, under complex conjugation

$$\begin{aligned} (g(\omega,p;z))^* = g(\omega^*,p^*;z), \qquad (\tilde{g}(\omega,p;z))^* = \tilde{g}(\omega^*,p^*;z) \\ (h_R(\omega,p;z))^* = h_A(\omega^*,p^*;z) = h_R(-\omega^*,p^*;z) \end{aligned} \tag{2.57}$$

Using 2.47 and 2.48, it then follows that

$$f^*(\omega,p) = f(-\omega^*,p^*), \qquad K^*(\omega,p) = K(-\omega^*,p^*) \ . \tag{2.58}$$

Due to the simple boundary conditions various solutions in 2.46 have simple analytic properties in the complex ω and p^2 planes. By writing the Schrodinger equation 2.34 in an integral form, using the techniques of [72] one can show that:

- 1. At given z, $g(\omega,p;z)$ and $\tilde{g}(\omega,p;z)$ are entire functions of ω and p [72];
- 2. $h_R(\omega,p;z)$ is analytic in the upper half ω plane. $h_A(\omega,p;z)$ is analytic in the lower half ω plane [72];
- 3. For a potential of the form 2.39, the only singularities of $h_R(\omega,p;z)$ in the

lower half ω-plane are simple poles, located at [73]

$$\omega = -i\frac{2\pi n}{\beta}, \qquad n = 1, 2, \cdots . \tag{2.59}$$

From these one can further deduce the following:

- 4. Since g and $\tilde{g}$ are entire functions of ω, p, it follows from 2.49 that $f(\omega, p)$ and $K(\omega, p)$ have the same analytic properties as $h_R(\omega, p; z)$, i.e. they are analytic in the upper half ω-plane and only have simple poles in the lower half ω-plane located at 2.59.

- 5. $f(\omega, p)$ can only have zeros in the upper half ω-plane along the imaginary ω-axis, which correspond to the bound states of 2.34. Suppose $f(\omega, p)$ has a zero at $\omega = \omega_0$ with $\mathrm{Im}\omega_0 > 0$ and $\mathrm{Re}\omega \neq 0$. It then follows from equation 2.47 that $g(\omega_0, p; z)$ is a normalizable solution of the Schrodinger equation 2.34 with a complex eigenvalue. This cannot be the case for a Hermitian Hamiltonian. As we remarked below 2.35, for real p, the potential 2.35 is positive definite for $z \in (0, \infty)$ and thus has no bound state. Thus $f(\omega, p)$ does have not any zeros in the upper half ω-plane for real spatial momentum. For pure imaginary p, it is possible for 2.35 to have bound states and $f(\omega, p)$ can indeed have zeros along the upper imaginary axis.

The above discussions and equations 2.52, 2.54 lead to the following analytic properties for the boundary correlation functions $G_+(\omega, p)$ and $G_R(\omega, p)$:

- 7. Since the poles of $f(\omega, p)$ at 2.59 cancel with the zeros of $e^{\beta\omega} - 1$ in 2.52, $G_+(\omega, p)$ is analytic at $\omega = \frac{2\pi i n}{\beta}$, $n \in \mathbf{Z}$.

- 8. The only singularities of $G_+(\omega, p)$ in the complex ω-plane are poles, arising from the zeros of $f(\omega, p)$ in the complex ω-plane[7]. Due to 2.58, the locations of

[7]From equation 2.50, the same zeros of f gives rise to the poles in the S-matrix of the Schrodinger problem 2.34. Recall that zeros of f on the upper imaginary axis correspond to bound states, those on the lower imaginary axis correspond to virtual states and those near the positive real axis correspond to resonances of the Schrodinger problem.

poles of G_+ obey a reflection symmetry: if there is a pole at ω_0, then there are poles at $-\omega_0, \omega_0^*, -\omega_0^*$. In other words, the poles are symmetric with respect to the real and imaginary ω-axes.

- 9. For G_R, from 2.54, the poles of $K(\omega, p)$ at 2.59 cancel with those of $f(\omega, p)$ at the same locations. Thus the only singularities of $G_R(\omega, p)$ in the ω-plane are poles, due to zeros of $f(\omega, p)$. For real p, $f(\omega, p)$ only has zeros in the lower half plane and thus G_R is analytic on the upper half plane. For pure imaginary p it then becomes possible for $G_R(\omega, p)$ to have poles on the upper half plane along the imaginary ω-axis.

Chapter 3

Two Point Correlators in the Black Hole Background

3.1 Approximate expressions for Lorentzian correlation functions for small l

The Schrodinger equation 2.34 cannot be solved exactly for $d > 3$. We review the results for $d = 2$ (i.e. a BTZ black hole) in Appendix A2. For $d = 4$ 2.34 is of Heun type. In this and the following sections we develop various approximation schemes to solve 2.34 and to find approximate expressions for $G_+(\omega)$ and $G_R(\omega)$. The first method applies to $d = 4$ with the angular momentum $l = 0$ (or linear momentum $p = 0$ in the case of $\mathbb{R}^3$). We are able to obtain closed expressions which are valid for generic values of ω and ν (not too small). Since this method gives rather explicit answers we present it first. The second method applies to $l = 0$ and $|\omega| \to \infty$ limit, but for any $d \geq 3$. The last method, which we discuss in detail in the next section, applies to the large operator dimension limit $\nu \to \infty$, with any l.

3.1.1 An approximation for $d = 4$

In this subsection we develop a uniform approximation (in r) to the solution of 2.34 with $d = 4$, i.e. for a Schwarzschild black hole in AdS_5. The approximation solution

is then used to compute various Lorentzian two-point functions in momentum space for strongly coupled $\mathcal{N} = 4$ SYM. A similar approximation has been also used by Siopsis [83] in deriving the quasinormal modes for the black hole. Our discussion below applies to both 2.35 and 2.36 with $d = 4$ and we will use a notation appropriate to 2.36.

Under the following transformations

$$\begin{aligned} r^2 &= r_0^2 \cosh^2\rho + r_1^2 \sinh^2\rho \\ \psi &= \sqrt{\frac{r(\rho)}{\sinh 2\rho}}\, u(\rho) \end{aligned} \tag{3.1}$$

equation 2.34 becomes

$$\begin{aligned} u'' + \Bigg[&\frac{h^2+1}{4\sinh^2\rho} + \frac{\tilde{h}^2-1}{4\cosh^2\rho} - \nu^2 + \\ &- \frac{(l+1)^2}{r_0^2\cosh^2\rho + r_1^2\sinh^2\rho} - \frac{r_1^2 r_0^2}{(r_0^2\cosh^2\rho + r_1^2\sinh^2\rho)^2} \Bigg] u(\rho) = 0 \end{aligned} \tag{3.2}$$

where

$$h = \frac{\omega\beta}{\pi}, \qquad \tilde{h} = \frac{\omega\tilde{\beta}}{\pi} \tag{3.3}$$

and $\beta, \tilde{\beta}$ were given in 2.3 and 2.14.

Note that $\rho \geq 0$ covers the region outside the horizon with the horizon at $\rho = 0$ and the boundary at $\rho = +\infty$. There is no known exact solution to 3.2. Instead we will find an approximation to it when l is small. At the lowest order of the approximation, we will drop the last two terms in the bracket. This follows from the observation that neither of these two terms dominates at the horizon $\rho = 0$ or at the boundary $\rho = \infty$. So dropping them will not affect the imposition of the boundary conditions there. Furthermore, if

$$h^2, \tilde{h}^2, \nu^2 \gg \frac{1}{r_0^2}, \frac{r_1^2}{r_0^2}, \frac{l^2}{r_0^2} \tag{3.4}$$

then the two discarded terms are always small compared to other terms anywhere outside the horizon. The first quantity on the right hand side of 3.4 is very small for a large black hole $r_0 \gg 1$. The second quantity is of order $O(1)$. The third quantity is also small for l not too large. We will solve 3.2 in this lowest order approximation and obtain the corresponding Lorentzian correlators. Higher order corrections to 3.2 can be developed systematically, but become rather complicated even to the next order. We will not pursue it further (see [70] for a discussion).

Without the last two terms in 3.2, the equation reduces to an equation of hypergeometric type, whose solutions can now be found in closed form. We present them in Appendix A3, along with explicit expressions for the functions f and K introduced in 2.47 and 2.48. From the results there we find that

$$\begin{aligned} G_R(\omega) &= 2\nu \left(\frac{2\pi}{|\mathcal{B}|}\right)^{2\nu} \frac{\Gamma(-\nu)}{\Gamma(\nu)} \frac{\Gamma(\frac{1+\nu}{2}-\frac{\omega\mathcal{B}}{4\pi})\Gamma(\frac{1+\nu}{2}+\frac{\omega\bar{\mathcal{B}}}{4\pi})}{\Gamma(\frac{1-\nu}{2}-\frac{\omega\mathcal{B}}{4\pi})\Gamma(\frac{1-\nu}{2}+\frac{\omega\bar{\mathcal{B}}}{4\pi})} \\ G_+ &= \frac{e^{\frac{1}{2}\beta\omega}}{\pi(\Gamma(\nu))^2} \left(\frac{2\pi}{|\mathcal{B}|}\right)^{2\nu} \Gamma\left(\frac{1+\nu}{2}-\frac{\omega\mathcal{B}}{4\pi}\right) \cdot \\ &\cdot \quad \Gamma\left(\frac{1+\nu}{2}-\frac{\omega\bar{\mathcal{B}}}{4\pi}\right) \Gamma\left(\frac{1+\nu}{2}+\frac{\omega\mathcal{B}}{4\pi}\right) \Gamma\left(\frac{1+\nu}{2}+\frac{\omega\bar{\mathcal{B}}}{4\pi}\right) \end{aligned} \tag{3.5}$$

where $\mathcal{B}$ was introduced in 2.14. Other Lorentzian and Euclidean correlators can be obtained using various formulae in section 2.3, e.g. 2.21 and 2.23. When ν is an integer, 3.5 should be modified and explicit expressions are given in Appendix A3.

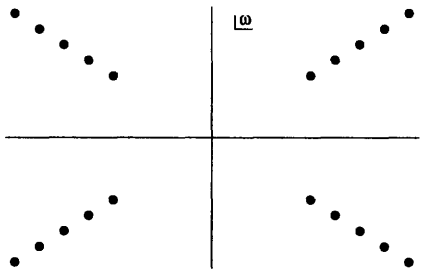

Figure 3-1: Poles for $G_+(\omega, p = 0)$ for $d = 4$ in the complex ω-plane. We use $r_0 = 1, r_1 = \sqrt{2}$.

We now summarize some salient features of 3.5–??:

- 1. From 3.5 $G_R(\omega)$ has poles in the lower ω complex plane located at

$$\omega_n = \frac{4\pi}{\mathcal{B}}\left(\frac{1+\nu}{2}+n\right), \quad \tilde{\omega}_n = -\omega_n^* = -\frac{4\pi}{\overline{\mathcal{B}}}\left(\frac{1+\nu}{2}+n\right), \quad n = 0, 1, \cdots \quad (3.6)$$

$G_+(\omega)$ also has poles in the upper half plane which are reflections of 3.6 with respect the real ω-axis (see 3-1). Note that when $\nu \gg 1$, all the values in 3.6 satisfy equation 3.4 and thus can be trusted. One notices the following features of each pole line: (i) the distance of first pole from the origin is proportional to ν for $\nu \gg 1$; (ii) the spacing between poles in each line is $\frac{4\pi}{\mathcal{B}}$ (or its complex conjugate), which is independent of ν. Recall that $\mathcal{B}$ is related to the complex Schwarzschild time that it takes for a radial null geodesics to go from the spatial boundary to the black hole singularity (see sec. 2.1). As we will see later, this feature persists for black holes in other dimensions as well for l not too big. We can also compute the residue at the poles for $G_R(\omega)$. We find that for large n, the residues for two sequences are

$$a_n \sim -\frac{8\pi}{\Gamma(\nu)^2\mathcal{B}}\left(\frac{\omega_n}{2}\right)^{2\nu}, \qquad -a_n^* \sim \frac{8\pi}{\Gamma(\nu)^2\overline{\mathcal{B}}}\left(-\frac{\tilde{\omega}_n}{2}\right)^{2\nu}$$

respectively.

- 2. When Fourier transformed back to coordinate space, the poles imply that the coordinate space correlation function decays exponentially with time with a parameter controlled by the imaginary part of the poles. Performing the Fourier transform $G_R(t) = \int \frac{d\omega}{2\pi} e^{-i\omega t} G_R(\omega)$ we get 0 for $t < 0$ as expected. For $t > 0$ closing the integration contour in the lower half plane we get:

$$G_R(t) = -i\sum_n (a_n e^{-i\omega_n t} - a_n^* e^{i\omega_n^* t}) = -i\sum_n e^{Im(\omega_n)t}\left(a_n e^{-iRe(\omega_n)t} - a_n^* e^{iRe(\omega_n)t}\right) \quad (3.7)$$

- 3. As $\omega \to +\infty$, we find that $G_+(\omega)$ is power-like [1]

$$G_+(\omega) = \frac{4\pi}{(\Gamma(\nu))^2}\left(\frac{\omega}{2}\right)^{2\nu}\left(1 - e^{-i\pi\nu + \frac{i\omega\mathcal{B}}{2}} - e^{i\pi\nu - \frac{i\omega\overline{\mathcal{B}}}{2}} + \cdots\right) \times \left(1 - \frac{(4\pi)^2}{12}\nu(\nu^2-1)\frac{\mathrm{Re}\mathcal{B}^2}{|\mathcal{B}|^4}\frac{1}{\omega^2} + \cdots\right) . \quad (3.9)$$

The behavior at $\omega \to -\infty$ can be obtained using that $G_{12}(\omega) = G_+(\omega)e^{-\frac{1}{2}\beta\omega}$ is an even function 2.24. Note that in the above expression there are both $1/\omega$ corrections and exponentially small tails of the form

$$e^{-\frac{1}{2}(n\omega\beta - im\omega\tilde{\beta})}, \qquad n \in \mathbf{Z}_+, \quad m \in \mathbf{Z} . \quad (3.10)$$

One can also find the asymptotic behavior of $G_+(\omega)$ in other quadrants of the asymptotic ω plane. For example as $\omega \to -i\infty$, we find it also decays exponentially

$$G_+(\omega) = \frac{4\pi}{(\Gamma(\nu))^2}\left(\frac{i\omega}{2}\right)^{2\nu} e^{-\frac{i}{2}\mathcal{B}\omega}\left(1 - e^{-i\pi\nu - \frac{i}{2}\omega\mathcal{B}} - e^{i\pi\nu - \frac{i}{2}\omega\overline{\mathcal{B}}} + \cdots\right) \times \left(1 - \frac{(4\pi)^2}{12}\nu(\nu^2-1)\frac{\mathrm{Re}\mathcal{B}^2}{|\mathcal{B}|^4}\frac{1}{\omega^2} + \cdots\right) . \quad (3.11)$$

Note that given 3.11 and 3.9 the asymptotic behaviour of $G_{12}(\omega) = G_+(\omega)e^{-\frac{1}{2}\beta\omega}$ along the real and imaginary ω axis is quite similar but for the exponential decay controlled by $\tilde{\beta}$ instead of β. Similar expressions can be worked out for G_R. As $\omega \to +\infty$ we get the following expansion:

$$G_R(\omega) = 2\nu\frac{\Gamma(-\nu)}{\Gamma(\nu)}e^{-i\nu\pi}\left(\frac{\omega}{2}\right)^{2\nu}\left[1 + 2i\sin(\pi\nu)e^{\frac{i}{2}\mathcal{B}\omega} + \cdots\right]\left(1 + O\left(\frac{1}{\omega}\right)\right) \quad (3.12)$$

[1] Here we used the following asymptotic expansions for $\Gamma(x)$ [21]:

$$\Gamma(x) \sim \sqrt{2\pi}x^{x-\frac{1}{2}}e^{-x}\left(1 + \frac{1}{12x} + O(x^{-2})\right) \quad x = |x|e^{i\theta} \quad |\theta| < \frac{\pi}{2} \quad (3.8)$$

$$\Gamma(-x) \sim \pm i\sqrt{2\pi}x^{-x-\frac{1}{2}}e^{x}\left(\sum_{n=0}^{\infty} e^{\pm 2\pi i(n+\frac{1}{2})x}\right)\left(1 - \frac{1}{12x} + O(x^{-2})\right) \quad x = |x|e^{\pm i\theta} \quad 0 < \theta < \frac{\pi}{2}$$

Along the imaginary axis for $\omega \to -i\infty$ we find

$$G_R(\omega) = 2\nu \frac{\Gamma(-\nu)}{\Gamma(\nu)} \left(\frac{i\omega}{2}\right)^{2\nu} \cdot \cdot \left[1 - 4i\sin(\pi\nu)\sinh\left(\frac{\beta\omega}{2}\right) e^{-\frac{i}{2}\omega\tilde{\beta}} + ..\right] \left(1 + O\left(\frac{1}{\omega}\right)\right) \tag{3.13}$$

while for $\omega \to +i\infty$:

$$G_R(\omega) = 2\nu \frac{\Gamma(-\nu)}{\Gamma(\nu)} \left(\frac{-i\omega}{2}\right)^{2\nu} \left(1 + O\left(\frac{1}{\omega}\right)\right) . \tag{3.14}$$

Note that in contrast to 3.9–3.13, there are no subdominant contributions in 3.14, only power corrections. This is because $G_R(\omega)$ does not have poles on the upper complex ω plane. From equation 2.23, also the Euclidean correlator $G_E(\omega)$ has only power corrections.

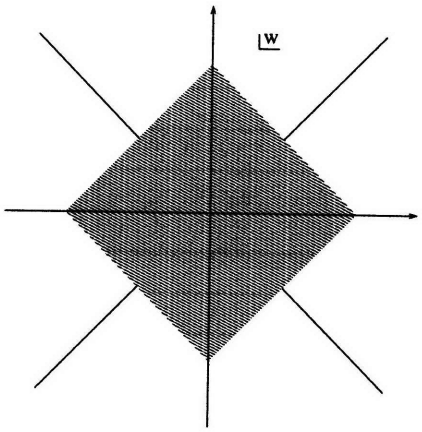

Figure 3-2: This picture shows the area in the complex ω plane where there are *no* subdominant contributions to $G_+(\omega)$ in the limit $\omega = \nu u$ and $\nu \to \infty$. The straight lines are lines of poles.

- 4. Now let us consider the following limit

$$\omega = \nu u, \qquad \nu \gg 1 , \tag{3.15}$$

and expand $G_+(\omega)$ in $1/\nu$. We find that

$$G_+(\omega) = 2\nu\, e^{\nu Z(u)} \left(1 + O(e^{-\nu X(u)})\right) \left(1 + \frac{1}{\nu} K_1 + \cdots\right) \tag{3.16}$$

The $1/\nu$ corrections follow from the standard Stirling formula. The exponentially subdominant terms exist only in certain regions of the complex plane as indicated in 3-2. The leading term $Z(u)$ has the form

$$Z(u) = -L(u) + iu\, t(u) \tag{3.17}$$

with

$$\begin{aligned} L(u) &= -\frac{1}{2}\log(A_+\tilde{A}_+ A_-\tilde{A}_-) \\ t(u) &= \frac{\beta}{4\pi}\log\left(\frac{A_+\tilde{A}_-}{A_-\tilde{A}_+}\right) - i\frac{\beta}{4\pi}\log\left(\frac{A_+\tilde{A}_+}{A_-\tilde{A}_-}\right) - \frac{i}{2}\beta \end{aligned} \tag{3.18}$$

and

$$A_\pm = \frac{\sqrt{2}\pi}{|\mathcal{B}|} \pm \frac{u}{\sqrt{2}} e^{i\theta_{\mathcal{B}}}, \qquad \tilde{A}_\pm = \frac{\sqrt{2}\pi}{|\mathcal{B}|} \pm \frac{u}{\sqrt{2}} e^{-i\theta_{\mathcal{B}}}\ . \tag{3.19}$$

We will see in the following sections that the quantities $Z(u), L(u)$ and $t(u)$ can be identified with geometric quantities associated with a bulk geodesic. One can also check that the following equation holds

$$\frac{dZ(u)}{du} = it(u) \tag{3.20}$$

i.e. $Z(u)$ and $L(u(t))$ are related by a Legendre transform. Note that in the limit 3.15 the lines of poles in 3-1 become branch cuts for the logarithms in 3.18, since the pole spacing is independent of ν and goes to zero when we scale ω with ν. This implies that in 3.18 the branch cuts of the logarithms cannot be chosen arbitrarily and should be straight lines extending radially from $\pm\frac{2\pi}{\mathcal{B}}$ and $\pm\frac{2\pi}{\bar{\mathcal{B}}}$ to ∞. This point will be important for our discussion.

- 5. Equation 3.16 implies that in the large ν limit, the shape of $G_{12}(\omega) = G_+(\omega)e^{-\frac{1}{2}\beta\omega}$ as a function ω does not change once we scale ω with ν. In particular $G_{12}(\omega)$ can be written as a superposition of Gaussians concentrated around the maxima of $Z(u)$. We are thus led to examine the maxima of $Z(u)$. One can check that for $\beta = \tilde{\beta}$, $Z(u)$ has a unique maximum at $u = 0$ with $Z(u) \sim -cu^4$ with c a positive constant. When $\tilde{\beta} > \beta$, the maximum splits into a minimum at $u = 0$ and two maxima. Recalling 2.14 for $r_0 \to \infty$ both β and $\tilde{\beta}$ go to 0 with $\frac{\tilde{\beta}}{\beta} = 1 - \frac{1}{2}r_0^{-2}$. In this limit the maxima are at $u = \pm\sqrt{3}$. In the opposite limit $r_0 \to 0$ the quantity $\tilde{\beta}$ approaches a constant while $\beta \to 0$ and the maxima are widely separated at $u = \pm\frac{2}{\pi r_0}$.

3.1.2 An alternative approximation

The above approximation is valid for $d = 4$ and to leading order $l = 0$. For ω large, one can also use the method developed in [25, 71] to find approximate expressions for G_R and G_+. We leave the details to appendix A4. The basic idea is to identify different regions in z for which 2.34 can be approximated by Bessel equations. For ω large enough the regions of validity of these approximations overlap and it is then possible to find a solution to 2.34 by matching solutions of Bessel equations in the overlap regions. This method works for large ω satisfying

$$|\omega|^{\frac{d-2}{d-1}} \gg l^2, \qquad |\omega|^{\frac{d}{d-1}} \gg \nu^2 \,. \tag{3.21}$$

In Appendix A4, one finds that for $d \geq 2$ the poles for $G_R(\omega)$ are located at

$$\begin{aligned} \omega_n &= \frac{4\pi}{\mathcal{B}}\left(\frac{1+\nu}{2} + n + \frac{i}{2}\log(2)\right), \\ \tilde{\omega}_n &= -\omega_n^* = -\frac{4\pi}{\mathcal{B}}\left(\frac{1+\nu}{2} + n - \frac{i}{2}\log(2)\right) \qquad n = 0, 1, \cdots . \end{aligned} \tag{3.22}$$

The locations of the poles 3.22 coincide for $d = 4$ with 3.6 except for a constant shift. Various expressions of $G_R(\omega)$ and $G_+(\omega)$ for large ω are also derived in appendix A4 D and for $d = 4$ have the same form as 3.9 – 3.14 with some difference in the

numerical coefficients in front of the subdominant terms that can be traced back to the constant shift in the position of the poles. For example, the asymptotic behavior for $G_R(\omega)$ and $G_+(\omega)$ as $\omega \to -i\infty$ are given by

$$\begin{aligned} G_R(\omega) &= 2\nu \frac{\Gamma(-\nu)}{\Gamma(\nu)} \left(\frac{i\omega}{2}\right)^{2\nu} \left(1 - 2i\sin(\pi\nu)\sinh\left(\frac{\beta\omega}{2}\right) e^{-i\frac{\omega\tilde{\beta}}{2}} + ...\right)\left(1 + O\left(\frac{1}{\omega}\right)\right) \\ G_+ &= -2\nu \frac{\Gamma(-\nu)}{\Gamma(\nu)} \left(\frac{i\omega}{2}\right)^{2\nu} \sin(\pi\nu) e^{-\frac{i}{2}\omega\mathcal{B}} \ . \end{aligned} \tag{3.23}$$

The asymptotic behavior in other regions of the complex plane can be found in Appendix A4.

3.2 A "semi-classical" approximation and relation with bulk geodesics

In the previous sections we used various techniques to get an idea of the analytic properties of various correlation functions. However, since the boundary correlation functions 2.52 and 2.54 are related to the bulk geometry in a very nonlocal way, even if one can solve the bulk Laplace equation exactly, it is very hard to extract from the resulting boundary correlation functions information about the bulk geometry, which is equivalent to solving a quantum inverse scattering problem.

In this section, we will develop another approximate method which will allow us to make a more direct connection between the boundary correlation functions and the bulk geometry. This will enable us to understand how the bulk geometry is encoded in the boundary correlators, in particular the manifestations of the regions beyond the horizon and the black hole singularities. This method also has the advantage of being applicable for arbitrary angular momentum.

Below we will use the notation appropriate for the flat case 2.35. The discussion applies without change to the sphere case 2.36 when $l < l_c$. There are some new complications for $l > l_c$ (see 2-3) which we will discuss in section 3.3.2 and Appendix A5. Also we will focus on $G_+(\omega, p)$ which captures all the important aspects of the

story. The discussions can be generalized to other real-time correlation functions without much difficulty[2].

3.2.1 A "semi-classical" approximation

Consider the following large ν limit with u and $\vec{k}$ fixed

$$\omega = \nu u, \qquad \vec{p} = \nu \vec{k}, \qquad \nu \gg 1 \ , \tag{3.24}$$

i.e. we take the mass m of ϕ to be large and "measure" the frequency ω and momentum $\vec{p}$ in units of m. In this limit, one can solve 2.34 approximately using the standard WKB method with $1/\nu$ playing the role of $\hbar$. More explicitly, writing $\psi = e^{\nu S}$ equation 2.34 becomes

$$-(\partial_z S)^2 - \frac{1}{\nu}\partial_z^2 S + V(z) + \frac{1}{\nu^2}Q(z) = u^2 \tag{3.25}$$

with

$$V(z) = f\left(1 + \frac{k^2}{r^2}\right) \tag{3.26}$$

and

$$Q(z) = f\left(\frac{(d-1)^2}{4r^d} - \frac{1}{4}\right) \ . \tag{3.27}$$

We first restrict to real $\vec{k}$, for which case the potential 3.26 (see 3-3) is a monotonically decreasing function for $z \in (0, +\infty)$, and consider positive energy scattering sates with $u > 0$. Solving 3.25 order by order in $1/\nu$, we find that, in the classically forbidden region (i.e. for $z < z_c$ in 3-3), the exponentially decreasing solution to 2.34

[2]The story for G_F and G_R is slightly more complicated since they correspond to propagators in the bulk with a source. These complications are not relevant for probing the singularities and the regions behind the horizon.

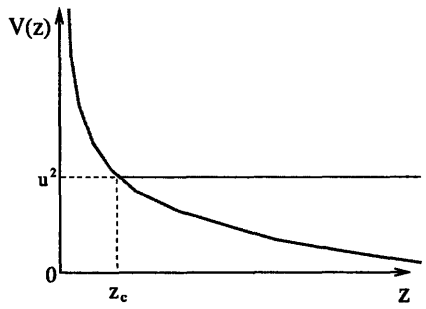

Figure 3-3: Schematic plot of the potential 3.26 for $\vec{k} \in R$. The boundary is at $z = 0$ the horizon at $z = \infty$.

can be written as

$$\psi_{\omega p}^{(wkb)}(z) = \frac{1}{\sqrt{\kappa(z)}} e^{\nu \mathcal{Z}} \left(1 + O\left(\nu^{-1}\right)\right) \tag{3.28}$$

with[3]

$$\begin{aligned} \mathcal{Z}(z) &= \int_{z_c}^{z} dz' \, \kappa(z'), \\ \kappa(z) &= \sqrt{V(r) - u^2} \, . \end{aligned} \tag{3.29}$$

$z_c = z(r_c)$ in the lower integration limit of 3.29 is the turning point with r_c given by the real positive root of equation

$$V(r) = f(r)\left(1 + \frac{k^2}{r^2}\right) = u^2 \, . \tag{3.30}$$

For $k^2, u^2 > 0$, equation 3.30 has a unique positive root $r_c > 1$. $\mathcal{Z}(z)$ satisfies the equation

$$\frac{1}{f}\mathcal{Z}'^2 - \frac{k^2}{r^2} + \frac{1}{f}u^2 = 1 \tag{3.31}$$

with $\mathcal{Z}'(z_c) = 0$. Note that to the order indicated in 3.28, the term in 3.25 proportional to $Q(z)$ does not contribute.

[3]The branch cuts for $\kappa(z)$ on the complex z-plane are chosen so that they do not intersect the integration contour in $\mathcal{Z}$.

The expression for $\psi_{\omega p}^{(wkb)}$ in the classically allowed region of the potential 3.26 (i.e. for $z_c < z < \infty$) follows from the standard connection formula

$$\psi_{\omega p}^{(wkb)} = \frac{2}{\sqrt{p(z)}} \cos\left(\nu W - \frac{\pi}{4}\right)\left(1 + O\left(\nu^{-1}\right)\right) \tag{3.32}$$

with

$$W = \int_{z_c}^{z} dz'\, p(z'), \qquad p(z) = \sqrt{u^2 - f\left(1 + \frac{k^2}{r^2}\right)} \tag{3.33}$$

Near the event horizon 3.32 has the form

$$\psi_{\omega p}^{(wkb)} = \frac{1}{\sqrt{u}} e^{i\omega z + i\delta_\omega}\left(1 + O\left(\nu^{-1}\right)\right) + c.c.$$

which fixes the relative normalization between $\psi_{\omega p}^{(wkb)}$ and $\psi_{\omega p}$ of 2.40 to be

$$\psi_{\omega p}^{(wkb)} = \frac{1}{\sqrt{u}} \psi_{\omega p}, \qquad u > 0, \quad \nu \to \infty \tag{3.34}$$

From 3.34 we find that in the limit 3.24 the boundary Wightman function G_+ is given by (for $u > 0$)

$$G_+(\omega, p) \approx 2\nu\, e^{\nu Z}\left(1 + O(\nu^{-1})\right) + \text{subdominant terms} \tag{3.35}$$

with

$$\begin{aligned} Z(u,k) &= \lim_{z,z' \to 0} (\mathcal{Z}(z) + \mathcal{Z}(z') - \log z' - \log z) \\ &= 2 \lim_{z \to 0} \left(-\log z + \int_{z_c}^{z} dz'\, \kappa(z')\right) . \end{aligned} \tag{3.36}$$

Higher order $1/\nu$ corrections in 3.35 can also be obtained from 3.25 using the standard WKB procedure. In particular, the term proportional to $Q(z)$ will be important at order ν^{-1}.

While equations 3.35–3.36 were obtained for $u > 0$ and real $k^2 > 0$, they can be

analytically continued to general complex values of u and k^2. The analytic continuation is a bit subtle and will be discussed below.

3.2.2 Relation with bulk geodesics

In the limit 3.24, the mass of the bulk particle goes to infinity with its velocity remaining finite. We expect the propagation of such a massive particle should follow geodesics. We now show that Z 3.36 has a simple interpretation in terms of geometric quantities associated with a bulk spacelike geodesic.

Due to translational invariance in the $(t, \vec{x})$ directions, a bulk spacelike geodesic is characterized by the integrals of motion:

$$E = -f\frac{dt}{ds}, \qquad \vec{q} = r^2\frac{d\vec{x}}{ds} \tag{3.37}$$

where s is the proper distance[4]. The geodesic satisfies the equation

$$\frac{1}{f}\left(\frac{dr}{ds}\right)^2 - \frac{1}{f}E^2 + \frac{q^2}{r^2} = 1\ . \tag{3.38}$$

Equation 3.38 is precisely 3.31 with the identification[5]

$$Z' = -\frac{dr}{ds}, \qquad u = iE, \qquad \vec{k} = i\vec{q} \tag{3.39}$$

where the sign for the first expression corresponds to have the geodesic moving away from the boundary. κ_r of 3.29 can be identified as the proper velocity of the geodesic along the r direction. Thus $Z(u,k)$ (equation 3.36) can be associated with a bulk (complex) spacelike geodesic with constants of motion $E = -iu, \vec{q} = -i\vec{k}$. The geodesic starts from $r \to +\infty$, moves inward, turns around at a turning point r_c, and

[4]We treat geodesics which are related by a translation in t and $\vec{x}$ directions as equivalent.

[5]Similarly one finds the equation satisfied by W in 3.33 coincides with that for a timelike geodesic with the identification

$$W' = \frac{dr}{ds}, \qquad u = E, \qquad \vec{k} = \vec{q}\ .$$

comes back to $r \to +\infty$. At the turning point r_c, $\frac{dr}{ds} = 0$ and

$$f(r_c)\left(\frac{q^2}{r_c^2} - 1\right) = E^2 \ . \tag{3.40}$$

which is equivalent to equation 3.30.

$Z(u = iE, k)$ can further be written as

$$Z(u = iE, k) = -Et(E, q) + \vec{q} \cdot \vec{x}(E, q) - L(E, q) \tag{3.41}$$

where $L(E, \vec{q})$ is the (regularized) proper length of the geodesic and $t(E, \vec{q})$, $\vec{x}(E, \vec{q})$ are the displacements in the t and $\vec{x}$ directions between the final and initial points,

$$\begin{aligned} L(E, \vec{q}) &= 2 \lim_{r \to \infty} \left(\int_{r_c}^{r} \frac{dr}{\sqrt{f + E^2 - \frac{f}{r^2} q^2}} - \log r \right) \\ t(E, \vec{q}) &= 2E \int_{r_c}^{\infty} \frac{dr}{f \sqrt{f + E^2 - \frac{f}{r^2} q^2}} \\ \vec{x}(E, \vec{q}) &= 2\vec{q} \int_{r_c}^{\infty} \frac{dr}{r^2 \sqrt{f + E^2 - \frac{f}{r^2} q^2}} \ . \end{aligned} \tag{3.42}$$

Also note that $t(E, q)$ and $x^i(E, q)$ can be obtained from Z by

$$\frac{\partial Z}{\partial E} = -t(E, \vec{q}), \qquad \frac{\partial Z}{\partial q_i} = x^i(E, \vec{q}) \ . \tag{3.43}$$

This shows that L and Z are related by a Legendre transform.

3.2.3 Analytic continuation

For a given real $(E, \vec{q})$, equations 3.37 and 3.38 specify a unique geodesic in the Lorentzian section of the black hole spacetime. Given the relation 3.39 between boundary theory momenta and bulk velocities, we need to consider complex geodesics with general complex $(E, \vec{q})$. It is important to note that $(E, \vec{q})$ does not specify a *complex* geodesic uniquely. Given a choice of root $r_c(E, \vec{q})$ of equation 3.40 and a contour in the complex r-plane from $r = +\infty$ to $r_c(E, \vec{q})$, 3.42 define a complex

spacelike geodesic in the bulk. For the same value of $E, \vec{q}$, a different choice of the root of 3.40 or a different contour which cannot be smoothly deformed into the previous one defines a different complex geodesic. For a general complex (u, k), the bulk geodesic which corresponds to $Z(u, k)$ of the boundary theory can be identified by the analytic continuation of the turning point $r_c(u, k)$ (equation 3.30) from the $k^2 > 0, u > 0$ region.

The analytic continuation of $r_c(u, k)$ from the $k^2 > 0, u > 0$ region is not unique, since for fixed k^2, $r_c(u, k)$ has branch points in the complex u-plane at which it merges with other solutions of 3.30. These are also branch points of $Z(u, k)$. More explicitly, the branch points u_b of $r_c(u, k)$ are given by

$$u_b^2 = V(z_0), \tag{3.44}$$

where $V(z)$ was given by 3.26 and z_0 are critical points of $V(z)$, i.e.

$$V'(z_0) = 0\ . \tag{3.45}$$

Note that not necessarily all solutions of 3.45 correspond to the branch points of r_c. It can happen that some of the solutions correspond to the merger of the other roots of 3.30. Those solutions do not give rise to the branch points of $Z(u, k)$ in the leading order analysis.

For $r_c(u, k)$ and $Z(u, k)$ to be single-valued, branch cuts have to be specified. The locations of the branch cuts can *not* be chosen arbitrarily, since different choices of branch cuts give rise to inequivalent analytic continuations, which will associate different bulk geodesics to $Z(u, k)$. Given that at finite ν the only singularities of G_+ in the complex ω-plane are poles (see discussion after 2.44), the analytic continuation of $Z(u, k)$ must be unique and its branch cuts should coincide[6] with the lines of poles of G_+ at finite ν. In section 3.1.1, in the discussion after equation 3.15 we have seen this explicitly for $d = 4$ and $k = 0$.

[6]This can happen if the spacings of the poles in ω-plane are independent of ν or grow with ν slower than the linear power.

Thus to properly identify which complex geodesic in the bulk is associated with the large ν limit of the boundary Wightman function $G_+(\nu u, \nu k)$ for a given (u, k), we need to determine the lines of poles of $G_+(\nu u, \nu k)$. When $k = 0$, the poles of $G_+(\omega)$ in various dimensions were determined before in [75, 25, 71, 83] and were reviewed in sec. 3.1. The poles for $k \neq 0$ will be determined in the next section and appendix A5. In particular, we obtain a simple formula for the locations of the poles in the large ν limit.

To summarize, the large ν limit 3.24 of the Wightman function $G_+(\nu u, \nu \vec{k})$ is given by the Legendre transform of the proper distance of a (complex) bulk spacelike geodesic with integrals of motion $E = -iu$ and $\vec{q} = -i\vec{k}$. The geodesic connects two boundary points and is specified by a turning point $r_c(u, \vec{k})$ in the bulk. From $G_+(\nu u, \nu \vec{k})$, one can use 3.43, 3.41 to find bulk geometric quantities like $t(E, \vec{q}), \vec{x}(E, \vec{q})$ and $L(E, \vec{q})$ for all (complex) values of $E, \vec{q}$, which can be used to reconstruct the bulk geometry[7]. As we will discuss more explicitly in the next chapter, as one varies $(u, \vec{k})$, the turning point scans over the full complexified bulk geometry and the boundary correlation functions can be used to probe the regions beyond the horizon and near the singularity.

3.3 Quasi-normal modes

In the last section we established an explicit relation between boundary momentum space correlation functions in the large operator dimension limit and bulk geodesics. As discussed there, to properly identify the bulk geodesic associated with $G_+(\nu u, \nu k)$ at a given (u, k), we need to determine the poles of $G_+(\nu u, \nu k)$, which become dense and appear as branch cuts of $Z(u, k)$ in the large ν limit 3.35. In this section we develop new techniques to find poles of $G_+(\nu u, \nu k)$, which in the gravity language, are also called quasi-normal frequencies.

The positions of the poles of $G_+(\nu u, \nu k)$ for general k (including $k = 0$) in the large ν limit can be obtained by generalizing the WKB analysis of the last section to include

[7]This is in some sense a classical inverse scattering problem.

higher order subdominant corrections. Near the positions of the poles, in addition to 3.35, an infinite number of subdominant corrections become equally important. When summing over them, one finds the locations of poles. In other words, the pole lines are anti-stokes lines for an infinite number of subdominant contributions. We present the detailed analysis of this more sophisticated WKB analysis in appendix A5 and give only the final results here.

When ν is large, we find that $G_+(\omega = \nu u, p = \nu k)$ has a line of poles starting at each of the branch points u_b of $r_c(u,k)$. As discussed around equation 3.44, at u_b, two solutions to the turning point equation 3.30 merge together. We denote the two turning points by $z_T = z(r_T)$ and $z_K = z(r_K)$. The locations of the poles are then given by the solutions the following equation

$$2\nu \mathcal{Z}(z_T, z_K) = i\pi(1+2n), \qquad n = 0, 1, \cdots \tag{3.46}$$

where[8]

$$\mathcal{Z}(z_T, z_K) = \int_{z_T}^{z_K} dz'\, \kappa(z') \tag{3.47}$$

and $\kappa(z') = \sqrt{V(z) - u^2}$ was defined in 3.29.

Equation 3.47 can be greatly simplified if u is close to u_b. Let $u = u_b + x$ with $x \sim O(\nu^{-1})$. Near $z_0 = z_T(u_b) = z_K(u_b)$ we can approximate the potential $V(z)$ as

$$V(z) \approx V(z_0) + \frac{1}{2}\partial_z^2 V(z_0)(z - z_0)^2$$

where we have used equation 3.45. We then find that

$$z_{T,K} \approx z_0 \pm a, \qquad a \equiv 2\sqrt{\frac{u_b\, x}{\partial_z^2 V(z_0)}} \tag{3.48}$$

[8]The precise determination of the multi-valued function $\mathcal{Z}(z_T, z_K)$ is given in Appendix A5.

and after integrating 3.47

$$\begin{aligned} \mathcal{Z}(z_T, z_K) &\approx \pm\tfrac{i\pi a^2}{2}\sqrt{\tfrac{\partial_z^2 V(z_0)}{2}} \\ &= \pm\tfrac{i\pi x}{\delta} \end{aligned} \tag{3.49}$$

with

$$\delta \equiv \sqrt{\frac{\partial_z^2 V}{2V}}\Big|_{z_0} . \tag{3.50}$$

Equation 3.46 then leads to the position u_n of the poles

$$u_n = u_b + (n + \frac{1}{2})\frac{\delta}{\nu}, \qquad n = 0, 1, \cdots \tag{3.51}$$

In terms of $\omega = \nu u$, the poles are uniformly spaced near $\omega_b = \nu u_b$

$$\omega_n = \omega_b + (n + \frac{1}{2})\delta, \qquad n = 0, 1, \cdots \tag{3.52}$$

with a spacing given by[9] 3.50 which is independent of ν.

The branch of the square root in 3.50 should be chosen so that δ points away (when there are no bound states) from the real axis at u_b[10]. In the infinite ν limit, the spacing in u goes to zero and the line of poles becomes a branch cut of $Z(u, k)$. In particular the phase of δ gives the direction of the branch cut.

To summarize, for large but finite ν,

- 1. The locations of the first few poles, i.e. with $\omega_n - \omega_b \sim O(\nu^0)$, are given by 3.52.

- 2. For poles which are of order $O(\nu)$ from ω_b in the ω-plane, 3.52 is no longer valid and one needs to use 3.46.

[9]The formula below does not apply to cases with $V(z_0) = 0$ or $\partial_z^2 V = 0$, for which the approximation breaks down.

[10]The determination of the sign in eq 3.50 follows from the analysis of Appendix A5. In the language introduced there for fixed k there are poles in the region of the complex u plane where the turning points Z_T and Z_K considered in 3.46 are both active. If the potential doesn't admit stable or unstable bound states there is only one active turning point in the vicinity of the real u axis.

- 3. At fixed $p = \nu k$ and ν, the locations of poles near $|\omega| \to \infty$ are given by 3.22 except for the log(2) factor which does not appear in this large ν expansion. Because of 3.21 the pole locations 3.22 are invalid in the limit 3.15.

3.3.1 Locations of poles in the large ν limit: infinite mass black hole

Let us now look at the explicit expressions of the branch points 3.44 and spacing 3.50 of the poles near the branch points for various dimensions. In this subsection we look at the cases of an infinite mass black hole 2.5.

Let us first consider $k = 0$, in which case

$$V(z) = f(r(z)) = r^2 - \frac{1}{r^{d-2}}$$

and equation 3.45 becomes

$$2r + \frac{d-2}{r^{d-1}} = 0 \tag{3.53}$$

Among d solutions of 3.53 only

$$r = \left(\frac{d-2}{2}\right)^{\frac{1}{d}} e^{\pm i\frac{\pi}{d}}$$

correspond to the merger of the turning point with the other roots of 3.30, leading to four branch points

$$u_b = \pm c_d e^{\pm i\frac{\pi}{d}}, \qquad c_d = \left(\frac{d-2}{2}\right)^{\frac{1}{d}} \sqrt{\frac{d}{d-2}}\,. \tag{3.54}$$

The spacing of poles can also be easily computed from 3.50

$$\delta = \pm\sqrt{d} c_d e^{\pm i\frac{\pi}{d}} \tag{3.55}$$

where each sign of 3.55 should be paired with that 3.54. Except for $d = 4$ (i.e. AdS_5),

3.55 is different from the spacings 3.22 at large ω, which are (using 2.11)

$$\tilde{\delta} = \pm d \sin\frac{\pi}{d} e^{\pm i\frac{\pi}{d}} \tag{3.56}$$

although they do point to the same directions. 3.55 and 3.56 do agree for $d = 4$.

The explicit expressions for the branch points and pole spacings for $k^2 \neq 0$ are rather complicated since they involve roots of a cubic equation. We will only point out some important features. For definiteness, we will restrict to k^2 real, i.e. k is real or pure imaginary. These are also the regions of main physical interests.

For $k^2 > 0$, the structure of poles is similar to that of $k^2 = 0$. There are four lines of poles. In particular, as $k^2 \to +\infty$, the branch points approach the real axis

$$u_b \approx \pm\left(k + \frac{1}{2}\left(\frac{d}{2}\right)^{\frac{2}{d+2}} e^{\pm\frac{2\pi i}{d+2}} k^{-\frac{d-2}{d+2}} + \cdots\right) \tag{3.57}$$

and the pole spacings near the branch points are

$$\delta \approx \pm\sqrt{d+2}\left(\frac{d}{2}\right)^{\frac{2}{d+2}} e^{\pm\frac{2\pi i}{d+2}} k^{-\frac{d-2}{d+2}} + \cdots \tag{3.58}$$

One can check the angle of the pole lines decrease monotonically as k^2 increases. Note that in the $k^2 \to \infty$ limit, the pole lines become the light cone cuts of G_+ at zero temperature.

For $k^2 = -q^2 < 0$, there are two additional lines of poles along the imaginary u axis with branch points located at $u_b = \pm iE_c$. For $q^2 \ll 1$, one finds that

$$E_c \approx \sqrt{\frac{2}{d}}\left(\frac{d}{d-2}\right)^{-\frac{d-2}{4}} q^{-\frac{d-2}{2}} \gg 1 \tag{3.59}$$

and

$$\delta = \pm i\frac{d}{\sqrt{2}}\left(\frac{d-2}{d}\right)^{\frac{d}{2}} q^{-(d-1)} \,. \tag{3.60}$$

E_c decrease monotonically to zero as q^2 increases to 1. For $q^2 \sim 1$ the gap δ between

successive poles becomes $\delta = id + O(q-1)$.

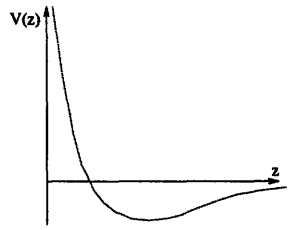

Figure 3-4: The potential 3.26 for $-k^2 = q^2 > 1$ admits bound states. In the z coordinate the boundary is at $z = 0$ and the horizon at $z = \infty$.

For $q^2 > 1$, the two lines of poles along the imaginary u-axis cross the real axis. This is due to the fact that for $q^2 > 1$, the Schrodinger problem 2.34 contains bound states, as is clear from the shape of the potential plotted in 3-4. The poles of the lower branch which lie in the upper half plane are bound state poles.

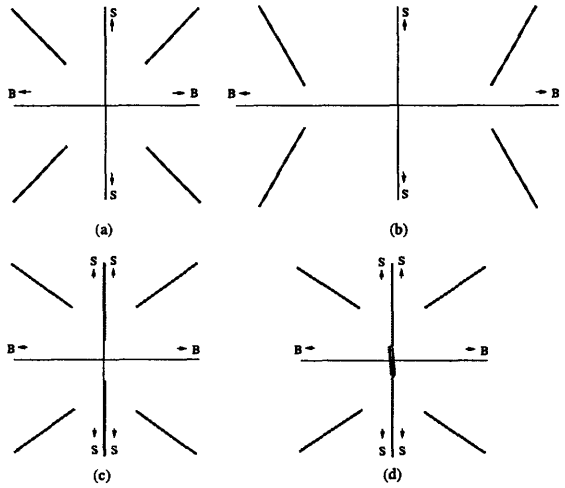

Figure 3-5: The structure of the branch cuts for (a): $k^2 = 0$, (b): $k^2 > 0$, (c): $-1 < k^2 < 0$, (d): $k^2 < -1$. At finite ν, the branch cuts become lines of poles. We also labeled the asymptotic regions by S or B, indicating whether the corresponding turning point approaches the black hole singularity (S) or the AdS boundary (B).

In 3-5, we plot configurations of the branch cuts of $Z(u,k)$ for various values of k^2 from the structure of the pole lines.

3.3.2 Long-lived quasi-particles for strongly coupled SYM theories on S^3

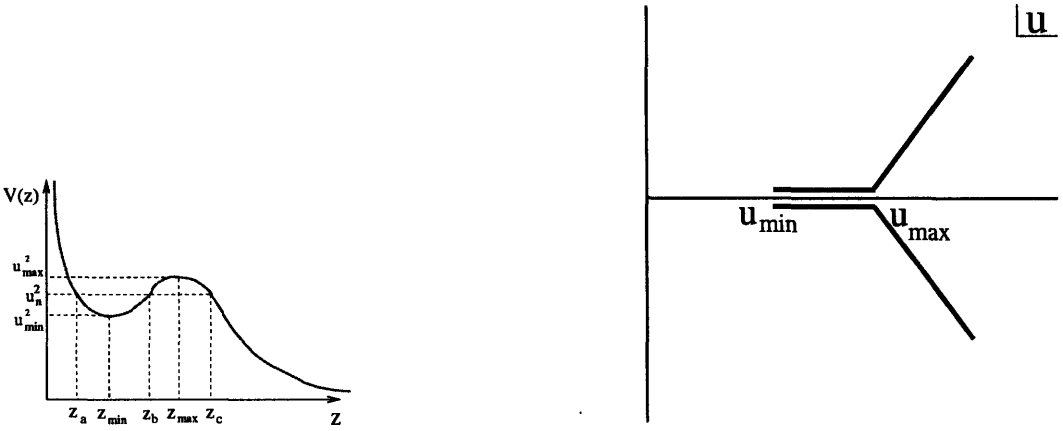

Figure 3-6: The figure at the left is a schematic plot for the potential $V(z)$ for $k > k_c$. The resulting pole lines in $G_+(\nu u, \nu k)$ are shown in the right plot. In the right plot we only show the right half of the complex u-plane. The poles in the left half are obtained by reflection with respect to the imaginary axis.

In this subsection we consider the pole structure of $G_+(\omega, p)$ for a finite mass black hole 2.1 and 2.2.

For small values of $k \in \mathbb{R}$, the potential $V(z)$ 3.26 is a monotonically decreasing function along the real z axis. The pole structure of $G_+(\nu u, \nu k)$ is very similar to that of an infinite mass black hole discussed in the last subsection and is captured by 3-5. For larger k however there exists a critical value k_c such that for $k > k_c$ the potential is no longer monotonic and looks like in 3-6. At $k = k_c$ we have $z_{min} = z_{max}$ and at $z = z_{min} = z_{max}$ both the first and second derivative of $V(z)$ are zero. By using the relation 2.8 between z and r and the explicit expression of $V(z)$ 3.26 k_c is the largest positive root of the coupled equations[11]

$$\begin{aligned} \frac{d^2}{dz^2}V(z) = 0 \quad &\Rightarrow \quad d((2+d)k_c^2 + (d-2)r^2)\mu - 8k_c^2 r^{d-2} = 0, \\ \frac{d}{dz}V(z) = 0 \quad &\Rightarrow \quad 2\,r^{2+d} - 2\,k_c^2\,r^{d-2} + (d-2)\,r^2\,\mu + d\,k_c^2\,\mu = 0\,. \end{aligned} \tag{3.61}$$

[11]For $d = 4$ eliminating r gives an equation $(k_c^2 - \mu)^3 - 27\mu^2 k_c^4 = 0$.

For $k > k_c$ the position $z_{min} = z(r_{min})$ of the local minimum and $z_{max} = z(r_{max})$ of the local maximum of the potential are given by the real and positive roots of the equation:

$$\frac{d}{dz}V(z) = 0 \quad \Rightarrow \; 2\,r^{2+d} - 2\,k^2\,r^{d-2} + (d-2)\,r^2\,\mu + d\,k^2\,\mu = 0\,. \tag{3.62}$$

For large $k \gg k_c$ the solutions of 3.62 are approximatively given by the solutions of: $r^4 = k^2$ and $2r^{d-2} = d\mu$. We see that there are 2 real positive solutions. The one corresponding to z_{min} is $r_{min} \sim \sqrt{k}$.

The form of the potential 3-6 for $k > k_c$ implies that it is classically possible for a particle with sufficient angular momentum to be in a bounded orbit outside the horizon of the black hole as the centrifugal potential provides a barrier to its falling in the horizon. Quantum mechanically however there will be a nonzero probability for the particle to tunnel through the centrifugal potential barrier and be absorbed by the black hole.

The situation just described (3-6) implies that the Schrodinger equation 2.34 in the large ν limit has resonances whose energies are given by $\omega_n = \nu u_n$ with u_n determined by

$$2\nu \int_{z_a}^{z_b} dz \sqrt{u_n^2 - V(z)} = 2\pi(n + \frac{1}{2}), \qquad n = 0, 1, \cdots \tag{3.63}$$

where $u_{min}^2 = V(z_{min}) < u_n^2 < V(z_{max}) = u_{max}^2$ and z_a, z_b are real solutions to $V(z) = u_n^2$ (see 3-6). The maximum energy for these quasi-stable states is u_{max}. These quasi-stable states can tunnel through the potential barrier between z_b and z_c (see 3-6) to fall into the horizon, with a decay rate given by

$$e^{-\Gamma_n} = \exp\left(-2\nu \int_{z_b}^{z_c} dz \sqrt{V(z) - u_n^2}\right)\,. \tag{3.64}$$

For small n and large ν the first few energy levels will be close to $V(z_{min})$ and it is therefore possible to approximate the potential with its quadratic part. One can

then get the following approximate formula for u_n

$$u_n = u_{min} + \frac{1}{\nu}\sqrt{\frac{\partial_z^2 V(z_{min})}{2V(z_{min})}}(\frac{1}{2}+n), \qquad n = 0, 1, \cdots, \qquad u_{min}^2 = V(z_{min})\ . \tag{3.65}$$

For example for the large k limit discussed below equation 3.62, we find that $\partial_z^2 V(z_{min}) = (f(r_{min}))^2 \partial_r^2 V(r_{min}) \sim 8k^2$ and then using 3.65:

$$u_{min} \sim k, \qquad u_{n+1} - u_n \sim \frac{2}{\nu} \tag{3.66}$$

The quasi-stable states described above generate poles in $G_+(\omega, l)$ which are very close but not exactly on the real axis. The distance of the poles from the real axis is inversely proportional to the decay rate of the corresponding quasi-stable states. More precisely the poles in $G_+(\omega, l)$ are located at

$$\omega_n = \nu u_n \pm \frac{i}{\pi} e^{-\Gamma_n}\ . \tag{3.67}$$

From the boundary theory point of view, these poles in $G_+(\omega, l)$ can be interpreted as excitations generated by an operator $\mathcal{O}$ over the thermal equilibrium which thermalize very slowly with a rate proportional to $e^{-\Gamma_n}$. These excitations have a natural interpretation of very long lived quasi-particle states in the boundary theory on S^{d-1}. In particular, for $d = 4$ this implies the existence of very long lived quasi-particles for $\mathcal{N} = 4$ SYM on S^3. The existence of these long-lived excitations should have to do with the fact that states with large angular momenta on S^{d-1} are highly degenerate, since the dimensions of the representations of $SO(d)$ grow like a power with angular momenta. In general we expect excitations associated with states with large of degeneracy should thermalize more slowly. The sharp appearance of these quasi-stable states when $k > k_c$ should be a consequence of the large N and large λ limit that we are working with.

As $\nu \to \infty$ the poles of $G_+(\omega, k)$ form branch cuts in the $u = \frac{\omega}{\nu}$ variable extending on the real axis from u_{min} to u_{max}. At u_{max} the branch cuts start deviating from the real axis as depicted in 3-6, this is due to that for large $|u| \gg u_{max}$ the position of

the branch cuts is qualitatively the same as the one for a monotonic potential.

To conclude this section, let us consider what happens to these long lived quasi-particles in the infinite black hole limit 2.4, which describes the boundary theory on $\mathbb{R}^{d-1}$. In momentum space, the limit 2.4 can be described as

$$\frac{\omega}{T} = \text{finite}, \qquad \frac{l}{T} = \text{finite}, \qquad T \to \infty \,. \tag{3.68}$$

From this equation it can be readily checked from equations 3.61 that as $T \to \infty$ (i.e. $\mu \to \infty$), k_c scales[12] with T as $T^{\frac{2d}{d-2}}$. It then follows that the frequencies (see 3.66) and angular momenta of the quasi-particles scale with T at least as fast as $T^{\frac{2d}{d-2}} > T$, which is much faster than 3.68. Thus we conclude that these quasi-particles are not present in the spectrum of the theory on $\mathbb{R}^{d-1}$. Indeed, as we discussed earlier the potential $V(z)$ for 2.6 is always monotonic and k_c does not exist.

[12]The scaling of k_c can be qualitatively understood by imposing that the approximate expressions for r_{min} and r_{max} valid at large k coincide that is $2k_c^{\frac{d-2}{2}} = d\mu$ and by recalling that as $\mu \to \infty$ the temperature scales as $T \sim \mu^{\frac{1}{d}}$.

Chapter 4

Excursions Beyond the Horizon

4.1 Decoding the bulk geometry

In chapter 3 we used three different approximation methods to solve the Laplace equation for a scalar field propagating in an AdS black hole geometry and to obtain real-time thermal boundary correlation functions. Since that chapter is somewhat technical, we briefly summarize here the main results obtained.

The method discussed in sec. 3.1.1 applies to $d = 4$ with $l = 0$ and ω not too small. The explicit expressions for $G_R(\omega)$ and $G_+(\omega)$ were presented in 3.5 and the poles of $G_R(\omega)$ in the complex ω-plane were given in 3.6. The large $|\omega|$ limits of 3.5 along various directions in the complex ω-plane were given in 3.9–3.14 and the large operator dimension limit (i.e. large ν) was given in 3.16.

The method discussed in sec. 3.1.2 and in detail in Appendix A4 applies to large ω, $l = 0$ and all dimensions. For $d = 4$, the results of sec. 3.1.1 were reproduced in the overlapping region of validity. In particular, it was found that all the essential features of the $d = 4$ results, including the locations of the poles and the asymptotic behavior of correlation functions, generalize to other dimensions.

The WKB method developed in sec. 3.2 concerns the large operator dimension limit ($\nu \to \infty$). The leading order expression for $G_+(\nu u, \nu k)$ was given by 3.35-3.36. Equation 3.36 can in principle be integrated for any u, k and general dimension d. But the integrations are rather complicated except for $d = 4, k = 0$ and $d = 2$. The

explicit expressions for various cases are presented in Appendix A6. For $d = 4, k = 0$, the result agrees with 3.17-3.18 obtained in sec. 3.1.1. For $d = 2$, the result agrees with that of Appendix A2 where the Laplace equation was solved exactly.

As discussed in the introduction, our main motivation is to understand how the bulk geometry is encoded in the boundary theory, in particular the manifestations of the regions behind the horizon and the presence of black hole singularities. The WKB method of sec. 3.2 provides important tools for answering these questions. There we found that for a given (u, k), $G_+(\nu u, \nu k)$ is given by the Legendre transform of the geodesic length of a complex spacelike geodesic in the bulk, whose constants of motion (E, q) along $t, \vec{x}$ are related to (u, k) by equation 3.39. The key question is then what are the regions of the black hole spacetime that the corresponding geodesics probe as we scan different values of (u, k). To answer this question, we can look at how the turning point $r_c(u, k)$ of a geodesic varies with (u, k). The discussion of sec. 3.2.1 indicates that (e.g. from 3-3) $r_c(u, k)$ always lies outside the horizon for any real u and k. Thus to see whether regions inside the horizon can be probed we should consider complex values of u and k. As explained in sec. 3.2.3, the analytic continuation of $r_c(u, k)$ to complex values of u and k is subtle, since $r_c(u, k)$ contains branch points and branch cuts have to be specified to make the analytic continuation unique. As discussed there the locations of the branch cuts for $r_c(u, k)$ should coincide with the locations of lines of poles of $G_+(\omega, p)$ at finite ν. We developed new techniques to determine such quasi-normal poles in sec. 3.3 and Appendix A5. The results are summarized in 3-5. We will now use 3-5 to discuss the analytic continuation of $r_c(u, k)$. We will show below that the analytic continuation to complex values of ω, k allows it to probe regions inside the horizon.

The behaviour of $r_1(u)$ in various parts of the complex u-plane (for a given k^2) can now be uniquely determined by analytic continuation from $u > 0$. In particular, 3-5 implies that the continuation should be done through the region around $u = 0$.

Let us first look at what are all the possible values of $(u, \vec{k})$ for which $r_1(u, k)$ approaches the singularity. From 3.30, when $r_1 \to 0$, $|u| \to \infty$, because f blows up at the singularity (large curvature effect). Conversely, $|u| \to \infty$ implies either

$r_1 \to 0$ or $r_1 \to \infty$. Thus along different directions to infinity in the complex u-plane, the turning point approaches either the boundary or the singularity, the choice being determined by the analytic continuation. The branch cuts in 3-5 divide the complex infinity of the u-plane into various asymptotic regions. The regions which correspond to either the singularity or the boundary are indicated in 3-5. Near the real u axis, the turning point approaches the boundary as $|u| \to +\infty$ as can be expected. As $|u| \to +\infty$ near the imaginary u axis, the turning point approaches the singularity.

For definiteness, we will restrict our discussion below to real k^2 and u^2 and examine in some detail how the turning point changes with u for fixed k^2 for the metric 2.6 . The discussion generalizes to finite μ as well.

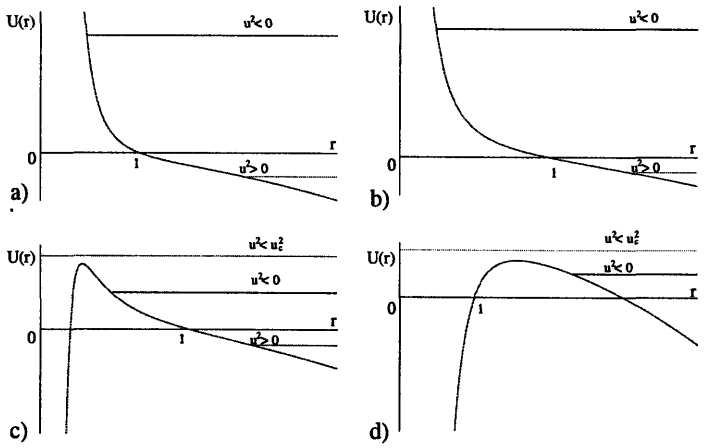

Figure 4-1: The potential U for (a): $k^2 = 0$, (b): $k^2 > 0$, (c): $-1 < k^2 < 0$, (d): $k^2 < -1$. The horizontal axis is r and vertical axis is $U(r)$. The horizon is at $r = 1$.

For this purpose, it is convenient to visualize how the turning point changes with u by treating equation 3.38 (or 3.31) as the motion of a one-dimensional particle of energy $E^2 = -u^2$, moving in a potential[1]

$$U = -V = -f\left(\frac{k^2}{r^2} + 1\right) \tag{4.1}$$

[1]Note that the potential V is inverted since we work in the classically forbidden region of the Schrodinger problem 2.34.

with the turning point satisfying the equation

$$f\left(1+\frac{k^2}{r^2}\right)=u^2 \tag{4.2}$$

In 4-1 we plot the potential U for various values of k^2 for $d=4$. The discussions below applies to all $d \geq 3$. Some important features of the plots can be summarized as:

- 1. For $k^2 \geq 0$, the potential U is monotonic for real $r>0$ with $U(r=0) \to +\infty$ and $U(\infty) \to -\infty$. When $u^2>0$, the turning point $r_1>1$, i.e. it lies outside the horizon. By continuing past $u^2=0$ to $u^2<0$ (corresponding to real energy E for the bulk geodesic), the turning point lies inside the horizon. In particular, as $E^2=-u^2 \to +\infty$, the turning point approaches the singularity.

- 2. For $k^2=-q^2<0$, the potential U has a maximum at $r_{max}>0$ with both $U(0)$ and $U(\infty)$ going to $-\infty$. For $q^2<1$, $r_{max}<1$, i.e. it lies inside the horizon, while for $q^2>1$, r_{max} lies outside the horizon. Thus in the latter case, the potential V has a minimum at r_{max} outside the horizon with $V(r_{max})<0$. One can check that this remains true for the full potential V_p 2.35 for ν not too small. This implies that the Schrodinger problem 2.34 can have bound states.

- 3. Denote $u_c^2=-E_c^2=-U(r_{max})$. For $u=u_c=\pm iE_c$, the turning point reaches r_{max}. u_c are precisely the branch points of r_1 on the imaginary u axis indicated in 3-5 c and 3-5 d. When $E^2>E_c^2=U(r_{max})$, the corresponding classical path has no real turning point and will hit the singularity. By giving E a small imaginary part, one can nevertheless continue them beyond the singularity to a complex turning point. While naively these geodesics appear to hit[2] the singularity, they are not good probes of it unless their complex turning point is also close to the singularity, since the integration contour itself can be smoothly deformed in the complex r-plane and the deformed contour does not have to be close to the singularity if the turning point is not.

[2]or with a small imaginary part for E, they seem to get very close to the singularity

The above discussions can be easily generalized to all complex values of k^2 and u using equation 4.2 . Generically, the turning point r_1 is complex.

4.1.1 UV/UV connection for physics beyond the horizon

The dependence of r_1 on u illustrates some interesting features in the relation between bulk and boundary scales. For definiteness, we illustrate them using $k^2 > 0$. For real $u \to +\infty$, the turning point is given by

$$r_1 \approx u \to +\infty \tag{4.3}$$

i.e. the turning point approaches the boundary. When u decreases, r_1 also decreases. The turning point r_1 reaches the horizon for $u = 0$ (see 4-1 a and 4-1 b) . This behavior reflects a familiar feature of the AdS/CFT correspondence, called IR/UV connection [63, 90], which relates long distances in the AdS spacetime to high energies in the boundary theory.

When dealing with physics inside the horizon, there appears to be a new feature. The turning point r_1 moves inside the horizon when u moves along the imaginary axis from the origin. Let $u = iE$. Then as E increases, r_1 decreases. For $E \to +\infty$, we find that

$$r_1 \approx \begin{cases} \frac{1}{E} & k = 0 \\ & \to 0 \, . \\ \sqrt{\frac{k}{E}} & k \neq 0 \end{cases} \tag{4.4}$$

To probe deeper inside the horizon requires larger E. Since the singularity may heuristically be considered as the UV of the bulk, we thus find a UV/UV connection when dealing with the physics inside the horizon.

4.2 Asymptotics of G_+ at finite k

In the last section, we found that the geometry around the black hole singularity is encoded in the behavior of Yang-Mills correlation functions in the complex ω-plane for $\omega \to \pm i\infty$. In this section we examine the manifestations of the singularity explicitly. For this purpose, we need to extract the large $|u|$ behaviors of the integrals 3.41-3.42 near the imaginary axis. The integrals in 3.42 are rather complicated for $k^2 \neq 0$ and general d. For an AdS_5 black hole, one can evaluate 3.42 explicitly in terms of elliptical integrals and we collect the results in Appendix A6 [3].

We present the large $|u|$ behaviors of $Z(u,k)$ as defined in 3.41 for a finite mass black hole in AdS_5 using the results in Appendices A.6 and A.7. The features discussed below should apply to finite mass black holes in generic dimension too. For definiteness we will restrict to $k^2 = -q^2 \geq 0$, in which case the structure of branch cuts and turning points in the complex u-plane is described in 3-5 a and 3-5 b.

First we consider the limit $u \to \pm\infty$ along the real axis. We find that

$$Z = -ut_0 + 2\log\left(\pm\frac{u}{2}\right) + 2 + \sum_{n=1}^{\infty} \frac{1}{u^{2n}} \widetilde{M}_n(k) \tag{4.5}$$

where the upper (lower) sign corresponds to $u \to +\infty$ $(-\infty)$ and

$$t_0 = \begin{cases} 0 & \mathrm{Re}u \to +\infty \\ \\ -i\beta & \mathrm{Re}u \to -\infty \end{cases} \tag{4.6}$$

where $\widetilde{M}_n$ is a polynomial in k^2 and μ of order at most k^{2n}. The expansion 4.5 applies

[3] Alternatively, one could extract the large $|u|$ expansions directly from the integrals using Mellin transformations, an approach which can in principle be applied to finite mass and generic dimensions. In this way one can check that the results presented here are universal. This method, while general, is also rather complicated and we will not illustrate it explicitly

for any finite value of k. Equation 4.5 implies that for $\omega \to \infty$ near the real axis

$$G_+(\omega) \approx \begin{cases} \frac{4\pi}{(\Gamma(\nu))^2}\left(\frac{\omega}{2}\right)^{2\nu}\left(1+O\left(\frac{1}{\omega^2}\right)\right) & \mathrm{Re}\omega \to +\infty \\ \\ \frac{4\pi}{(\Gamma(\nu))^2}\left(-\frac{\omega}{2}\right)^{2\nu} e^{\beta\omega}\left(1+O\left(\frac{1}{\omega^2}\right)\right) & \mathrm{Re}\omega \to -\infty \end{cases} \tag{4.7}$$

This is precisely what one would expect based on conformal invariance[4] and is consistent with the asymptotic expansion 3.9 which is the result of a different approximation of $G_+(\omega)$ valid for $k = 0$.

Having analyzed the asymptotic behaviour of $Z(u,k)$ along the real u axis we can now consider the case $u \to \pm i\infty$. Letting $u = iE$ and taking $\mathrm{Re}E \to +\infty$ along the real E axis we find that Z has the following large E expansion

$$Z = -t_0 E + 2\log\frac{E}{2} + 2 + k^2 \sum_{n=0}\left(\frac{1}{(kE\sqrt{\mu})}\right)^{n+\frac{1}{2}} T_n(k) + \sum_{n=1}\frac{1}{E^{2n}}\widetilde{L}_n(k) \tag{4.8}$$

where t_0 is

$$t_0 = \frac{\overline{\mathcal{B}}}{2}, \qquad \mathrm{Re}E \to +\infty \tag{4.9}$$

and $\mathcal{B}$ was defined in equation 2.12. For $\mathrm{Re}E \to -\infty$ along the real E axis, one takes $E \to -E$ in 4.8 except for the first term for which one uses instead

$$t_0 = -\frac{\mathcal{B}}{2}, \qquad \mathrm{Re}E \to -\infty \tag{4.10}$$

In 4.8, $T_n(k)$ is a polynomial in k^2 and μ up to at most k^{2n}. $\widetilde{L}_n(k)$ is a polynomial of k^2 and μ containing powers up to k^{2n}. The expansions for other quantities in 3.42 are similar,

$$L = -2\log\left(\pm\frac{E}{2}\right) + \cdots$$

[4]When real $\omega \to +\infty$, one expects the correlation function to recover the zero temperature form. The second line of equation 4.7 follows from the general properties of the Wightman function at finite temperature.

$$
\begin{aligned}
t &= t_0 - \frac{2}{E} + \cdots \\
x^i &= 0 + \cdots
\end{aligned} \tag{4.11}
$$

where $\cdots$ in 4.11 denotes terms of similar structure to the last two terms in 4.8.

Since the first series in the expansion 4.8 contains negative powers of k, it breaks down when k is small ($O(E^{-1})$).

The asymptotic expansions of $Z(u,k)$ along the real and imaginary u axis for fixed k are therefore extremely different. Along the real axis the expansion is valid for any finite value of k while along the imaginary axis the limits $k \to 0$ and $u \to \pm i\infty$ do not commute. While the physics of the spacelike geodesics close to the boundary is quite indifferent to the presence of the transverse S^3 for small values of k as the geodesics approach the singularity the effect of a small deviation of k from 0 is important. This is particularly evident from the expansion of x_i whose first term is not linear in k but of order $O\left(\frac{k_i}{\sqrt{kE}}\right)$

When $|kE| < \sqrt{\mu}$ the expansions 4.8 is replaced by

$$
Z = -Et_0 + 2\log\left(\pm\tfrac{E}{2}\right) + 2 + \textstyle\sum_{n=1}^{\infty} \frac{1}{E^{2n}} k_n(\epsilon) \tag{4.12}
$$

where $\epsilon = -\frac{k^2E^2}{\mu}$ and $k_n(s)$ are power series in ϵ. For example, for $n = 1$

$$
k_1(\epsilon) = \frac{\pi}{2}\epsilon + \frac{3\pi}{16}\epsilon^2 + O(\epsilon^3) \tag{4.13}
$$

The expansions for quantities in 3.42 are given by 4.11 but with $\cdots$ replaced by terms of the same structure as the last term of 4.12. The appearance of the expansion parameter ϵ for small k can be attributed to the presence of the branch point 3.59 at $2qE \approx \mu$ for large E. The expansion 4.8 applies in the limit $|E| \to \infty$ for any given finite k, no matter how small. 4.12 is only relevant for the expansion near $k = 0$. Note that 4.12 implies that the derivatives of Z over k evaluated at $k = 0$ diverge in the large E limit[5].

[5]The expansion in 4.12 can be generalized to other dimensions. In particular the divergent behaviour of the derivatives of Z over k for $E \to \pm\infty$ and $k = 0$ is a generic feature that will be

Equations 4.8–4.12 imply that as $\omega = \nu u \to \pm i\infty$, the boundary correlation function behaves as

$$G_+(\omega,\vec{p}) \approx \frac{4\pi}{(\Gamma(\nu))^2}\left(\mp i\frac{\omega}{2}\right)^{2\nu} e^{\pm i\omega\left(\frac{\tilde{\beta}}{2}\pm\frac{i\beta}{2}\right)}\left(1+O\left(\frac{1}{\sqrt{\omega}}\right)\right) \tag{4.14}$$

where the upper (lower) sign corresponds to $\omega \to +i\infty$ $(-i\infty)$. Note that the correlation function decays exponentially along these directions. The exponential decay is controlled by the quantity $\tilde{\beta}$. This behavior is due to the fact that for $|E| \to \infty$, $t(E,\vec{q}) \to$ const.

We therefore notice two main differences between the expansions of $G_+(\omega,\vec{p})$ for $\omega \to \infty$ along the real and imaginary axes.

- 1 The exponential decay along $w \to \pm i\infty$ present in 4.14 cannot be obtained by analytical continuation from the expansion 4.7 valid for $\omega \to \pm\infty$. This is due to the presence of the quasi-normal pole lines.

- 2 While along the real ω axis the finite p corrections organize in powers of ω^{-2} along the imaginary axis they organize in powers of $\omega^{-\frac{1}{2}}$. Moreover along the imaginary ω axis these diverge in the limit $p \to 0$ as the series expansion breaks down for $p \sim \omega^{-1}$.

Some further remarks:

- 1. While naively it appears from the second equation of 3.42 that $t(E,q)$ is an odd function of E, one has to be careful about the contribution of the pole at $r = 1$ when analytically continuing the integral from the $k^2 > 0, u > 0$ region. It can indeed be checked from equations 4.9,4.10, 4.6) that except for the imaginary part of the constant term t_0, the rest of the function $t(E,q)$ is indeed odd in E.

- 2. Note that the leading behaviors of various quantities in 4.11 are *universal.* They simply follow from the fact that as $r_1 \to 0$, the geodesic becomes null. For

related in the next section to the presence of a singularity in the bulk

example, the constant t_0 in the expansion of $t(u, \vec{k})$ for u approaching imaginary infinity is precisely the Schwarzschild time that it takes for a null geodesic to go from the boundary to the singularity and to come back (recall 2.11). In particular, the results apply without change to finite mass black holes (see appendix A7) and black hole in other $d \geq 3$ provided one uses the corresponding $\mathcal{B}$ appropriate for each background.

- 3. While 4.14 and 4.7 were derived in the large ν limit, it is important to emphasize that they should hold for all ν, since the limit $|u| \to \infty$ should coincide with the limit $|\omega| = \nu|u| \to \infty$ regardless of the value of ν. This can be explicitly checked for AdS_4 black holes by comparing with the large ω behavior of $G_{12}(\omega) = e^{-\frac{1}{2}\beta\omega} G_+(\omega)$ described by 3.9 and 3.11 or for generic $d \geq 3$ by using the results of the approximation described in appendix A4.

- 4. In the above we have computed only the leading order approximation to G_+ in the large ν limit. It would be interesting to compute the next order in the $1/\nu$ expansion. In particular, the function $Q(z)$ 3.25 will start contributing to next order. Since $Q(z)$ becomes singular at $r \to 0$, it would be interesting to see whether it yields new manifestations of the singularity in the boundary theory correlation functions.

4.2.1 Light-cone limit

Another interesting limit is the light-cone limit $u \to +\infty$ with $k \sim u$. The results for this case are derived for the $\mu \to \infty$ rescaled metric 2.6 in appendix A7. We have seen in section 3.3.2 that for finite μ as $k \to \infty$ there are branch cuts for the function $Z(u, k)$ starting at $u \sim k$ on the real u axis. We also have seen in 3.57 that these branch cuts do not reach the real axis in the limit $\mu \to \infty$ for any finite k. This feature shows up in the asymptotic behaviour of $Z(u, k)$. Defining the variable $g = \frac{u^2}{k^2} - 1$ we have for $k \to \infty$ and $g \gg k^{-\frac{4}{3}}$:

$$Z = \log(u^2 - k^2) + 2 - \log(4) + O(\frac{1}{g^3 k^4})$$

The divergence as $u^2 - k^2 = 0$ however is not present for any finite k as the expansion changes for $g \sim k^{-\frac{4}{3}}$ reflecting the fact that the branch cuts 3.57 remain at a finite distance from the real axis. There is no divergence for $u \sim k$ and $Z(u,k)$ remains finite. At finite μ on the contrary a singularity is present on the real u axis.

4.3 Manifestations of singularities in boundary theories

We argued that for large ω along the imaginary axis the boundary theory correlation functions encode information about the region of spacetime beyond the horizon and close to the singularity. In this section we will reconsider the asymptotic behaviour of $G_+(u,k)$ for large u imaginary and pinpoint two features which are manifestations of the singularity.

As $\omega = \nu u \to \pm i\infty$, the boundary correlation function behaves as

$$G_+(\omega) \approx \frac{1}{\pi(\Gamma(\nu))^2}\left(\mp i\frac{\omega}{2}\right)^{2\nu} e^{\pm i\omega t_0} \tag{4.15}$$

where the upper (lower) sign corresponds to $\omega \to +i\infty$ $(-i\infty)$. We have obtained this asymptotic behaviour using two different methods in section 3.1 and also in the large ν limit in the previous section. This result remains valid for finite ν and for all values of $d \geq 2$.

In the large ν limit we have established a direct connection between the quantity

$$t_0 = \left(\frac{\tilde{\beta}}{2} \pm \frac{i\beta}{2}\right) \tag{4.16}$$

appearing in 4.15 and the Schwarzschild time that it takes for a null geodesic to go from the boundary to the singularity and to come back. The real part $\tilde{\beta}$ in particular measures the departure of the Penrose diagram (2-1) from a square as was first pointed out in [28].

Notice that as $t_0 \neq 0$ the asymptotic behaviour of $G_+(\omega)$ along the imaginary axis

cannot be obtained by analytic continuation from the asymptotic expansion valid in the limit $\omega \to +\infty$:

$$G_+(\omega) \sim \frac{1}{\pi(\Gamma(\nu))^2} \left(\frac{\omega}{2}\right)^{2\nu}$$

This reflects the presence of the quasinormal poles accumulating for $|\omega| \to \infty$. They separate the region probing the geometry outside the horizon from the region probing the geometry beyond it. One particular case we have to pay particular attention to is the BTZ black hole. As shown in appendix A2 in this case the quasinormal poles lines are parallel to the imaginary ω axis and separate a distinct asymptotic region only for $k \in \mathbb{R}$ and $k \neq 0$. For $k = 0$ the quasinormal poles are on the imaginary ω axis.

For $d \neq 2$ at $r = 0$ we have a curvature singularity. One consequence is that the transverse S_{d-1} in the metric shrinks as $r \to 0$. The geodesics that we take in consideration to approximate $G_+(\nu u)$ at $k = 0$ have zero angular momentum on the S_{d-1} and therefore are not sensible to the shrinking radius of curvature. However as soon as we consider derivatives of $Z(u, k)$ with respect to k at $k = 0$ we have from 4.13 :

$$\frac{d^{2n}}{dk^{2n}} Z(E, k) \mid_{k=0} \sim E^{2n} \qquad E \to \infty \tag{4.17}$$

which diverge as E goes to infinity reflecting the fact that the transverse S_{d-1} is shrinking in size[6] as the turning point $r_1 \sim \frac{1}{E} \to 0$. In the BTZ case the situation is different as there is no curvature singularity and the derivatives considered in 4.17 do not diverge as $E \to \infty$.

Finally a generic consequence of the presence of the horizon is that in the Schrodinger problem 2.34 the potential $V_l(z) \to 0$ as $z \to \infty$. This is due to the explicit factor of $f(r(z))$ in 2.36 which goes to zero at the horizon. Therefore the problem admits a continuous spectrum; moreover for real values of l and ω there are no bound states and therefore all singularities in the Wightman function $G_+(\omega)$ computed at $N \to \infty$

[6] in [27] a class of gauge theory observables directly sensible to this curvature divergence was proposed

and $\lambda \to \infty$ are away from the real axis. We have seen in 3.7 that as a consequence their Fourier transforms will decay as $t \to \infty$. In the absence of an horizon 2.34 only admits bound states, the spectrum off all correlation functions is discrete (for S_3 of finite radius) and they do not decay in time.

4.4 Discussions: Resolution of black hole singularities at finite N ?

There are two limits in which the theory can be approximated by a continuous spectrum. One is the large N limit. For a typical many-body system, one expects the spacing of the highly excited states to be of order $\hbar^{-K}$, where in our case K is of order N^2, thus we expect the level spacing to be exponentially small in N^2 when N is large. In the large N one has a continuous spectrum. The other limit is the limit of $R \to \infty$, in which case the theory lives on $\mathbb{R}^3$. Due to the underlying conformal invariance, this is the same as the high temperature limit of the theory.

In this chapter we established a direct relation between the large operator dimension limit of the boundary Wightman function $G_+(\omega, \vec{p})$ and bulk geodesics with integrals of motion $E = -i\nu^{-1}\omega$ and $\vec{q} = -i\nu^{-1}\vec{p}$. In particular, we find that in the complex ω-plane, there exist lines of poles separating the complex ω-plane into several sectors (see 3-5). Roughly speaking, the sectors near the real axis describe the physics outside the horizon while the sectors near the imaginary axis describe the physics inside the horizon. At complex infinity, one either approaches the boundary or the singularity. The presence of the curvature singularity of a black hole is reflected in a certain exponential falloff of $G_+(\omega, \vec{p})$ near imaginary infinity. The falloff is controlled by a complex parameter $\mathcal{B}$ (introduced in 2.12) which characterizes the black hole geometry. These results are quite generic and are applicable to finite mass black holes in various dimensions.

The rich analytic behavior observed for G_+ in the complex ω-plane is tied to the fact that in the large N limit, the boundary theory has a continuous spectrum,

even though it lives on a compact space. In the bulk, the continuous spectrum arises because of the presence of the horizon. At finite N, no matter how large, the boundary theory on an S^{d-1} has a discrete spectrum. In particular, the finite temperature Wightman function should have the form

$$G_+(\omega) = 2\pi \sum_{m,n} e^{-\beta E_m} \rho_{mn} \delta(\omega - E_n + E_m) \tag{4.18}$$

which is a sum of delta functions along the real ω-axis, where m, n sum over the physical states of the theory. G_+ in equation 4.18 does not have an unambiguous continuation off the real axis. In particular, the procedures of analytically continuing G_+ to complex ω and taking the large N limit do not commute. Equation 4.15 arises by taking the large N limit first and then doing the analytic continuation. This appears to imply that at finite N, geometric notions associated with a black hole, such as the event horizon and the singularity, no longer exist. This is not surprising since the black hole geometry arises as a saddle point in the path integral of the boundary theory in a $1/N$ expansion. If one does not use such an expansion, the geometric notions lose their meaning.

Nevertheless, when N is large, in a typical situation the asymptotic expansion in $1/N$ becomes an arbitrarily good approximation and the geometric interpretation is valid. The presence of the black hole singularity seems to imply that for certain questions such an expansion breaks down no matter how large N is[7]. That is, in order to make the theory consistent, one has to take into account corrections non-perturbative in N. In the boundary theory it is difficult to identify these questions, since they are typically related to local physics inside the horizons. We hope the relation between the boundary correlation functions and the bulk geometry we have found may help to pinpoint such questions.

In the above we argued that the fact that the boundary theory on S^{d-1} has a discrete spectrum at finite N may indicate the resolution of the singularity at finite N. The story becomes somewhat less trivial in the high temperature limit.

[7]One example of such a breakdown is in the long time behaviors of Lorentzian correlation functions [64], although it does not seem to be directly related to the singularity.

The boundary manifold decompactifies in this limit and the boundary theory has a continuous spectrum even at finite N. In this case, one has to disentangle the effects due to large N from those due to noncompact directions. We believe that the analytic structure indicated in 3-5 may yield important clues for resolving this issue. The presence of various lines of poles opens up new asymptotic regions near the imaginary axis which describe physics inside the horizon. This might be considered as a manifestation of the horizon in a boundary theory living on $\mathbb{R}^{d-1}$. It would be interesting to understand what happens to this feature and the exponential decay of G_+ near imaginary infinity at finite N. We have examined a few examples in free theories at finite N. In these examples, all the poles in the complex ω-plane lie along the imaginary axis and no new asymptotic regions appear other than those associated with the standard large frequency behavior.

Chapter 5

The Arrow of Time and Thermalization in Large N Gauge Theory

As described in the introduction we now turn to investigate the physics of a continuous spectrum and time decay in the large N limit of the boundary theory. This constitutes a first step towards the achievement of the goal of understanding the resolution of spacelike singularities in String theory. The plan of the chapter is as follows. In section 5.1.1 we introduce the subject of our study: a family of matrix quantum mechanical systems including $\mathcal{N} = 4$ SYM on S^3. We highlight some relevant features of the energy spectrum of these theories. Motivated by the classical mixing properties, we introduce observables which could signal time irreversibility. The simplest of them are real-time correlation functions at finite temperature, which describe non-equilibrium linear responses of the systems. The rest of the chapter is devoted to studying these observables, first in perturbation theory, and then using a non-perturbative statistical method. In sec 5.2 we compute real-time correlation functions in perturbation theory. We find that at any finite order in perturbation theory, the arrow of time does not emerge. In sec 5.3 we argue that the planar perturbative expansion has a zero radius of convergence and cannot be used to understand the long time behavior of the system. In section 5.4 we give a simple physical explanation for the breakdown of perturbation

theory. We argue that for any nonzero 't Hooft coupling, an exponentially large (in N^2) number of free theory states of wide energy range (or order N) mix under the interaction. As a consequence small λ and long time limits do not commute at infinite N. In section 5.5 we develop a statistical approach to studying the dynamics of the theories in highly excited states, which indicates that time irreversibility occur for any nonzero 't Hooft coupling λ. We conclude in section 5.6 with a discussion of implications of our results.

5.1 Prelude: theories and observables of interest

In this section we introduce the systems and observables we want to study.

5.1.1 Matrix mechanical systems

We consider generic matrix quantum mechanical systems of the form

$$S = N\mathrm{tr}\int dt\left[\sum_{\alpha}\left(\frac{1}{2}(D_t M_\alpha)^2 - \frac{1}{2}\omega_\alpha^2 M_\alpha^2\right)\right] - \int dt\, V(M_\alpha;\lambda) \tag{5.1}$$

which satisfy the following requirements:

- 1. M_α are $N\times N$ matrices and $D_t M_\alpha = \partial_t - i[A, M_\alpha]$ is a covariant derivative. One can also include fermionic matrices, but they will not play an important role in the following and for simplicity of notations we suppress them.
- 2. The frequencies ω_α in 5.1 are nonzero for any α, i.e. the theory has a mass gap and a unique vacuum.
- 3. The number of matrices is greater than one and can be infinite. When there are an infinite number of matrices, we require the theory to be obtainable from a renormalizable field theory on a compact space, in which case ω_α are integer or half-integer multiples of a finite number of fundamental frequencies.
- 4. $V(M_\alpha;\lambda)$ can be written as a sum of *single-trace* operators and is controlled by a coupling constant λ, which remains fixed in the large N limit.

$\mathcal{N} = 4$ SYM on S^3 is an example of such systems with an infinite number of matrices (including fermions) when the Yang-Mills and matter fields are expanded in terms of spherical harmonics on S^3 (see e.g. [56, 2]). In this case, ω_α are integer or half-integer multiples of a fundamental frequency $\omega_0 = 1/R$ with R the radius of the S^3. The number of modes with frequencies $\omega_\alpha = \frac{k}{R}$ increases with k as a power. $V(M_\alpha; \lambda)$ can be schematically written as[1]

$$V = N\left(\sqrt{\lambda}V_3(M_\alpha) + \lambda V_4(M_\alpha)\right) \tag{5.2}$$

where V_3 and V_4 contain infinite sums of single-trace operators which are cubic and quartic in M_α and $\partial_t M_\alpha$. $\lambda = g_{YM}^2 N$ is the 't Hooft coupling.

In this chapter we work in the large N limit throughout. Our discussion will only depend on the large N scaling of various physical quantities and not on the specific structure of the theories in 5.1 like the precise field contents and exact forms of interactions. For purpose of illustration, we will often use as a specific example the following simple system

$$S = \tfrac{N}{2}\mathrm{tr}\int dt\ [(D_t M_1)^2 + (D_t M_2)^2 - \omega_0^2(M_1^2 + M_2^2) - \lambda M_1 M_2 M_1 M_2] \ . \tag{5.3}$$

5.1.2 Energy spectrum

5.1 has a $U(N)$ gauge symmetry and physical states are singlets of $U(N)$. One can classify energy eigenstates of a theory by how their energies scale with N in the large N limit. We will call the sector of states whose energies (as measured from the vacuum) are of order $O(1)$ the low energy sector. As motivated in the introduction, we are mainly interested in the sector of states whose energies are of order μN^2 with μ independent of N, which will be called the high energy sector. The density of states in the low energy sector is of order $O(1)$, i.e. independent of N, while that of the

[1]The precise form of the interactions depends on the choice of gauge. It is convenient to choose Coulomb gauge $\nabla \cdot \vec{A} = 0$, in which the longitudinal component of the gauge field is set to zero. In this gauge, M_α include also non-propagating modes coming from harmonic modes of ghosts and the zero component of the gauge field.

high energy sector can be written in a form

$$\Omega(E) \sim e^{s(\mu)N^2}, \qquad E = \mu N^2 \tag{5.4}$$

with $s(\mu)$ some function independent of N. 5.4 follows from the fact that the number of ways to construct a state of energy of order $O(N^2)$ from $O(N^2)$ oscillators of frequency of $O(1)$ is an exponential in N^2. The presence of interaction should not change this behavior at least for μ sufficiently large. 5.4 is the reason why we restrict to more than one matrix in 5.1 For a gauged matrix quantum mechanics with a single matrix one can reduce the matrix to its eigenvalues and 5.4 does not apply. When μ is sufficiently large, $s(\mu)$ should be a monotonically increasing function[2] of μ and we will restrict our definition of high energy sector to such energies.

For $\mathcal{N} = 4$ SYM, states in the low energy sector correspond to fundamental string states in the AdS spacetime, while the states in the high energy sectors may be considered as black hole microstates[3].

A convenient way to study a system in excited states is to put it in a canonical ensemble with a temperature $T = \frac{1}{\beta}$. The partition function and free energy are defined by (tr denotes sum over all physical states and H is the Hamiltonian)

$$Z = \mathrm{tr} e^{-\beta H} = e^{-\beta F} \ . \tag{5.5}$$

We will always keep T fixed in the large N limit. Below low and high temperature refers to how the temperature is compared with the mass gap of a theory[4]. As one varies T, different parts of the energy spectrum are probed. For the family of matrix quantum mechanical systems 5.1, there are two distinct temperature regimes. At low temperature, one probes the low energy sector and the free energy F is of order $O(1)$. At high temperature F is of order $O(N^2)$ and the high energy sector is probed. It may seem surprising at first sight that one can probe the sector of energies of $O(N^2)$ using

[2]That is, the theory should have a positive specific heat for μ sufficiently large.
[3]Note that at a sufficiently high energy, the most entropic object in AdS is a big black hole.
[4]For example for $\mathcal{N} = 4$ SYM on S^3, low (high) temperature means $T \ll \frac{1}{R}$ ($T \gg \frac{1}{R}$)

a temperature of $O(1)$. This is due to the large entropy factor 5.4 which compensates the Boltzmann suppression. For $\mathcal{N} = 4$ SYM theory at strong coupling, there is a first order phase transition separating the two regimes at a temperature of order $1/R$, where R is the AdS radius [45, 96, 97]. A first order phase transition has also been found for various theories in the family of 5.1 at weak coupling [88, 1, 2].

An important feature of the high energy sector is that the large N limit is like a thermodynamic limit with N^2 playing the analogous role of the volume factor. In this limit the number of degrees of freedom goes to infinity while the average excitations per degree of freedom remain finite. The thermal partition function

$$Z(\beta) = \mathrm{tr} e^{-\beta H} = \int dE\, \Omega(E) e^{-\beta E} \tag{5.6}$$

is sharply peaked at an energy $E_\beta \sim O(N^2)$ (with a width of order $O(N)$) determined by

$$\left.\frac{\partial S(E)}{\partial E}\right|_{E_\beta} = \beta, \qquad S(E) = \log \Omega(E) \tag{5.7}$$

Note that the leading N dependence of $S(E)$ has the form $S(E) = N^2 s(\mu)$ (see 5.4) with $\mu = E/N^2$ characterizing the average excitations per oscillator degree of freedom. Equation 5.7 can also be interpreted as the equivalence between canonical and microcanonical ensemble[5]. Note that since $F \sim O(N^2)$, the high temperature phase can be considered a "deconfined" phase [93, 97].

5.1.3 Observables

In a classical Hamiltonian system, time irreversibility is closely related with the mixing property of the system, which can be stated as follows. Consider time correlation functions

$$C_{AB}(t) = \left\langle A(\Phi^t X) B(X) \right\rangle - \langle A \rangle \langle B \rangle \tag{5.8}$$

[5]In contrast such an equivalence does not exist for the low energy sector.

where A, B are functions on the classical phase space parameterized by X. $\Phi^t X$ describes the Hamiltonian flow, where Φ^t is a one-parameter group of volume-preserving transformations of the phase space onto itself. $\langle ... \rangle$ in 5.8 denotes phase space average over a constant energy surface. The system is mixing[6] iff [94]

$$C_{AB}(t) \to 0, \qquad t \to \infty \tag{5.9}$$

for any *smooth* L^2 functions A and B.

The closest analogue of 5.8 for the matrix quantum mechanical systems we are considering would be

$$G_i(t) = \langle i|\mathcal{O}(t)\mathcal{O}(0)|i\rangle - \langle i|\mathcal{O}(0)|i\rangle^2 \tag{5.10}$$

where $|i\rangle$ is a generic energy eigenstate in the high energy sector, and $\mathcal{O}$ is an arbitrary gauge invariant operator which when acting on the vacuum creates a state of finite energy of order $O(1)$. More explicitly, denoting $|\psi_\mathcal{O}\rangle = \mathcal{O}(0)\,|\Omega\rangle$ with $|\Omega\rangle$ the vacuum, we require $\langle\psi_\mathcal{O}|H|\psi_\mathcal{O}\rangle \sim O(1)$. Note that for $\mathcal{N} = 4$ SYM on S^3, a *local* operator $O(t, \vec{x})$ of dimension $O(1)$ on S^3 is not allowed by this criterion since $O(t, \vec{x})$ creates a state of infinite energy. To construct a state of finite energy one can smear the local operator over a spatial volume, e.g. by considering operators with definite angular momentum on S^3. Without loss of generality, we can take $\mathcal{O}$ to be of the form

$$\mathcal{O} = \mathrm{tr}(M_{\alpha_1} \cdots M_{\alpha_{n_1}})\mathrm{tr}(M_{\beta_1} \cdots M_{\beta_{n_2}}) \cdots \mathrm{tr}(M_{\gamma_1} \cdots M_{\gamma_{n_k}}) \tag{5.11}$$

with the total number of matrices $K = \sum_{i=1}^{k} n_k$ independent of N. We will call such operators small operators. The reason for restricting to small operators is that they have a well defined large N limit in the sense defined in [98]. More explicitly, if one treats the large N limit of a matrix quantum mechanics as a classical system,

[6]Note that mixing is a stronger property than ergodic which involves long time average. The ergodic and mixing properties can also be characterized in terms of the spectrum of the Koopman operator. For example, a system is mixing iff the eigenvalue 1 is simply degenerate and is the only proper eigenvalue of the Koopman operator [94].

then 5.11 with $K \sim O(1)$ are *smooth* functions on the corresponding classical pase space. From AdS point of view, such operators correspond to fundamental string probes which do not deform the background geometry. If for all small operators $\mathcal{O}$ and generic states $|i\rangle$ in the high energy sector

$$G_i(t) \to 0, \qquad t \to \infty \tag{5.12}$$

one can say the system develops an arrow of time. In particular, 5.12 implies that one cannot distinguish different initial states from their long time behavior (i.e. information is lost).

Energy eigenstates are hard to work with. It is convenient to consider microcanonical or canonical averages of 5.10, for example, the thermal *connected* Wightman functions (see Appendix B1.1 for a precise definition of "connected" and the constant C below)

$$G_+(t) \ = \langle \mathcal{O}(t)\mathcal{O}(0)\rangle_\beta = \tfrac{1}{Z}\mathrm{tr}\left(e^{-\beta H}\mathcal{O}(t)\mathcal{O}(0)\right) - C \tag{5.13}$$

and retarded functions

$$G_R(t) = \frac{1}{Z}\mathrm{tr}\left(e^{-\beta H}[\mathcal{O}(t), \mathcal{O}(0)]\right) \ . \tag{5.14}$$

We shall take the temperature T to be sufficiently high so that E_β determined from 5.7 lies the high energy sector. Equation 5.12 implies that[7]

$$G_R(t) \to 0, \qquad G_+(t) \to 0, \qquad t \to +\infty \ . \tag{5.15}$$

Note that $G_R(t)$ measures the linear response of the system to external perturbations caused by $\mathcal{O}$. That $G_R(t) \to 0$ for $t \to \infty$ implies that any small perturbation of the system away from the thermal equilibrium eventually dies away. In a weaker sense than 5.12, 5.15 can also be considered as an indication of the emergence of an arrow

[7] 5.12 in fact implies the following to be true for any ensemble of states.

of time.

In frequency space, the Fourier transform[8] of 5.13 and 5.14 can be written in terms of a spectral density function $\rho(\omega)$ (see Appendix B1.1 for a review)

$$\begin{aligned} G_+(\omega) &= \frac{1}{1-e^{-\beta\omega}}\rho(\omega) \\ G_R(\omega) &= -\int_{-\infty}^{\infty}\frac{d\omega'}{2\pi}\frac{\rho(\omega')}{\omega-\omega'+i\epsilon} \end{aligned} \tag{5.16}$$

5.15 may be characterized by properties of the spectral density $\rho(\omega)$. For example from the Riemann-Lebesgue theorem, 5.15 should hold if $\rho(\omega)$ is an integrable function on the real axis. Since other real-time correlation functions can be obtained from G_+ (or spectral density function $\rho(\omega)$) from standard relations, for the rest of the chapter, we will focus on G_+ only.

For $\mathcal{N}=4$ SYM at strong coupling, it is convenient to take $\mathcal{O}$ to have a definite angular momentum l on S^3. 5.13 and 5.14 can be studied by considering a bulk field propagating in an eternal AdS black hole geometry and one does find the behavior 5.15 as first emphasized in [64]. In the bulk language, 5.15 can be heuristically interpreted as the fact that any small perturbation of the black hole geometry eventually dies away by falling into the horizon. Furthermore, by going to frequency space, one finds that the Fourier transform $G_+(\omega,l)$ has a rich analytic structure in the complex ω-plane[9], which encodes that the bulk black hole geometry contains a horizon and singularities. The main features can be summarized as follows [27]:

- 1. $G_+(\omega,l)$ has a continuous spectrum with $\omega\in(-\infty,+\infty)$. This is due to the presence of the horizon in the bulk.

- 2. In the complex ω-plane, the only singularities of $G_+(\omega,l)$ are poles. The decay rate for $G_+(t)$ at large t is controlled by the imaginary part of the poles closest to the real axis, which is of order β.

[8]We use the same letter to denote the Fourier transform of a function, distinguishing them by the argument of the function.

[9]Similar things can also said about $G_R(\omega,l)$ which can be obtained from $G_+(\omega,l)$ using standard relations.

- 3. The presence of black hole singularities in the bulk geometry is encoded in the behavior of $G_+(\omega, l)$ at the imaginary infinity of the ω-plane[10]. In particular,

  3a. $G_+(\omega, l)$ decays exponentially as $\omega \to \pm i\infty$.

  3b. Derivatives of $G_+(\omega, l)$ over l evaluated at $l = 0$ are divergent as $\omega \to \pm i\infty$.

As emphasized in [27], none of the above features survives at finite N, in which case[11]

$$G_+(\omega) = 2\pi \sum_{m,n} e^{-\beta E_m} \rho_{mn} \delta(\omega - E_n + E_m)$$

has a discrete spectrum and is a sum of delta functions supported on the real axis. This indicates that concepts like horizon and singularities only have an approximate meaning in a semi-classical limit (large N limit).

To understand the information loss paradox and the resolution of black hole singularities, we need to understand how and why they arise in the classical limit of a quantum gravity. In Yang-Mills theory, this boils down to understanding what physics is missed in the large N limit and why missing it is responsible for the appearance of singularities and the loss of information. With these motivations in mind, we are interested in understanding the following questions

- 1. Can one find a qualitative argument for the emergence of an arrow of time in the large N limit?

- 2. Does the analytic behavior observed at strong coupling persist to weak coupling?

which we turn to in the following sections.

[10] See also [28] for signature of the black hole singularities in coordinate space.

[11] Note that even though $\mathcal{N} = 4$ SYM on S^3 is a field theory, at finite N the theory can be effectively considered as a theory with a finite number of degrees of freedom, since for any given energy E, there are only a finite number of modes below that energy. Furthermore, given that the number of modes with frequency $\frac{k}{R}$ grows with k only as a power, it is more entropically favorable to excite modes with low k for $E \sim O(N^2)$ and modes with $\omega_\alpha \sim O(N)$ are almost never excited.

5.2 Non-thermalization in perturbation theory

In this section we consider 5.13 in perturbation theory in the planar limit. We will find that real-time correlation functions have a discrete spectrum and oscillatory behavior. Thus the theory does not thermalize in the large N limit.

In perturbation theory, $G_+(t)$ can be computed using two methods. In the first method, one computes $G_E(\tau)$ with $0 < \tau < \beta$ in Euclidean space using standard Feynman diagram techniques. $G_+(t)$ can then be obtained by taking $\tau = it + \epsilon$. An alternative way is to double the fields and use the analogue of the Schwinger-Keldysh contour to compute the Feynman function $G_F(\omega)$ in frequency space [74], from which $G_+(\omega)$ can be obtained. In the Euclidean-time method it is more convenient to do the computation in coordinate space since one does not have to sum over discrete frequencies, while in the real-time method frequency space is more convenient to use.

We look at the free theory first.

5.2.1 Free theory

To evaluate 5.13 in free theory, it is convenient to use the Euclidean method. The Euclidean correlator

$$G_E^{(0)}(\tau) = \langle \mathcal{O}(\tau)\mathcal{O}(0)\rangle_{0,\beta}, \qquad 0 \le \tau < \beta \tag{5.17}$$

with $\mathcal{O}$ of the form 5.11 can be computed using the Wick contraction[12]

$$\underbrace{M_{ij}^{\alpha_1}(\tau)\, M_{kl}^{\alpha_2}(0)} = \frac{\delta_{\alpha_1\alpha_2}}{N} \sum_{m=-\infty}^{\infty} g_E^{(0)}(\tau - m\beta; \omega_{\alpha_1}) U_{il}^{-m} U_{kj}^{m} \tag{5.18}$$

where $g_E^{(0)}$ is the propagator at zero temperature

$$g_E^{(0)}(\tau;\omega) = \frac{1}{2\omega} e^{-\omega|\tau|}\,. \tag{5.19}$$

[12] see e.g. [24] for a derivation of the following equation and some examples of correlation functions in free theory.

In 5.18 U is a unitary matrix which arises due to covariant derivatives in 5.1 and can be understood as the Wilson line of A wound around the τ direction. In the evaluation of free theory correlation functions $\langle \cdots \rangle_{0,\beta}$ in 5.17, one first preforms the Wick contractions 5.18 and then performs the unitary matrix integral over U, which plays the role of projecting the intermediate states to the singlet sector. In the large N limit, the U integral can be evaluated by a saddle point approximation. Note in particular that [1]

$$U \to 1, \qquad T \to \infty \tag{5.20}$$

Equation 5.20 indicates that the singlet condition should not play an important role for states of sufficiently high energy.

For definiteness, we now restrict to theories with a single fundamental frequency ω_0 like $\mathcal{N} = 4$ SYM or 5.3. Wick contractions in 5.17 give rise to terms of the form $e^{n\omega_0\tau}$ for some integer n, while the U-integral computes the coefficients of these terms. Thus 5.17 always has the form

$$G_E^{(0)}(\tau) = \sum_{n=-\Delta}^{\Delta} c_n(\beta) e^{n\omega_0\tau} \tag{5.21}$$

where Δ is the dimension of the operator[13]. Analytically continuing 5.21 to real time, we find that

$$G_+^{(0)}(t) = \sum_{n=-\Delta}^{\Delta} c_n(\beta) e^{-in\omega_0 t} \tag{5.22}$$

and

$$G_+^{(0)}(\omega) = 2\pi \sum_{n=-\Delta}^{\Delta} c_n(\beta)\delta(\omega - n\omega_0) \ . \tag{5.23}$$

Thus in the large N limit, the correlation function always shows a discrete spec-

[13]Note that for $\mathcal{N} = 4$ SYM the dimension of M_α is given by $\frac{\omega_\alpha}{\omega_0}$. For other matrix quantum mechanical systems without conformal symmetry one can use a similar definition in free theory. For bosonic operators, Δ are integers.

trum is quasi-periodic. The results are generic. If the theory under consideration has several incommensurate fundamental frequencies, one simply includes a sum like those 5.21 and 5.23 for each such frequency. The maximal number of independent exponentials is 2^K, where K is the total number of matrices in $\mathcal{O}$.

It is also instructive to obtain 5.22 using a different method. By inserting a complete set of free theory energy eigenstates in 5.13 we find that

$$G_+^{(0)}(t) = \frac{1}{Z_0} \sum_{a,b} e^{-\beta \epsilon_a} \rho_{ab} e^{i(\epsilon_a - \epsilon_b)t} \tag{5.24}$$

where $|a\rangle$ is a free theory state with energy ϵ_a and $\rho_{ab} = |\langle a|\mathcal{O}(0)|b\rangle|^2$. To understand the structure of 5.24 we expand $\mathcal{O}(0)$ in terms of creation and annihilation operators associated with each $(M_\alpha)_{ij}$, from which we find that

- A. Due to energy conservation, $\mathcal{O}$ can connect levels whose energy differences lie between $-\Delta\omega_0$ and $\Delta\omega_0$, i.e. ρ_{ab} can only be non-vanishing for $|\epsilon_a - \epsilon_b| < \Delta\omega_0$.

- B. $\mathcal{O}$ can only connect states whose energy differences are integer multiples of ω_0 i.e. ρ_{ab} can only be non-vanishing for $\epsilon_a - \epsilon_b = n\omega_0$ with $|n| < \Delta$ integers (or half integers if $\mathcal{O}$ is fermionic).

As a result, 5.24 must have the form 5.22. Note that the argument based on 5.24 applies not only to the thermal ensemble, but in fact to correlation functions in any density matrix (or pure state).

To summarize, one finds that in free theory a real-time thermal two-point function always has a discrete spectrum and is quasi-periodic in the large N limit. This implies that once one perturbs the theory away from thermal equilibrium, the system never falls back and keeps oscillating. This is not surprising since the system is free and there is no interaction to thermalize any disturbance. Note that this is distinctly different from the behavior 5.15 found at strong coupling. In particular, this implies that the bulk description of the high temperature phase in free theory looks nothing like a black hole. Also note that the story here is very different from that of the orbifold CFT in the AdS_3/CFT_2 correspondence. There the mass gap in free theory

goes to zero in the large N limit in the long string sector [65]. As a result, one finds that free theory correlation functions in the long string sector do resemble those from a BTZ black hole [64, 5].

5.2.2 Perturbation theory

In this subsection we use a simple example 5.3 for illustration. The general features discussed below apply to generic theories in 5.1 including $\mathcal{N} = 4$ SYM.

In perturbation theory $G_E(\tau)$ can be expanded in terms of λ as

$$G_E(\tau) = \sum_{n=0}^{\infty} \lambda^n G_E^{(n)}(\tau) \tag{5.25}$$

where $G_E^{(0)}$ is the free theory result. We will be only interested in the connected part of $G_E(\tau)$. Higher order corrections are obtained by expanding $e^{-\lambda \int d\tau V}$ in the path integral with V given by the quartic term in 5.3. More explicitly, a typical contribution to $G_E^{(n)}(\tau)$ in 5.25 has the form

$$\frac{(-1)^n}{n!} \int_0^\beta d\tau_1 \cdots \int_0^\beta d\tau_n \, \langle \mathcal{O}(\tau)\mathcal{O}(0)\, V(\tau_1) \cdots V(\tau_n) \rangle_{\beta,0} \tag{5.26}$$

The free theory correlation function inside the integrals in 5.26 can be computed by first using Wick contraction 5.18 and then doing the U integral. The general structure of 5.26 can be summarized as follows:

- 1. The planar diagram contribution to $G_E^{(n)}(\tau)$ scales like N^0, while diagrams of other topologies give higher order $1/N^2$ corrections. The number R_n of planar diagrams grows like a power in n, i.e. is bounded by C^n with C some finite constant [92].

- 2. The τ-integrations are over a compact segment and are all well defined. A typical term in 5.26 after the integration has the structure

$$g_{kj}^{(n)}(\beta) \tau^l e^{k\omega_0 \tau} \tag{5.27}$$

where l and k are integers. l can take values from 0 to n, while k from $-2n-\Delta$ to $2n+\Delta$ where Δ is the dimension of $\mathcal{O}$ in free theory.

Analytically continuing 5.25 to Lorentzian time by taking $\tau = it + \epsilon$, we find

$$G_+(t,\lambda) = \sum_{n=0}^{\infty} \lambda^n G_+^{(n)}(t) \tag{5.28}$$

where typical terms in $G_+^{(n)}(t)$ have the t-dependence of the form

$$g_{kl}^{(n)}(\beta) t^l e^{ik\omega_0 t} \tag{5.29}$$

with the range of l and k given after equation 5.27. After Fourier transforming to frequency space we find that at each order in the perturbative expansion $G_+^{(n)}(\omega)$ (and thus the spectral density function $\rho(\omega)$) consists of sums of terms of the form

$$g_{kl}^{(n)} \delta^{(l)}(\omega - k\omega_0) \tag{5.30}$$

where the superscript l denotes the number of derivatives.

One origin of t^l terms in 5.29 is the shifting of frequency from the free theory value. For example, suppose the free theory frequency is shifted to $\omega = \omega_0 + \lambda\omega_1 + \cdots$, one would get terms of the form 5.29 when expanding the exponential $e^{i\omega t}$ in λ. One can in principle improve the perturbation theory by resumming such contributions using Dyson's equations. However, there appears no systematic way of doing this for a composite operator 5.11. In Appendix B1.2, we prove that real-time correlation functions of fundamental modes M_α again have a discrete spectrum in the improved perturbative expansion.

5.3 Break down of Planar perturbation theory

It is well known that at zero temperature the planar expansion of a matrix quantum mechanics has a finite radius of convergence in the λ-plane (see e.g. [92] for a recent

discussion and earlier references). If this persists at finite temperature, properties of the theory at zero coupling or in perturbation theory should hold at least for the coupling constant being sufficiently small. In particular, from our discussion of last section, one would conclude that real-time correlation functions for generic gauge invariant operators should be quasi-periodic and an arrow of time does not emerge at small 't Hooft coupling. In this section, we argue that the planar perturbative expansion in fact breaks down for real-time correlation functions and thus perturbation theory cannot be used to understand the long-time behavior of the system at any nonzero coupling.

From our discussion in section 5.2, we expect the Euclidean correlation function 5.25 should have a finite radius of convergence for any given $\tau \in (0, \beta)$. After analytic continuation to real time, the convergence of the expansion in Euclidean time implies that 5.28 should have a finite radius $\lambda_c(t)$ of convergence for any given t. However, it does not tell how $\lambda_c(t)$ changes with t in the limit $t \to \infty$. In this section we argue that the radius of convergence goes to zero in the large t limit. Note that the convergence of the perturbative expansion depends crucially on how $g_{kl}^{(n)}$ in 5.30 fall off with n. We will argue below that the falloff is slow enough that perturbation theory breaks down in the long time limit. In frequency space, one finds that n-th order term in the expansion grows like $n!$[14].

We will again use 5.3 as an illustration. The argument generalizes immediately to generic systems in 5.1. For simplicity, we will consider the high temperature limit 5.20 in which we can replace U in 5.18 by the identity matrix, e.g.

$$\underbrace{M_{1ij}(\tau)\, M_{1kl}(0)} = \frac{1}{N} \sum_{m=-\infty}^{\infty} g_E^{(0)}(\tau - m\beta; \omega_0)\delta_{il}\delta_{kj} = \frac{1}{N}\delta_{il}\delta_{kj}\, g_E(\tau; \omega) \tag{5.31}$$

where

$$g_E(\tau; \omega) = \frac{1}{2\omega}\left(e^{-\omega\tau}(1 + f(\omega)) + e^{\omega\tau} f(\omega)\right), \qquad \tau \in (0, \beta) \tag{5.32}$$

[14]Note that in frequency space the relation between real-time and Euclidean correlation functions is not simple, since Euclidean correlation functions are only defined at discrete imaginary frequencies.

with

$$f(\omega) = \frac{1}{e^{\beta\omega} - 1} \ . \tag{5.33}$$

Note that outside the range in 5.32, $g_E(\tau)$ is periodic.

For our purpose it is enough to examine the Wightman function for M_1,

$$D_+(t) = \frac{1}{Z(\beta)} \mathrm{tr} \left(e^{-\beta H} M_1(t) M_1(0) \right) \ . \tag{5.34}$$

An exactly parallel argument to that of the last section leads to the expansion

$$D_+(t, \lambda) = \sum_{n=0}^{\infty} \lambda^n D_+^{(n)}(t) \tag{5.35}$$

where typical terms in $D_+^{(n)}(t)$ have the t-dependence of the form

$$d_{kl}^{(n)}(\beta) t^l e^{ik\omega_0 t} \tag{5.36}$$

The convergence of series depends on how $d_{kl}^{(n)}$ fall off with n. For our purpose it is enough to concentrate on the term with the highest power t in each order, i.e. the coefficients of t^n with given k. More explicitly, we will look at a term of the form

$$D_+(t, \lambda) = D_+^{(0)}(t) \sum_{n=0}^{\infty} c_n \lambda^n t^n + \cdots \tag{5.37}$$

where $D_+^{(0)}$ is the free theory expression.

As before we will first compute 5.37 in Euclidean time and then perform an analytic continuation. Calculating c_n explicitly at each loop order for all n is of course impractical. Our strategy is as follows. We will identify a family (in fact infinite families as we will see below) of planar Feynman diagrams of increasing loop order and show that their contribution to c_n falls off like a power in n. Barring any unforseen magical cancellation[15], this would imply that the perturbation series 5.28 has a zero

[15]Note that since we are in the high temperature phase, in which supersymmetry is badly broken, there is no obvious reason for suspecting such magical cancelations.

radius of convergence in the $t \to \infty$ limit. The simplest set of diagrams which meet our purpose are given by:

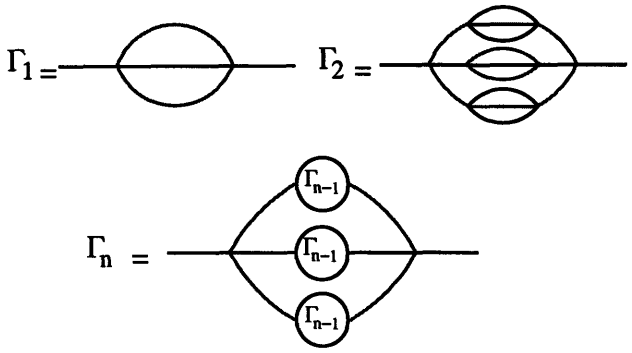

Figure 5-1: A family of diagrams which indicates that the perturbation theory break down in the long time limit. Black and red lines denote propagators of M_1 and M_2 respectively.

These graphs appear at orders $d_1 = 2, d_2 = 8, d_3 = 26, \cdots$ of perturbation theory where

$$d_i = 3d_{i-1} + 2 = 3^i - 1, \qquad i = 1, 2 \cdots . \tag{5.38}$$

We denote the contribution of each diagram by $\Gamma_i(\tau)$. For our purpose, it is not necessary to compute the full graph. We will only need to calculate the term in each graph with the highest power of τ, i.e. the term proportional to τ^{d_i}. Also note that in each diagram, the symmetry factor is exactly 1. Let us start with Γ_1, which is given by

$$\Gamma_1(\tau - \tau') = \lambda^2 \int_0^\beta d\tau_1 d\tau_2 \, g_E(\tau - \tau_1; \omega_0) g_E^3(\tau_1 - \tau_2; \omega_0) g_E(\tau_2 - \tau'; \omega_0) \tag{5.39}$$

Note the identity

$$g_E^3(\tau; \omega_0) = \frac{3}{(2\omega_0)^2} f^2(\omega_0) \left(e^{\beta\omega_0} g_E(\tau; \omega_0) + \frac{f(\omega_0)}{f(3\omega_0)} g_E(\tau; 3\omega_0) \right) \tag{5.40}$$

Now plug 5.40 into 5.39. It is easy to convince oneself that the term proportional to

$g_E(\tau;3\omega_0)$ in 5.40 will not generate a term proportional to τ^2 and we will ignore it. The contribution of the term proportional to $g_E(\tau;\omega_0)$ can be found by noting the identity

$$\int_0^\beta d\tau_1 d\tau_2\; g_E(\tau-\tau_1;\omega_0)g_E(\tau_1-\tau_2;\omega_0)g_E(\tau_2-\tau';\omega_0) = \frac{1}{2}\frac{\partial^2}{(\partial\omega_0^2)^2}g_E(\tau-\tau';\omega_0) \quad (5.41)$$

The right hand side of 5.41 contains a piece $\frac{1}{2}\frac{(\tau-\tau')^2}{(2\omega_0)^2}g_E(\tau-\tau')$ plus parts with smaller powers of $\tau-\tau'$. Thus the term in 5.39 proportional to $(\tau-\tau')^2$ is given by

$$\Gamma_1(\tau-\tau') = \frac{\alpha\lambda^2}{2}(\tau-\tau')^2 g_E(\tau-\tau') + \cdots \quad (5.42)$$

where

$$\alpha = \frac{3f(1+f)}{(2\omega_0)^4}, \qquad f = f(\omega_0) \quad (5.43)$$

The term proportional to τ^{d_i} for higher order diagrams $\Gamma_i(\tau)$ can now be obtained by iterating the above procedure. A useful identity is

$$\begin{aligned}&\int_0^\beta d\tau_1 d\tau_2\; g_E(\tau-\tau_1;\omega_0)g_E(\tau_1-\tau_2;\omega_0)\,(\tau_1-\tau_2)^n\, g_E(\tau_2-\tau';\omega_0) = \\ &= \frac{(\tau-\tau')^{n+2}}{(2\omega_0)^2}\frac{1}{(n+2)(n+1)}g_E(\tau-\tau';\omega_0) + \cdots \end{aligned} \quad (5.44)$$

where we kept only the term with the highest power of $\tau-\tau'$, as lower power terms will not contribute to the terms in which we are interested. We find that the term proportional to τ^{d_i} in $\Gamma_i(\tau)$ is given by

$$\Gamma_i(\tau) = F_i\lambda^{d_i}\tau^{d_i}g_E(\tau;\omega_0) + \cdots \quad (5.45)$$

where F_i satisfy the recursive relation

$$F_{i+1} = F_i^3\frac{\alpha}{d_{i+1}(d_{i+1}-1)}\,. \quad (5.46)$$

Thus F_i can be written as

$$F_i = \alpha^{\frac{d_i}{2}} \Lambda_i \tag{5.47}$$

with

$$\Lambda_i = \prod_{k=0}^{i-1} \left(\frac{1}{d_{i-k}(d_{i-k}-1)} \right)^{3^k} \tag{5.48}$$

Λ_i in the large i limit can be easily estimated and we find

$$\Lambda_i \approx e^{-\frac{3}{2}d_i}, \qquad i \gg 1 \, .$$

Summing all our diagrams together and analytically continuing to Lorentzian time with $\tau = it + \epsilon$, we find that[16]

$$\sum_i \Gamma_i(t) \approx D_+^{(0)}(t) \sum_{i=1}^{\infty} (-1)^i \left(\frac{\lambda t}{h_c} \right)^{d_i} + \cdots \tag{5.49}$$

with h_c given by

$$h_c = \frac{e^{\frac{3}{2}}}{\sqrt{\alpha}} = \frac{e^{\frac{3}{2}}(2\omega_0)^2}{\sqrt{3f(1+f)}} \tag{5.50}$$

Equation 5.49 implies that the radius of convergence in λ is given by

$$\lambda_c(t) \sim \frac{1}{t} \tag{5.51}$$

which goes to zero as $t \to \infty$.

It is also instructive to repeat the computation of 5-1 in frequency space using the real-time method. The calculation is straightforward and we will only summarize the result. One finds that the contribution of Γ_i to the Feynman function $D_F(\omega)$ grows like $d_i!$. Thus one expects that the perturbative expansion in frequency space is not

[16]Since we are only interested in the asymptotic behavior of the sum for large i we have replaced F_i by its asymptotic value.

well defined for any frequency. Note that the non-analyticity in frequency space can be expected since in going to frequency space one has to integrate the full real time-axis and the Fourier transform is sensitive to the long time behavior. Also note that the $n!$ factorial behavior in perturbation theory often implies an essential singularity at $\lambda = 0$ (see also below).

We conclude this section with some remarks:

- 1. In the zero-temperature limit $h_c \to \infty$ and the set of terms in 5.49 all go to zero.

- 2. To simplify our discussion, we have only considered diagrams in 5-1. There are in fact many other diagrams of similar type contributing at other orders in λ. For example, by including those in fig.2, one can get contributions for all even orders in λ rather than only 5.38. The qualitative conclusion we reached above is not affected by including them[17].

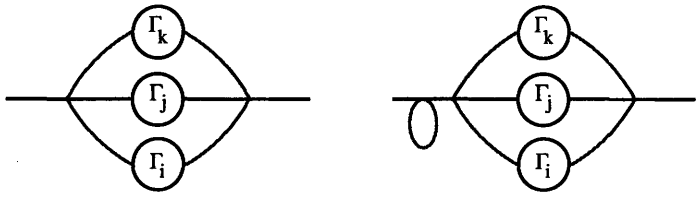

Figure 5-2: By including the diagrams on the left with all possible $i, j, k \geq 0$ we can get contribution at every even order of λ instead of 5.38. Γ_0 denotes a single propagator. Diagrams on the right can also contribute to the odd orders if 5.3 contains additional interactions of the form $\mathrm{tr}A^2B^2$.

- 3. By taking in consideration the diagrams on the left of 5-2 the sum in 5.49 is extended [18] to all even powers of λt and is oscillating therefore the singularities in λt should lie on the imaginary axis. Let us suppose that for a given λ, $D_+(t)$ has a singularity in t at q_c/λ with q_c lying in the upper half plane[19]. Now Fourier

[17]There are also potentially an infinite number of other sets of diagrams which can lead to the behavior 5.51, e.g. one can replace Γ_1 by any diagram whose highest power in t is the same as the order of perturbation and then iterates.

[18]the value of h_c also changes

[19]Note that q_c^*/λ must also be a singularity of $D_+(t)$.

transforming $D_+(t)$ we find that

$$D_+(\omega) = \int_{-\infty}^{\infty} dt\, e^{i\omega t}\, D_+(t) \tag{5.52}$$

The presence of q_c/λ and q_c^*/λ implies $D_+(\omega)$ contains a term of the form for $\omega > 0$

$$D_+(\omega) \sim e^{i\omega \frac{q_c}{\lambda}} \tag{5.53}$$

Thus $D_+(\omega)$ contains an essential singularity at $\lambda = 0$.

- 4. The $n!$ behavior in perturbative expansion in frequency space (say in the computation of $D_F(\omega)$) arises from a *single* class of Feynman diagrams. This is reminiscent of renormalons in field theories [37, 59, 91]. In particular, when Borel resumming the divergent series, depending on whether ω is greater or smaller than ω_0, the singularities on the Borel plane can appear on the positive or negative real axis[20], also reminiscent of the IR and UV renormalons.

- 5. Note that in the limit $T \to \infty$, h_c in 5.50 scales with T as $h_c \sim \frac{\omega_0^3}{T}$, i.e.

$$\lambda_c(t) \sim \frac{\omega_0^3}{tT} \tag{5.54}$$

For fixed λ, we expect a singularity for $D_+(t)$ at

$$t \sim \frac{\omega_0^3}{\lambda T} \tag{5.55}$$

Note that the right hand side of 5.55 is reminiscent of the magnetic mass scale for a Yang-Mills theory (see e.g. [38]). However, in our matrix quantum mechanics, there is no infrared divergence and it is not clear whether there is a connection.

- 6. The discussion can be straightforwardly applied to a generic theory in 5.1 with cubic and quartic couplings. In fact the argument also applies to a single

[20]Since we only have contributions to even order in λ, we cannot make a conclusion from our discussion so far.

anharmonic oscillator at finite temperature, even though in that case one does not expect the perturbative expansion to converge anyway[21]. Similarly, the argument also applies to a single-matrix quantum mechanics if one does not impose the singlet condition. When imposing the singlet condition, the matrix U in equation 5.18 cannot be set to 1 and our argument does not apply. Similarly our argument does not apply to 5.1 in the low energy sector, in which U is always important. Indeed using the results of [24, 30], one can show that to leading order in the large N limit, correlation functions at finite temperature can be written in terms of those at zero temperature and we do expect that the perturbation theory has a finite radius of convergence.

- 7. Our argument indicates that perturbation theory breaks down in the long time limit for a generic theory in 5.1. However, for any specific theory (say $\mathcal{N} = 4$ SYM theory) we cannot rule out magical cancelations which could in principle make the coefficients of n-th order term much smaller than indicated by the diagrams we find. If magical cancelations do occur in some theory, that would also be extremely interesting since it indicates some hitherto unknown hidden structure[22].

5.4 Physical explanation for the breakdown of planar expansion

In this section we give a simple physical explanation for the breakdown of perturbation theory in the long time limit. The discussion below should apply to a generic theory in 5.1. For definiteness we use $\mathcal{N} = 4$ SYM as an illustration example.

We first set up some notations. We write the full Hamiltonian as

$$H = H_0 + V(\lambda) \tag{5.56}$$

[21] In Appendix B3, we present an alternative argument for the breakdown of perturbation theory for the case of a single anharmonic oscillator.

[22] Since we are working at a finite temperature, supersymmetry alone should not be sufficient for the cancelations.

with H_0 the Hamiltonian of the free theory and V the interaction. We denote a free theory energy eigenstate by $|a\rangle$ with energy ϵ_a. $|0\rangle$ is the (unique) free theory vacuum. The energy eigenstates of the interacting theory H are denoted by $|i\rangle$ with energy E_i. $|\Omega\rangle$ is the interacting theory vacuum. We can expand

$$|i\rangle = \sum_a c_{ia} |a\rangle \tag{5.57}$$

with c_{ia} satisfying

$$\sum_a |c_{ia}|^2 = \sum_i |c_{ia}|^2 = 1 \ . \tag{5.58}$$

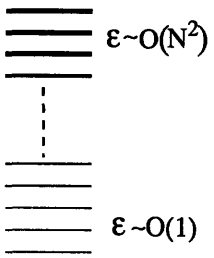

Figure 5-3: The energy spectrum of free $\mathcal{N} = 4$ SYM on S^3 is quantized. Typical degeneracy for an energy level $\epsilon \sim O(1)$ is of order $O(1)$. Typical degeneracy for a level of energy $\epsilon \sim O(N^2)$ is of order $e^{O(N^2)}$.

We first recall some relevant features of the free theory energy spectrum of $\mathcal{N} = 4$ SYM on S^3. Since ω_α in 5.1 are all integer or half-integer multiples of $\omega_0 = \frac{1}{R}$, the free theory energy spectrum is quantized in units $\frac{1}{2}\omega_0$. Typical energy levels are degenerate. The degeneracy is of $O(1)$ in the low energy sector and of order $e^{O(N^2)}$ in the high energy sector. The exponentially large degeneracy in the high energy sector can be seen as follows. From 5.7 the density of states $\Omega_0(\epsilon)$ in the high energy sector is of order $e^{O(N^2)}$. Since the energy levels are equally spaced with spacings order $O(1)$, it must be that typical energy levels have a degeneracy of order $e^{O(N^2)}$. Alternatively, the number of ways to construct a state of energy of order $O(N^2)$ from $O(N^2)$ oscillators of frequency of $O(1)$ is clearly exponentially large in N^2.

Now let us turn on the interaction $V(\lambda)$ 5.2 with a tiny but nonzero λ. We will

focus on the high energy sector. Given that free theory energy levels are highly degenerate, one would like to apply degenerate perturbation, say to diagonalize V in a degenerate subspace of energy $E \approx \mu N^2$ and of dimension $e^{O(N^2)}$. For this purpose we need to choose a basis in the degenerate subspace. This is a rather complicated question, due to difficulties in imposing singlet conditions[23]. However, when μ is sufficiently large we expect the singlet condition not to play an important role[24]. So to simplify our discussion we will ignore the singlet condition below. A convenient orthonormal basis of energy eigenstates for H_0 are then monomials of various oscillators (appropriately normalized), i.e.

$$\prod_{\alpha} \prod_{i,j=1}^{N} \left(M^{\dagger}_{\alpha ij}\right)^{n_{\alpha ij}} |0\rangle \ . \tag{5.59}$$

In the basis 5.59, if the full theory is not integrable, V can be effectively treated as an (extremely) sparse random matrix[25]. The sparseness is due to that each term in V can connect a given monomial state to at most N^k other states, where k is an $O(1)$ number[26]. Randomness has to do with the large dimension of the subspace and to the fact that there is no preferred ordering for the states within the same subspace. Diagonalizing V, we thus expect, from general features of a sparse random matrix (see Appendix B2,B4 for a summary),

- 1. The degeneracy of the free theory will generically be broken[27].
- 2. A number of states of order $e^{O(N^2)}$ will mix under the perturbation.
- 3. The typical level spacing between energy levels should be proportional to the inverse of the density of states and is thus exponentially small, of order $e^{-O(N^2)}$.

[23]The trace relations are important for states of such energies.

[24]As remarked earlier, in the high temperature limit the saddle point for U (in 5.18) approaches the identity matrix.

[25]Here we restrict V to a single energy level. When including all energy levels V is banded and sparse. The banded structure is due to energy conservation.

[26]This is because each term in V is a monomial of a few matrices.

[27]For Yang-Mills theories on S^3, there are remaining degeneracies associated with the isometry group $SO(4)$ of S^3. Except when one considers the sectors with very large angular momenta on S^3, typical representations of $SO(4)$ are rather small and should not affect our general argument.

The story is in fact a little more intricate. We expect the degenerate perturbation to be a good guide if the spread of energy eigenvalues after diagonalizing V in a subspace is smaller than the spacings between nearby energy levels. The spread Γ of eigenvalues of V can be estimated by (see Appendix B4)

$$\Gamma^2 \sim \Gamma_a^2 = \sum_{a \neq b} |\langle a|V|b\rangle|^2 \sim O(N^2) \tag{5.60}$$

for any nonzero λ, where the sum restricts to a degenerate subspace. Note that 5.60 only depends on that V is a single trace operator and does not depend on the specific structure of it. That $\Gamma \sim O(N)$ implies that it is not sufficient to diagonalize V within a degenerate subspace. It appears more appropriate to diagonalize[28] it in a subspace with energy spread of order $O(N)$. Thus in addition, we expect that:

- 4. an interacting theory eigenstate $|i\rangle$ is strongly coupled to free theory states $|a\rangle$ within an energy shell of order $O(N)$.

This statement will be justified in the next section from a somewhat different perspective. That $\Gamma \sim O(N)$ for any nonzero λ in the 't Hooft limit indicates a tiny λ may not really be considered as a small perturbation after all.

Various features discussed above when turning on a small λ are clearly non-perturbative in nature. However, it may be hard to probe them directly using Euclidean space observables like partition functions and Euclidean correlation functions. These observables probe only average behaviors within an energy difference range of order $O(T)$ or larger and thus may not be sensitive to the changes in level spacings at smaller scales[29]. In contrast, real-time correlation functions are much more sensitive.

[28]This statement is of course only heuristic since there is no sharp criterion to decide what should be the precise size of the subspace. However, we expect the N scaling should be robust.

[29]Of course if one is able to compute Euclidean observables exactly, one should be able to extract all the interesting physics. After all, real-time observables can be obtained from Euclidean ones by analytic continuation. It is just often the case that real-time physics is encoded in a very subtle way in Euclidean observables.

For example, consider the Lehmann spectral decomposition of $G_+(t)$, i.e.

$$\begin{aligned} G_+(t) &= \frac{1}{Z}\mathrm{tr}\left(e^{-\beta H}\mathcal{O}(t)\mathcal{O}(0)\right) \\ &= \frac{1}{Z}\sum_{i,j} e^{-\beta E_i + i(E_i - E_j)t} |\langle i|\mathcal{O}(0)|j\rangle|^2 \end{aligned} \tag{5.61}$$

where we have inserted complete sets of energy eigenstates $|i\rangle$ of the interacting theory. From 5.61, it is clear that $G_+(t)$ can in principle probe any small energy differences, provided one takes t to be large enough. This explains the breakdown of perturbation theory in the long time limit observed in $G_+(t)$. At large N, the $\lambda \to 0$ and $t \to \infty$ limits do not commute. We conclude this section the following remarks:

- 1. The argument presented in this section, while strongly indicating that the planar perturbation theory should break down in the long time limit, does not however tell us why it breaks down at a time scale 5.55. It would be interesting to have a concrete physical understanding of the relevance of 5.55.

- 2. As discussed as the end of section 5.3, the same Feynman diagram calculation of that section would indicate that the perturbation theory for anharmonic oscillators (say take $N = 1$ in 5.3) also breaks down at a time scale 5.55. We emphasize that while from the Feynman diagram point of view the discussion for anharmonic oscillators is almost identical to that for a matrix quantum mechanics (except that for matrix quantum mechanics one restricts to planar diagrams), the underlying physics for the breakdown of perturbation theory is rather different. In the case of anharmonic oscillators, the issues discussed in the earlier part of this section do not arise. See Appendix B3 for a discussion on the underlying reason for an anharmonic oscillator.

5.5 A statistical approach

The argument of section 5.4 shows that the planar perturbation theory breaks down in the large time limit, but it does not tell us what the long time behavior is. Non-

perturbative tools are needed to understand the long time behavior of real time correlation functions in the large N limit. Here we develop a statistical approach, taking advantage of the extremely large density of states in the high energy sector. In this section we outline the main idea and the results, leaving detailed calculations to various appendices. The statistical approach enables us to derive some qualitative features satisfied by the Wightman function for a generic operator at finite temperature, including that it has a continuous spectral density function and should decay to zero in the long time limit. The features we find here are also shared by the Wightman function at strong coupling found from supergravity analysis.

Our starting point is the Lehmann spectral decomposition of $G_+(t)$ 5.61,

$$G_+(t) \ = \frac{1}{Z}\sum_{i,j} e^{-\beta E_i + i(E_i - E_j)t}\rho_{ij} \tag{5.62}$$

where

$$\rho_{ij} = |\ \langle i|\mathcal{O}(0)|j\rangle\ |^2 = |\mathcal{O}_{ij}|^2 \tag{5.63}$$

In momentum space

$$G_+(\omega) = \frac{1}{Z}\sum_{i,j} e^{-\beta E_i}\delta(\omega + E_i - E_j)\rho_{ij}\ . \tag{5.64}$$

Matrix elements $\mathcal{O}_{ij}$ can in turn be expressed in terms of those of free theory using (c_{ia} was introduced in 5.57)

$$\mathcal{O}_{ij} = \langle i|\mathcal{O}(0)|j\rangle = \sum_{a,b} c^*_{ia}c_{jb}\langle a|\mathcal{O}|b\rangle = \sum_{a,b} c^*_{ia}c_{jb}\mathcal{O}_{ab} \tag{5.65}$$

where we have inserted complete sets of free theory states and $\mathcal{O}_{ab} = \langle a|\mathcal{O}(0)|b\rangle$.

Since for sufficiently high temperature, the sums in 5.64 and 5.65 are peaked at an energy with an extremely large density of states, one should be able to obtain the qualitative behavior of ρ_{ij} and $G_+(\omega)$ from statistical properties of $\mathcal{O}_{ab}$ and c_{ia}. As discussed in the last section, in the interacting theory, we expect typical level

spacings scale with N like $e^{-O(N^2)}$. In the large N limit, E_i can be considered as taking continuous values. Note that this by itself does not imply that $G_+(\omega)$ has a continuous spectral decomposition, since it is possible that ρ_{ij} only has support for states with finite energy differences. We argue below that ρ_{ij} has nonzero support between states with any $E_i - E_j \in (-\infty, \infty)$, which is independent of N, and thus $G_+(\omega)$ does have a continuous spectrum.

Let us first look at the statistical behavior of c_{ia}. For this purpose, consider the following density functions

$$\rho_a(E) = \sum_i |c_{ia}|^2 \delta(E - E_i) \tag{5.66}$$

$$\chi_i(\epsilon) = \sum_a |c_{ia}|^2 \delta(\epsilon - \epsilon_a) \tag{5.67}$$

$\rho_a(E)$, first introduced by Wigner [95], is also called the local spectral density function or strength function in the literature[30]. Using normalization properties of c_{ia}, one finds that

$$\int dE\, \rho_a(E) = 1, \qquad \int d\epsilon\, \chi_i(\epsilon) = 1 \tag{5.68}$$

$\rho_a(E)$ can be considered as the distribution of interacting theory eigenstates of energy E coupling to a free theory state $|a\rangle$. Similarly, $\chi_i(\epsilon)$ gives the distribution of free theory states of energy ϵ coupling to an exact eigenstate $|i\rangle$. The mean and the variances of the two distributions are given by

$$\overline{E}_a = \int dE\, E\, \rho_a(E) = \langle a|H|a\rangle \tag{5.69}$$

$$\sigma_a = \Gamma_a^2 = \int dE\, (E - \overline{E}_a)^2\, \rho_a(E) = \sum_{b \neq a} |\, \langle a|V|b\rangle\, |^2 \tag{5.70}$$

[30]These density functions have been frequently used in quantum chaos literature, see e.g. [31]

$$\bar{\epsilon}_i = \int d\epsilon\, \epsilon\, \chi_i(\epsilon) = E_i - \langle i|V|i\rangle \tag{5.71}$$

$$\Sigma_i = \Delta_i^2 = \int d\epsilon\, (\epsilon - \epsilon_i)^2\, \chi(E_i, \epsilon) = \sum_{j\neq i} |\, \langle i|V|j\rangle\, |^2 \tag{5.72}$$

$\overline{E}_a$ and Γ_a give the center and the spread of interacting theory energy eigenstates coupling to a free state $|a\rangle$. Similarly, $\bar{\epsilon}_i$ and Δ_i give the center and the spread of free theory states coupling to an interacting theory energy eigenstate $|i\rangle$. Γ_a can be considered as a measure of correlation among energy levels of the interacting theory (since states whose energies differ by Γ_a could couple to the same free theory state and are thus correlated). Δ_i characterizes the range of free theory states which are mixed by perturbation. Note that the heuristic discussion after equation 5.60 implies that $\Delta_i \sim O(N)$, which we will confirm below using a different method.

Individual energy eigenstates are rather hard to work with. We will consider microcanonical averages of 5.66 and 5.67. After all, for 5.62 and 5.64 we only need the behavior of ρ_{ij} averaged over states of similar energies. We will denote the average[31] of $\chi_i(\epsilon)$ over interacting theory states of energy E by $\chi_E(\epsilon)$ and similarly the average of $\rho_a(E)$ over free theory states $|a\rangle$ of similar energy ϵ by $\rho_\epsilon(E)$. Since the averages involve a huge number of states and the large N limit is like a thermodynamic limit in the high energy sector, we will assume that $\chi_E(\epsilon)$ is a smooth *slow* function[32] of E, i.e. it depends on E only through E/N^2. Similarly $\rho_\epsilon(E)$ is assumed to depend on ϵ only through ϵ/N^2. The center and variance of $\chi_E(\epsilon)$ and $\rho_\epsilon(E)$ will be denoted by $\bar{\epsilon}(E)$, $\Sigma(E) = \Delta^2(E)$, $\overline{E}(\epsilon)$, and $\sigma(\epsilon) = \Gamma^2(\epsilon)$ respectively[33]. These quantities should also be slow functions of E or ϵ as they inherit the property from $\chi_E(\epsilon)$ and $\rho_\epsilon(E)$.

[31]More explicitly, the average can be written as

$$\chi_E(\epsilon) = \frac{1}{\Omega(E)} \sum_{E_i\in(E-\delta,E+\delta)} \chi_i(\epsilon) \tag{5.73}$$

where δ is small enough that $\Omega(E)$ does not vary significantly in the range $(E-\delta, E+\delta)$.

[32]Note that a function $f(E)$ is considered a slow function if it can be written in a form $f(E) = N^a g(E/N^2)$, where $g(x)$ is a function independent of N.

[33]which can also be obtained by the average of various quantities 5.69-5.72 to leading order in large N.

In the Appendix B4 we estimate these quantities and find that

$$\begin{aligned} \overline{\epsilon}(E) &= N^2 g(\lambda, E/N^2) \\ \Sigma(E) &= N^2 h(\lambda, E/N^2) \\ \overline{E}(\epsilon) &= N^2 \tilde{g}(\lambda, \epsilon/N^2) \\ \sigma(\epsilon) &= N^2 \tilde{h}(\lambda, \epsilon/N^2) \end{aligned} \tag{5.74}$$

We emphasize that the large N scalings above only depend that V is given by N times single trace operators. Given that the underlying theory is not integrable and the extremely large number of states, we will thus approximate c_{ia} for fixed i as a random unit vector which centers at $\overline{\epsilon}_i$ with a spread of order $\Delta_i \sim O(N)$.

Now we turn to the statistical properties of $\mathcal{O}_{ab}$. Our earlier discussion for V in the free state basis 5.59 can be carried over to any operator $\mathcal{O}$ of dimension $O(1)$. Thus $\mathcal{O}_{ab}$ can be considered as an sparse banded random matrix. The matrix is banded since from energy conservation $\mathcal{O}$ can only connect states whose energy difference is smaller than the dimension of $\mathcal{O}$. Note that even though $\mathcal{O}_{ab}$ is sparse, for each row (or column), the number of nonzero entries grows with N as a power.

To summarize, we will assume the following statistical properties for c_{ia} and $\mathcal{O}_{ab}$:

- 1. For a given i, c_{ia} is a random unit vector with support inside an energy shell of width $O(N)$. In particular, the c_{ia} satisfy the same distribution for $|a\rangle$ of the same energy.

- 2. $\mathcal{O}_{ab}$ is banded sparse random matrix, with the number of nonzero entries growing with N as a power.

Now consider any two states $|i\rangle$ and $|j\rangle$, with energies E_i and E_j respectively, for which $\omega = E_i - E_j \sim O(1)$. One finds that $\overline{\epsilon}_i - \overline{\epsilon}_j \sim O(1)$ and the energy shells of the two states overlap significantly. Given that the number of nonzero entries in a row or column of $\mathcal{O}_{ab}$ grows with N as a power and that each element of c_{ia} satisfies the same distribution, one concludes from 5.65 that $\mathcal{O}_{ij}$ should have support for any $\omega = E_i - E_j \sim O(1)$ and $G_+(\omega)$ has a continuous spectrum for $\omega \in (-\infty, +\infty)$. Note that

the fact that $\Delta \sim O(N)$ is crucial for having a continuous spectrum $\omega \in (-\infty, +\infty)$. Suppose $\Delta \sim O(1)$, the spectrum cannot extend to $\pm\infty$ due to energy conservation.

One can further work out more detailed properties of ρ_{ij}. Leaving the detailed calculation in various appendices, we find that (after averaging ρ_{ij} over states of similar energies)

$$\rho_{E_1 E_2} = \frac{1}{\Omega(E)} A(\omega; E) = e^{-S(E)} A(\omega; E) \tag{5.75}$$

where $\Omega(E)$ and $S(E) = \log \Omega(E)$ are the density of states and entropy of the interacting theory respectively and

$$E = \frac{E_1 + E_2}{2}, \qquad \omega = E_1 - E_2 \ .$$

Equation 5.75 is derived in Appendix B6 along with properties of $A(\omega; E)$ stated below. Some useful formulas used in the derivation are collected in Appendix B5. $A(\omega; E)$ can be expressed in terms of an integral of $\chi_E(\epsilon)$ and $\bar{\epsilon}(E)$ (see equations (G.3) and (G.8)) and satisfies the following properties:

- 1. $A(\omega; E)$ is an even function of ω, i.e.

$$A(-\omega; E) = A(\omega; E) \tag{5.76}$$

- 2. As $\omega \to \infty$

$$A(\omega; E) \propto e^{-\frac{1}{2}\beta(E)|\omega|}, \qquad \beta(E) = \frac{\partial S(E)}{\partial E} \tag{5.77}$$

- 3. $A(\omega, E)$ is integrable along the real axis and can at most have integrable singularities of the form

$$A(\omega; E) \propto \frac{1}{|\omega - \omega_s|^{\alpha_s}}, \qquad \alpha_s < 1 \ . \tag{5.78}$$

- 4. $A_E(\omega)$ depends on E only through E/N^2, i.e. it can be written as

$$A(\omega; E) = A(\omega; \mu), \qquad \mu = \frac{E}{N^2} \tag{5.79}$$

and A is a function independent of N.

Note that property 2 implies that in the large N limit, $\rho_{E_1 E_2} \sim 0$ for $E_1 - E_2 \sim N^a$ with $a > 0$.

The expression for $G_+(\omega)$ in momentum space can now be obtained by plugging 5.75 into 5.64 and using a saddle point approximation. We find that

$$\begin{aligned} G_+(\omega) &= \frac{1}{Z}\int dE\, e^{-\beta E}\, e^{S(E)+S(E+\omega)} e^{-S(E+\omega/2)} A(\omega, E/N^2) \\ &= \frac{1}{Z}\int dE\, e^{-\beta E + S(E)} \left[e^{S(E+\omega)-S(E+\omega/2)} A(\omega, E/N^2)\right] \\ &= e^{\frac{\beta\omega}{2}} A(\omega, \mu_\beta) \end{aligned} \tag{5.80}$$

where

$$\mu_\beta = \frac{E_\beta}{N^2}, \qquad \left.\frac{\partial S(E)}{\partial E}\right|_{E_\beta} = \beta\ . \tag{5.81}$$

Note that since in the large N limit, E can be treated as continuous and ρ_{ij} has support for any energy difference, it is appropriate to approximate the sum in 5.64 by an integral. Also from the second line to the third line we have used that the quantity inside the bracket depends on E slowly and performed a saddle point approximation. We conclude this section with some remarks:

- 1. $G_+(\omega)$ has a continuous spectrum with $\omega \in (-\infty, +\infty)$ in the large N limit (note that ω does not scale with N).

- 2. Since $A(\omega, \mu)$ can at most have integrable singularities of the form 5.78 on the real axis, after a Fourier transform to coordinate space, $G_+(t)$ must go to zero in the limit $t \to \infty$. If $A(\omega; \mu)$ is a smooth function on the real axis, then $G_+(t)$ must decay exponentially with time.

- 3. Considering the last line of 5.80 as a definition for $A(\omega;\mu)$, for $\mathcal{N}=4$ SYM on S^3 at strong coupling, the corresponding $A(\omega;\mu)$ can be found by solving the Laplace equation for a scalar field in an AdS black hole geometry and be expressed in terms of boundary values of renormalizable wave functions for the scalar field [27]. In particular, $A(\omega;\mu)$ found at strong coupling satisfy all the properties 5.76–5.79 (it is a smooth function on the real axis).

- 4. It should be possible to obtain an explicit expression for $A(\omega;\mu)$ (and thus $G_+(\omega)$) using the expressions found in the appendices (e.g. equation (G.3)) if one can find the density functions 5.66 and 5.67 for a sparse banded random matrix with varying density of states. While those for constant density of states have been discussed in the literature (see e.g. [31]), not much appears to be known for the non-constant density of states.

5.6 Discussions

In this chapter we first showed that in perturbation theory, real-time correlation functions in the high temperature phase of 5.1 have a discrete spectrum and the system does not thermalize when perturbed away from thermal equilibrium. We then argued that the perturbative expansions for real-time correlation functions break down in the long time limit. The breakdown of perturbation theory indicates that at large N the $\lambda \to 0$ and $t \to \infty$ limits do not commute. The reason for the breakdown is that a wide energy range (of order $O(N)$) of degenerate free theory energy eigenstates mix under the interaction. The level spacings in the energy spectrum of $O(1)$ in the free theory become $e^{-O(N^2)}$. As a result, real-time correlation functions develop a continuous spectrum for any nonzero λ. The continuous spectrum was argued from a statistical approach developed in section 5.5, where we also show that real-time correlation functions should decay to zero as $t \to \infty$ and the system becomes time irreversible.

We should emphasize that our arguments in this chapter are qualitative in nature and far from foolproof. For example, instead of being a random vector, c_{ia} could have

some structure (e.g. being very sparse) within the range of its spread, in which case our statistical argument will not be valid.

It is also important to emphasize our results only apply to the high energy sector and in the low energy sector (or in the low temperature), there is no indication of breakdown of the planar expansion. In particular the results we describe here are not inconsistent with that the sector near the vacuum might be integrable in the large N limit [68, 13, 20, 55, 86, 14].

Our results indicate that there is a large N "phase transition" at $\lambda = 0$, i.e. physical observables undergo qualitative changes in the limit $\lambda \to 0$. The "phase transition" we find here is somewhat unusual, since it is not manifest in the Euclidean quantities like the partition function. The partition function appears to be smooth in the $\lambda \to 0$ limit. The "phase transition" is in real-time correlation functions and their Fourier transforms. Real-time correlation functions decay to zero at large time at any finite λ, while oscillatory for $\lambda = 0$. In frequency space there is an essential singularity at $\lambda = 0$.

It would be interesting to understand whether one can continue the physics at small λ to large λ. If there is no further large N "phase transition" in λ, we expect that the analytic structure of various correlation functions observed at strong coupling should also be present at small λ. Such structure include the signatures of black hole singularities [28, 27] and the bulk-cone singularities [52].

Given that an arrow of time emerges for small λ in the large N limit, it is natural to ask what should be the string theory interpretation of the high temperature phase for $\mathcal{N} = 4$ SYM on S^3 at weak coupling, or from the microcanonical point of view, what is the bulk interpretation for a generic state in the high energy sector.

From the parameter relations in AdS/CFT,

$$\frac{l_s^2}{R^2} = \frac{1}{\sqrt{\lambda}}, \qquad \frac{G_N}{R^8} = \frac{1}{N^2}, \qquad G_N = l_p^8 \sim g_s^2 l_s^8, \quad . \tag{5.82}$$

one might conclude that at weak coupling $\lambda \ll 1$, $l_s \gg R$, i.e. the string length l_s is much bigger than the AdS curvature radius R. However, it seems unlikely one can

give an invariant meaning to the statement. For example, even starting with a metric with $R \ll l_s$, one could perform a field redefinition of the form $g_{\mu\nu} \to g_{\mu\nu} + \alpha' R_{\mu\nu} + \cdots$. In terms of new metric one then has $R \sim l_s$. Thus it seems to us that even for $\lambda \ll 1$, the corresponding bulk string theory should describe a spacetime of stringy scale, rather than sub-stringy scale. This is also expected from the gauge theory point of view. At weak coupling the only mass scale is the inverse radius of the sphere and there are no other lighter degrees of freedom. Thus the string scale has to be of the same order as that of the AdS curvature scale.

Can one interpret the bulk configuration corresponding to the high temperature phase at weak coupling as a stringy black hole? It seems to us the answer is likely to be yes. Let us list the properties that the corresponding bulk configuration should satisfy as expected from gauge theory, assuming there is no further large N "phase transition" between weak and strong couplings:

- 1. The bulk configuration should have an entropy and free energy of order $O(1/g_s^2)$.
- 2. The object absorbs all fundamental probes (since boundary correlation functions decay with time).
- 3. The bulk geometry should have a horizon (since the boundary theory has a continuous spectrum).
- 4. The bulk configuration is likely to have singularities (since the signatures of the black hole singularities in gauge theory at strong coupling cannot disappear as the coupling is changed if there is no phase transition).
- 5.A generic matter distribution will collapse into such a configuration (since in the boundary theory, a generic initial state will approach the thermal equilibrium).
- 6. Results in [1, 88] indicate that the Euclidean time circle in the dual geometry for the theory in the high temperature phase should become contractible[34].

[34]Note that this alone cannot imply that the bulk geometry is a black hole since even at zero cou-

From the properties above, it seems appropriate to call it a stringy black hole.

Finally let us mention that it is possible that a stronger version of equation 5.75 holds, i.e. for two generic states $|i\rangle$, $|j\rangle$ in the high energy sector,

$$\rho_{ij} = \frac{1}{\Omega(E)} A(\omega; E)\mathcal{R}_{ij}, \tag{5.83}$$

with

$$E = \frac{E_i + E_j}{2}, \qquad \omega = E_i - E_j$$

and $\mathcal{R}_{ij}$ a random matrix. Equation 5.83 is considered to be the hallmark of quantum chaos [78, 85][35]. Thus it is possible that $\mathcal{N} = 4$ SYM is chaotic in the high energy sector. Such a chaotic behavior, if it exists, might be related to the BKL behavior near a spacelike singularity [18].

pling the time circle becomes contractible. As we argued earlier in this chapter real-time correlation functions in free theory do not behave like those of a black hole.

[35]It has also been argued in [85] that if 5.83 holds, then thermalization always occurs.

Chapter 6

Conclusion

In the first part of this thesis we have considered an eternal Schwarzschild black hole embedded in AdS_5. For large enough mass this classical supergravity background is dual to $\mathcal{N} = 4$ $SU(N)$ SYM at finite temperature in the large N and large coupling λ limit. The question we tried to address was if and how the gauge theory correlators probed the region beyond the horizon and near the singularity of the black hole.

By considering two point wightman functions $G_+(\omega)$ of scalar operators of large conformal dimension we established a direct relation between the complex ω plane and the Penrose diagram of the spacetime. For each complex ω a particular spacelike geodesic gives most of the contribution to the correlator. For real values of ω the geodesic does not probe the region beyond the horizon; as $\omega \to \infty$ it stays closer and closer to the boundary of spacetime. For imaginary values of ω however the geodesic enters the region beyond the horizon and comes closer and closer to the singularity as $\omega \to i\infty$. By studying this limit we pinpointed two features of the correlation function which directly reflect the presence of the singularity in the bulk spacetime. One of this signatures in particular, the exponential decay of $G_+(\omega)$ as $\omega \to \pm i\infty$, persists without change as the dimension of the operators is made smaller as can be established by computing the correlation function in many different approximation schemes.

Some avenues of future research that stem from these results are the following:

- Extend the analysis to higher point correlation functions. These should encode the singularity in more striking way as their computation involves integrating interaction vertices over the bulk geometry.

- The relation between imaginary frequencies and bulk geometry should be investigated further. The usual UV/IR correspondence in AdS/CFT associates the energy scale of objects in the CFT side with the "distance" of their duals from the boundary; can we establish an intuitive dual description of the time coordinate inside the horizon?

- The CFT evolves according to the bulk Schwarzschild time; is there a dual description for the proper time as measured by observers falling freely into the black hole? It can be that an answer to this question could be obtained by analyzing the behaviour of bulk to boundary correlators instead of limiting us to the boundary to boundary case.

- The eternal black hole solution is a background of choice due to its high degree of symmetry. Is it possible to generalize our analysis to a gravitational collapse scenario?

Having established the presence of signatures of the bulk singularity in the CFT at large N and large coupling λ the question arises to try to use them to understand how the singularity is resolved by stringy (finite λ) effects or quantum gravity (finite N). As N is made finite the gauge theory has a discrete spectrum for any λ preventing the analytic continuation of correlators to imaginary frequencies. The signatures of the singularity we have found therefore disappear. It could still be though, that even in the large N limit finite λ is sufficient to resolve the singularity. A first step towards the understanding of this issue is that of determining what is the physical origin of the continuous spectrum in the CFT in the large N limit.

As we have seen in the introduction the presence of a continuous spectrum in the CFT is related to thermalization and the presence of an arrow of time and an horizon in the bulk description. On the other end its presence requires the large

N limit necessarily as for any finite λ the CFT is a bounded quantum mechanical system. In the second part of this thesis we addressed the question of how an arrow of time arises in the CFT in the large N limit and for what values of the coupling it happens.

Working in the large N limit we first established that at no finite order in perturbation theory a continuous spectrum is generated. We also found strong indications that the perturbative series does not converge for any nonzero value of λ at high enough temperature. We gave the following interpretation to this breakdown of perturbation theory: at high temperatures the gauge theory probes properties of the spectrum at energies of order N^2. In the free theory at these energies the energy levels are extremely degenerate e^{cN^2}. As soon as a nonzero interaction is turned on states with energies differing by $O(\lambda N)$ interact strongly and produce a very dense spectrum which appears as continuous in the large N limit. We also established that the resulting correlation functions have spectral properties compatible with those found at strong coupling using the black hole background.

This analysis provides some indications that the singularity could survive string corrections and be resolved only by quantum gravitational effects. If this were true the states in the gauge theory of energy $O(N^2)$ would be dual to the microstates of a stringy black hole. In order to be able to substantiate this assertions however the following problems have to be addressed:

- Even if λ is small we have established that the large N perturbation theory breaks down at high temperature signaling the presence of a large N phase transition at $\lambda = 0$. It would be useful to develop the tools necessary to establish the presence at small λ of the singularity signatures described in the first part of this work. This goal could be reached either by explicit resummation of the perturbation theory series or by improving the statistical methods introduced in the last chapter. Also these should be extended from the toy models taken in consideration so far to the case of gauge theories reduced on S^3 if an explicit comparison with the strong coupling results is sought.

- It would then be necessary to exclude the presence of a phase transition at finite λ in the large N limit which would prevent us to follow the singularity present at large λ to the small coupling regime.

- Finally we could study the resolution of the singularity due to quantum gravitational effects by looking at the gauge theory at finite λ.

The final hope and the motivation of our study is that of giving a contribution to the understanding of spacelike singularities and their resolution in string theory. As we have seen a possible window to this problem is provided by the AdS-CFT correspondence. Progress in this direction, besides providing us with further hints as to the structure of a theory of quantum gravity could give us new tools and ways to look at gauge theories which could find a useful application elsewhere in the future.

Appendix A

Appendix A

A.1 Bulk propagators in the Hartle-Hawking vacuum

In the Hartle-Hawking vacuum (see e.g. [22]), one has the mode expansion

$$\phi = \sum_{i=1}^{2} \int_0^\infty \frac{d\omega}{2\pi} \int \frac{d\vec{p}}{(2\pi)^{d-1}} \left(H^{(i)}_{\omega p} b^{(i)}_{\omega p} + H^{(i)*}_{\omega p} b^{(i)\dagger}_{\omega p} \right) \tag{A.1}$$

where

$$\begin{aligned} H^{(1)}_{\omega p} &= \cosh\theta_\omega \phi^{(1)}_{\omega p} + \sinh\theta_\omega \phi^{(2)}_{\omega p}, \\ H^{(2)}_{\omega p} &= \cosh\theta_\omega \phi^{(2)*}_{\omega p} + \sinh\theta_\omega \phi^{(1)*}_{\omega p} \ . \end{aligned} \tag{A.2}$$

$\phi^{(1,2)}$ denote a complete sets of normalizable modes supported only in the right (R) and left (L) quadrants of the black hole spacetime respectively, i.e.

$$\begin{aligned} \phi^{(1)}_{\omega p} &= \begin{cases} e^{-i\omega t + i\vec{p}\cdot\vec{x}} r^{-\frac{d-1}{2}} \psi_{\omega p}(r) & R \\ 0 & L \end{cases} \\ \phi^{(2)}_{\omega p} &= \begin{cases} 0 & R \\ e^{-i\omega t + i\vec{p}\cdot\vec{x}} r^{-\frac{d-1}{2}} \psi_{\omega p}(r) & L \end{cases} \ . \end{aligned} \tag{A.3}$$

$\psi_{\omega p}$ is given by the solutions of 2.34 which satisfy the boundary conditions 2.40–2.41. It is an even function of ω. In A.2, θ_ω is given by

$$\tanh\theta_\omega = e^{-\frac{\omega\beta}{2}} \ .$$

$b^{(i)}_{\omega p}$ satisfy the commutation relations

$$[b^{(i)}_{\omega p}, b^{(j)\dagger}_{\omega' p'}] = (2\pi)^d \delta(\omega-\omega')\delta(\vec{p}-\vec{p}')\delta_{ij}, \qquad i,j=1,2$$

Plugging in A.1 into 2.28 one finds that when both points are located in the right quadrant, the expression for $\mathcal{G}_+$ in momentum space is given by

$$\mathcal{G}_+(\omega,p;r,r') \ = \frac{1}{2\omega}\frac{e^{\beta\omega}}{e^{\beta\omega}-1}(rr')^{-\frac{d-1}{2}}\psi_{\omega p}(r)\psi_{\omega p}(r') \tag{A.4}$$

If instead one of the points is located in the left quadrant, then one finds the Fourier transform of the corresponding quantity (which we denote by $\mathcal{G}_{12}$) is given by

$$\mathcal{G}_{12}(\omega,p;r,r') = e^{-\frac{1}{2}\beta\omega}\mathcal{G}_+(\omega,p;r,r') \tag{A.5}$$

A.5 gives rise to 2.27 when taking $r,r' \to \infty$. By passing we note that the bulk Feynman and retarded propagators in the momentum space are given by (with both points in the right quadrant)

$$\begin{aligned}
\mathcal{G}_F(\omega,p;r,r') &= (rr')^{-\frac{d-1}{2}}\int_{-\infty}^{\infty}\frac{d\omega'}{2\pi}\frac{1}{1-e^{-\beta\omega'}}\frac{1}{\omega'^2-\omega^2-i\epsilon}\psi_{\omega' p}(r)\psi_{\omega' p}(r') \\
\mathcal{G}_R(\omega,p;r,r') &= (rr')^{-\frac{d-1}{2}}\int_{0}^{\infty}\frac{d\omega'}{2\pi}\frac{1}{\omega'^2-(\omega+i\epsilon)^2}\psi_{\omega' p}(r)\psi_{\omega' p}(r')
\end{aligned} \tag{A.6}$$

Introducing the spectral density function

$$\rho(\omega,p;r,r') = \frac{1}{2\omega}(rr')^{-\frac{d-1}{2}}\psi_{\omega p}(r)\psi_{\omega p}(r'), \tag{A.7}$$

one finds that various propagators can be written in terms of ρ as

$$\begin{aligned}
\mathcal{G}_+(\omega,p;r,r') &= \frac{e^{\beta\omega}}{e^{\beta\omega}-1}\rho(\omega,p;r,r') \\
\mathcal{G}_R(\omega,p;r,r') &= -\int_{-\infty}^{\infty}\frac{d\omega'}{2\pi}\frac{\rho(\omega',p;r,r')}{\omega-\omega'+i\epsilon} \\
\mathcal{G}_F(\omega,p;r,r') &= \mathcal{G}_R(\omega,p;r,r')+\frac{i}{e^{\beta\omega}-1}\rho(\omega,p;r,r')
\end{aligned} \tag{A.8}$$

which is exactly what one would expects of a thermal theory.

A.2 BTZ

In this appendix, we look at the example of a non-rotating BTZ black hole [7] in which case the corresponding boundary G_+ can be found exactly. In particular we will be able to check explicitly the relation between the bulk geodesics and the large ν limit of G_+ proposed in the main text.

A.2.1 Exact solution

For a non-rotating BTZ black hole, the metric can be written as

$$ds^2 = -f dt^2 + \frac{1}{f}dr^2 + r^2 dx^2 \tag{A.9}$$

with

$$f = r^2 - 1 \tag{A.10}$$

and x a periodic variable. The complexified temperature is $\mathcal{B} = 2i\pi$ that is $\beta' = 0$ and the Penrose diagram 2-1 is a square. The tortoise coordinate z is given by

$$r = \coth z\ . \tag{A.11}$$

The potential 2.35 becomes

$$\begin{aligned} V_p &= (r^2-1)\left[\frac{p^2+\frac{1}{4}}{r^2}+\nu^2-\frac{1}{4}\right] \\ &= \frac{p^2+\frac{1}{4}}{\cosh^2 z}+\frac{\nu^2-\frac{1}{4}}{\sinh^2 z} \end{aligned} \tag{A.12}$$

Changing variables in 2.34 to

$$y = 1-\frac{1}{r^2} = \frac{1}{\cosh^2 z}$$

and letting

$$\psi_{\omega p} = y^{\frac{i}{2}\omega}(1-y)^{\frac{\nu}{2}+\frac{1}{4}}w(y)$$

$w(x)$ satisfies the hypergeometric equation

$$y(1-y)\frac{d^2w}{dy^2}-[c-(a+b+1)y]\frac{dw}{dy}-abw=0 \tag{A.13}$$

with parameters

$$a = q_+ + i\frac{\omega+p}{2}, \qquad b = q_+ + i\frac{\omega-p}{2}, \qquad c = 1+i\omega, \qquad q_+ = \frac{1}{2}(1+\nu)$$

Various functions defined in 2.46 are then given by

$$g(y) = y^{\frac{i\omega}{2}}(1-y)^{\frac{\nu}{2}+\frac{1}{4}}F\left(q_+ + i\frac{\omega+p}{2}, q_+ + i\frac{\omega-p}{2}; 2q_+; 1-y\right) \tag{A.14}$$

and

$$\begin{aligned} h_A(y) &= \left(\frac{y}{4}\right)^{\frac{i\omega}{2}}(1-y)^{\frac{\nu}{2}+\frac{1}{4}}F\left(q_+ + i\frac{\omega+p}{2}, q_+ + i\frac{\omega-p}{2}; 1+i\omega; y\right) \\ h_R(y) &= \left(\frac{y}{4}\right)^{-\frac{i\omega}{2}}(1-y)^{\frac{\nu}{2}+\frac{1}{4}}F\left(q_+ - i\frac{\omega-p}{2}, q_+ - i\frac{\omega+p}{2}; 1-i\omega; y\right) \end{aligned} \tag{A.15}$$

One finds that

$$g(y) = \frac{1}{2i\omega}\left(h_A f(\omega,p) - h_R f(-\omega,p)\right) \tag{A.16}$$

with the Jost function

$$f(\omega,p) = -\frac{2^{i\omega+1}\Gamma(2q_+)\Gamma(1-i\omega)}{\Gamma(q_+ - i\frac{\omega+p}{2})\Gamma(q_+ - i\frac{\omega-p}{2})} \tag{A.17}$$

It then follows from 2.52

$$G_+ \ = \frac{e^{\pi\omega}}{\pi(\Gamma(\nu))^2}\Gamma(q_+ - i\tfrac{\omega+p}{2})\Gamma(q_+ - i\tfrac{\omega-p}{2})\Gamma(q_+ + i\tfrac{\omega+p}{2})\Gamma(q_+ + i\tfrac{\omega-p}{2}) \tag{A.18}$$

A.2.2 Structure of poles

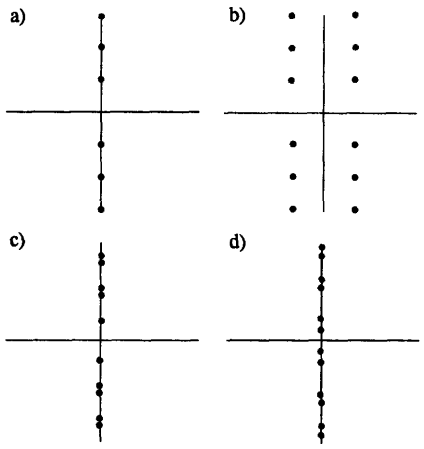

Figure A-1: The structure of poles for G_+ for (a): $p^2 = 0$, (b): $p^2 > 0$, (c): $-\nu^2 < p^2 < 0$, (d): $p^2 < -\nu^2$. In (d), the blue dot in the upper half ω-plane correspond to a bound state.

The poles of A.18 arise from zeros of $f(\omega,p)$ and $f(-\omega,p)$. Equation A.17 has two lines of zeros at

$$\omega = -2i(n+q_+) - p, \qquad \omega = -2i(n+q_+) + p, \qquad n = 0,1,\cdots \tag{A.19}$$

We consider $p = i\nu q$ $(q > 0)$ pure imaginary, then zeros of f are at

$$\omega = -i(2n+1) - i\nu(1+q), \qquad \omega = -i(2n+1) + i\nu(q-1), \qquad n = 0,1,\cdots$$

When $q > 1 + \frac{1}{\nu}$, there are zeros on upper half plane at

$$\omega = i\nu(q-1) - i, \quad i\nu(q-1) - 3i, \quad \cdots, \quad i\nu(q-1) - (2m-1)i \tag{A.20}$$

where m satisfies $\nu(q-1)-(2m-1) > 0$ and $\nu(q-1)-(2m+1) < 0$. A.20 correspond to the bound states of the system. The structure of poles for G_+ is plotted in A-1.

For $p^2 > 0$ the lines of poles do not lie on the imaginary ω axis and therefore in the limit 3.15 divide the asymptotic $u = \frac{\omega}{\nu}$ plane in four different asymptotic regions.

A.2.3 Asymptotic behavior of G_+

We now examine the behavior of G_+ in the limit of large ω along various directions of the complex plane. For real $p > 0$ we find that

$$G_+ \approx \begin{cases} \frac{4\pi}{(\Gamma(\nu))^2}\left(\frac{\omega}{2}\right)^{2\nu} & \omega \to +\infty \\ \frac{4\pi}{(\Gamma(\nu))^2}\left(-\frac{\omega}{2}\right)^{2\nu} e^{2\pi\omega} & \omega \to -\infty \\ \frac{4\pi}{(\Gamma(\nu))^2}\left(\frac{|\omega|}{2}\right)^{2\nu} e^{\pi\omega - \pi p} & \omega \to \pm i\infty \end{cases} \tag{A.21}$$

The opening of four distinct asymptotic region in the ω plane for $p^2 > 0$ is reflected in the different asymptotic behaviour for $\omega \to \infty$ along the real and imaginary axis.

A.2.4 Large ν limit

We now consider large ν limit with $\omega = \nu u$ and $p = \nu k$. Then equation A.18 can be expanded as

$$G_+(\omega, p) = 2\nu\, e^{\nu Z}\left(1 + O(e^{-\nu u})\right)\left(1 + O(\nu^{-1})\right) \tag{A.22}$$

with

$$Z = \pi u + A_+ \log A_+ + A_- \log A_- + \tilde{A}_+ \log \tilde{A}_+ + \tilde{A}_- \log \tilde{A}_- \tag{A.23}$$

and

$$A_\pm = \frac{1}{2} \pm \frac{i}{2}(u+k), \qquad \tilde{A}_\pm = \frac{1}{2} \pm \frac{i}{2}(u-k)$$

In the large ν limit the series of poles become branch cuts with the branch points located at

$$u = \pm k \pm i \qquad \text{or} \qquad u^2 = -(1 \pm ik)^2$$

The branch cuts are parallel to the imaginary axis.

A.2.5 Geodesic approximation

One can check that equation A.23 can be obtained using the geodesic approximation 3.41 and 3.42. The real physical momenta k and u correspond to complex geodesics with pure imaginary $E = -iu$ and $q = -ik$, while real bulk geodesics with real E, q describe behaviors of G_+ along the imaginary axis. More explicitly, various quantities in 3.42 can be integrated directly to obtain

$$\begin{aligned} L(u,k) &= -\frac{1}{2}\log(A_+\tilde{A}_+A_-\tilde{A}_-) \\ t(u,k) &= \frac{1}{2}\log\left(\frac{A_+\tilde{A}_+}{A_-\tilde{A}_-}\right) - \frac{i\beta}{2} \\ x(u,k) &= -\frac{1}{2}\log\left(\frac{A_+\tilde{A}_-}{A_-\tilde{A}_+}\right) \end{aligned} \tag{A.24}$$

We note that for $k > 0$ real, $u \to +i\infty$, we find that

$$t \approx -i\pi, \qquad x \approx -i\pi$$

which reproduces the third line of A.21. Note that in this limit the geodesics becomes approximately null and its turning point (given by $r_1^2 = -\frac{k^2}{u^2}$) approaches the singularity. The fact that t is pure imaginary is a consequence of that the Penrose diagram

of a BTZ black hole is a square.

A.3 Solutions to 3.2

Without last two terms in 3.2, the equation reduces to the hypergeometric type. To see this explicitly, considering a change of coordinate

$$y = \tanh^2 \rho = \frac{r^2 - r_0^2}{r^2 + r_1^2}, \qquad r^2 = \frac{r_0^2 + r_1^2 y}{1 - y} \tag{A.25}$$

where the horizon is at $y = 0$ and the boundary is at $y = 1$. Let

$$u(y) = y^{p-\frac{1}{4}}(1-y)^{q_- - \frac{1}{2}} w(y) \tag{A.26}$$

with

$$p = \frac{1}{2} - \frac{ih}{4}, \qquad q_\pm = \frac{1}{2}(1 \pm \nu), \qquad \nu = \sqrt{4 + m^2}$$

then $w(y)$ satisfies the standard form of the hypergeometric differential equation

$$y(1-y)\frac{d^2 w}{dy^2} - [c - (a+b+1)y]\frac{dw}{dy} - abw = 0 \tag{A.27}$$

with parameters

$$b = q_- - \frac{\omega \mathcal{B}}{4\pi}, \qquad a = q_- + \frac{\omega \overline{\mathcal{B}}}{4\pi}, \qquad c = 2p = 1 - \frac{ih}{2}\,. \tag{A.28}$$

We now write down various solutions with specified boundary conditions and various functions discussed in sec. 2.3. The solution $h_R(\omega, y)$ specified by equation 2.46 corresponds to

$$h_R(\omega, y) \;\; = \sqrt{\tfrac{2}{r_0}} e^{-i\omega\gamma} F(a, b, c; y) \tag{A.29}$$

where γ is constant independent of ω. Then by working out the behavior near the boundary we obtain

$$h_R(y) = \sqrt{\frac{2}{\beta}} e^{-i\omega\gamma} \left(\frac{\Gamma(c)\Gamma(\nu)}{\Gamma(c-a)\Gamma(c-b)} (r_0^2 + r_1^2)^{-\frac{\nu}{2}} \tilde{g}(y) + \frac{\Gamma(c)\Gamma(-\nu)}{\Gamma(a)\Gamma(b)} (r_0^2 + r_1^2)^{\frac{\nu}{2}} g(y) \right)$$

with $\tilde{g}$ and g as defined in 2.46. From the above expression using 2.54 and 2.48 and 2.52 we find that

$$\begin{aligned} G_R(\omega) &= 2\nu \left(\frac{2\pi}{|\mathcal{B}|}\right)^{2\nu} \frac{\Gamma(-\nu)}{\Gamma(\nu)} \frac{\Gamma(\frac{1+\nu}{2} - \frac{\omega\mathcal{B}}{4\pi})\Gamma(\frac{1+\nu}{2} + \frac{\omega\bar{\mathcal{B}}}{4\pi})}{\Gamma(\frac{1-\nu}{2} - \frac{\omega\mathcal{B}}{4\pi})\Gamma(\frac{1-\nu}{2} + \frac{\omega\bar{\mathcal{B}}}{4\pi})} \\ G_{12} &= \frac{1}{\pi(\Gamma(\nu))^2} \left(\frac{2\pi}{|\mathcal{B}|}\right)^{2\nu} \Gamma\left(\frac{1+\nu}{2} - \frac{\omega\mathcal{B}}{4\pi}\right) \cdot \\ &\cdot \Gamma\left(\frac{1+\nu}{2} - \frac{\omega\bar{\mathcal{B}}}{4\pi}\right) \Gamma\left(\frac{1+\nu}{2} + \frac{\omega\mathcal{B}}{4\pi}\right) \Gamma\left(\frac{1+\nu}{2} + \frac{\omega\bar{\mathcal{B}}}{4\pi}\right) \end{aligned} \tag{A.30}$$

For $\nu = n,\ n = 1, 2, \cdots$, equation A.30 should be replaced by

$$G_R = \frac{2(-1)^n}{(\Gamma(n))^2} \left(\frac{2\pi}{|\mathcal{B}|}\right)^{2n} P_{2n}(\omega) \left[\psi\left(\frac{n+1}{2} - \frac{\omega\mathcal{B}}{4\pi}\right) + \psi\left(\frac{n+1}{2} + \frac{\omega\bar{\mathcal{B}}}{4\pi}\right) \right] \tag{A.31}$$

where P_{2n} is a polynomial of order $2n$

$$P_{2n}(\omega) = \frac{\Gamma\left(\frac{1+n}{2} - \frac{\omega\mathcal{B}}{4\pi}\right) \Gamma\left(\frac{1+n}{2} + \frac{\omega\bar{\mathcal{B}}}{4\pi}\right)}{\Gamma\left(\frac{1-n}{2} - \frac{\omega\mathcal{B}}{4\pi}\right) \Gamma\left(\frac{1-n}{2} + \frac{\omega\bar{\mathcal{B}}}{4\pi}\right)} \tag{A.32}$$

and $\psi(z)$ is the Digamma function. When we use A.31 to compute G_{12} we obtain exactly the same expression as the non-integer case ??. For integer $\nu = n$, ?? can also be written as

$$G_{12} = \frac{\pi}{(\Gamma(n))^2} \left(\frac{2\pi}{|\mathcal{B}|}\right)^{2n} Q_{2n}(\omega) \frac{1}{\cos\left(\frac{n\pi}{2} + \frac{\omega\mathcal{B}}{4}\right) \cos\left(\frac{n\pi}{2} + \frac{\omega\bar{\mathcal{B}}}{4}\right)} \tag{A.33}$$

with Q_{2n} another polynomial of order $2n$

$$Q_{2n}(\omega) = \frac{\Gamma\left(\frac{1+n}{2} - \frac{\omega\mathcal{B}}{4\pi}\right) \Gamma\left(\frac{1+n}{2} - \frac{\omega\bar{\mathcal{B}}}{4\pi}\right)}{\Gamma\left(\frac{1-n}{2} - \frac{\omega\mathcal{B}}{4\pi}\right) \Gamma\left(\frac{1-n}{2} - \frac{\omega\bar{\mathcal{B}}}{4\pi}\right)} .$$

A.4 An alternative approximation

In this section we present another approximation of $G_R(\omega)$ and $G_+(\omega)$ which applies when $|\omega|$ is sufficiently large. The method described below was developed in [25, 71] to find the quasi-normal modes of AdS black holes. While not explicitly discussed there, approximate expressions for $G_R(\omega)$ for large $|\omega|$ can be easily extracted from the discussion of [25, 71], which we reproduce here. First the approximation and its regime of validity are briefly reviewed then we use it to determine the asymptotic expansion of $G_R(\omega)$ and $G_+(\omega)$ for real and imaginary ω.

In order to find $G_R(\omega)$ we start from the Schrodinger problem 2.34. Various solutions with different asymptotics at the boundary or at the horizon are defined in 2.46. In particular the solution $h_R(\omega)$ is a linear superposition of the solutions $g(\omega)$ and $\tilde{g}(\omega)$:

$$h_R(\omega) = C_- g(\omega) + C_+ \tilde{g}(\omega) \tag{A.34}$$

Then from 2.54 we get $G_R(\omega) = \frac{C_+}{C_-}$. Therefore we must find approximate expressions for C_+ and C_-.

We start with the Schrodinger equation 2.34 in the tortoise coordinate:

$$-\frac{d^2\psi_{\omega l}}{dz^2} + V_l(z)\psi_{\omega l} = \omega^2 \psi_{\omega l} \tag{A.35}$$

where the potential $V_l(z)$ is defined implicitly via r as:

$$V_l(z) = f(r)\left(\frac{(2l+d-2)^2-1}{4r^2} + \nu^2 - \frac{1}{4} + \frac{\mu(d-1)^2}{4r^d}\right) \tag{A.36}$$

ν was defined in 2.26 and the field $\psi(z)$ in eq A.35 has been expanded in spherical harmonics on S^3 ($\hat{e}$ is a point on S^3):

$$\psi(t,\hat{e},z) = \sum_l \int \frac{d\omega}{2\pi} e^{-i\omega t} Y_l(\hat{e})\psi_{\omega l}(z)$$

Below for notation simplicity, we will suppress the subscript ω l on ψ. We are

interested in approximating the differential equation A.35 for large $|\omega|$ with Bessel equations both near the singularity ($r = 0$) and close to the boundary ($r \to \infty$). When the regions of validity of these approximations overlap it is possible to match their solutions to obtain an approximation to h_R valid for any z. In the following we will consider $d > 2$ and μ fixed and we will find the values of ν and l for which the approximation works.

At the singularity $r \to 0$, one has $z \approx z_0 + \frac{1}{\mu(d-1)} r^{d-1}$ and the most divergent term in the potential is:

$$V_l(z) \approx -\frac{\mu^2(d-1)^2}{4r^{2d-2}} \approx -\frac{1}{4(z-z_0)^2} \tag{A.37}$$

Notice that this term of the potential is equal to ω^2 for $r = r* = \left(\frac{\mu(d-1)}{\omega}\right)^{\frac{1}{d-1}}$.

The potential A.37 would give an equation of Bessel type, however for l or ν large there are terms in the full potential proportional to $\frac{l^2}{r^d}$ and $\frac{\nu^2}{r^{d-2}}$ which could dominate over both ω^2 and $-\frac{\mu^2(d-1)^2}{4r^{2d-2}}$ for certain values of $r \sim 0$. In order for this not to be the case we must impose that these terms are $\ll \omega^2$ at $r = r*$ that is:

$$\begin{aligned} l^2\omega^{\frac{d}{d-1}} &\ll \omega^2 \Rightarrow l^2 \ll \omega^{\frac{d-2}{d-1}} \\ \nu^2\omega^{\frac{d-2}{d-1}} &\ll \omega^2 \Rightarrow \nu^2 \ll \omega^{\frac{d}{d-1}} \end{aligned} \tag{A.38}$$

If these conditions are satisfied A.37 is the only contribution to the potential to be considered for all values of r not close to the boundary.

It is useful to introduce a parameter j such that when $z \to 0$ the potential behaves like:

$$V(z) \approx \frac{j^2 - 1}{4(z-z_0)^2} \tag{A.39}$$

We will consider the equation for arbitrary j and we will recover the results for $j = 0$ by continuity. With A.39 equation A.35 reduces to a Bessel equation and

$$\psi(z) \sim A_+(2\pi\omega(z_0 - z))^{\frac{1}{2}} J_{j/2}(\omega(z_0 - z)) + A_-(2\pi\omega(z_0 - z))^{\frac{1}{2}} J_{-j/2}(\omega(z_0 - z)) \ . \tag{A.40}$$

This solution is a valid approximation everywhere except near the boundary ($r \sim \infty \quad z \sim 0$) as the term $(\nu^2 - \frac{1}{4})r^2$ in the potential becomes dominant over ω^2 for $r \sim O(\omega)$.

Near the spatial boundary , we have $z \approx \frac{1}{r}$ and,

$$V_l(z) \approx \left(\nu^2 - \frac{1}{4}\right) r^2 \approx \frac{\left(\nu^2 - \frac{1}{4}\right)}{z^2} \tag{A.41}$$

With A.41 equation A.35 also reduces to a Bessel equation and we find that

$$\psi(z) \quad \sim B_+(2\pi\omega z)^{\frac{1}{2}} J_\nu(\omega z) + B_-(2\pi\omega z)^{\frac{1}{2}} J_{-\nu}(\omega z) \tag{A.42}$$

That is by comparing the asymptotic form at the boundary with 2.46 :

$$\psi(z) = (2\pi\omega)^{\frac{1}{2}} \left[\frac{B_+}{\Gamma(1+\nu)} \left(\frac{\omega}{2}\right)^{\nu} \tilde{g}(z + \frac{B_-}{\Gamma(1-\nu)} \left(\frac{\omega}{2}\right)^{-\nu} g(z) \right] . \tag{A.43}$$

This form of the solution is valid everywhere except near the singularity $r(z) \sim r*$

We would like to find B_+, B_- in A.42 and A.43 for the solution h_R defined in 2.46

$$h_R(z) = \psi(z) \sim e^{i\omega z}, \qquad z \to \infty \tag{A.44}$$

In the large ω limit, the validity region of A.42 overlaps with that of A.40. In order to match these solutions unambiguously, it is convenient to take their arguments ωz and $\omega(z - z_0)$ real so that they exhibit an oscillatory behavior. For this purpose we will match these solutions along the line $z = sz_0, \quad s \in R$ in the complex z-plane and take ωz_0 real. The matching will give us expressions for B_+, B_- along the curve $\omega = \lambda z_0^{-1}$ in the complex ω-plane. We will then obtain their behaviors for other values of ω by analytic continuation. In order to understand what are the values of z_0 to use we impose that there are no branch points for $V(z)$ between the positive real z axis and the straight line $z = sz_0$ because otherwise the asymptotic behaviour of the solution for $Re(z) \to +\infty$ cannot be considered the same as the one on the real

axis given by A.44 . By considering the determination of the function $r(z)$ described in appendix A8 we then see that the two possible values for z_0 are given by $\frac{\mathcal{B}}{4}$ and $\frac{\overline{\mathcal{B}}}{4}$. The straight line $z = sz_0$ starts at $z = 0$ for $s = 0$ reaches the singularity at $s = 1$ and finally approaches the horizon for $s \to +\infty$. We cannot therefore match directly the form of the solution at the boundary $z = 0$ A.42 with the expected behavior at $z \to \infty$ as the matching line goes through the singularity. We will therefore first match A.44 and A.40 and then A.40 with A.42.

Consider first $z_0 = \frac{1}{4}(\beta' - i\beta) = \frac{\overline{\mathcal{B}}}{4}$. For ωz_0 real, we need $\omega = \lambda z_0^{-1}$. We will first consider $\lambda \in R_-$. For $z = sz_0$ and $s \to +\infty$, using the asymptotic expansion of the Bessel function we find that A.40 can be written as

$$\psi(z) \sim \left(A_+ e^{-i\pi\frac{(1+j)}{4}} + A_- e^{-i\pi\frac{(1-j)}{4}}\right) e^{i\omega(z_0-z)} + \left(A_+ e^{i\pi\frac{(1+j)}{4}} + A_- e^{i\pi\frac{(1-j)}{4}}\right) e^{-i\omega(z_0-z)}$$

The purely ingoing boundary condition A.44 at the horizon requires that the coefficient of $e^{-i\omega z}$ vanishes, which leads to

$$\frac{A_-}{A_+} = -e^{-\frac{i\pi j}{2}} \ . \tag{A.45}$$

The asymptotic behavior of $\psi(z)$ for $0 < (1 - s) \ll 1$, and $|\omega(z - z_0)| \gg 1$ can be obtained by rotating the argument $(z_0 - z)$ of the Bessel function of an angle π counterclockwise in the complex plane[1]. Using the fact that around $z = 0$ we have $J_s(e^{-i\pi}z) = e^{-i\pi s}J_s(z)$ we obtain

$$\psi(z) \sim \left(A_+ e^{i\pi\frac{(1+j)}{4}} + A_- e^{i\pi\frac{(1-j)}{4}}\right) e^{i\omega(z-z_0)} + \left(A_+ e^{3i\pi\frac{(1+j)}{4}} + A_- e^{3i\pi\frac{(1-j)}{4}}\right) e^{-i\omega(z-z_0)}$$

The asymptotic form of A.42 for $0 < s \ll 1 \quad |\omega z| \gg 1$ is given by

$$\psi(z) \sim \left(B_+ e^{\frac{-i\pi(1+2\nu)}{4}} + B_- e^{\frac{-i\pi(1-2\nu)}{4}}\right) e^{-i\omega z} + \left(B_+ e^{\frac{i\pi(1+2\nu)}{4}} + B_- e^{\frac{i\pi(1-2\nu)}{4}}\right) e^{i\omega z} \tag{A.46}$$

[1]in such a way not to cross the branch cut emanating from $z = z_0$ as described in appendix A8

Matching the two expressions above we find that

$$\begin{aligned} -2A_+e^{\frac{i\pi(1-j)}{4}}\sin(\pi j) &= e^{-i(\omega z_0+\frac{\pi}{4})}\left(B_+e^{-i\frac{\pi\nu}{2}}+B_-e^{i\frac{\pi\nu}{2}}\right) \\ 2iA_+e^{\frac{i\pi(1-j)}{4}}\sin(\frac{\pi j}{2}) &= e^{i(\omega z_0+\frac{\pi}{4})}\left(B_+e^{i\frac{\pi\nu}{2}}+B_-e^{-i\frac{\pi\nu}{2}}\right) \end{aligned} \tag{A.47}$$

which gives

$$\frac{B_+}{B_-} = -\frac{\cos\left(-\frac{\pi\nu}{2}+\omega z_0-\frac{i}{2}\ln(2\cos(\frac{j\pi}{2}))\right)}{\cos\left(\frac{\pi\nu}{2}+\omega z_0-\frac{i}{2}\ln(2\cos(\frac{j\pi}{2}))\right)} \tag{A.48}$$

For $\lambda > 0$, the steps are exactly parallel except that in this case it will be convenient to change the sign of the arguments of all the Bessel functions. We find that the matching gives us

$$\frac{B_+}{B_-} = -e^{-i\pi\nu} \tag{A.49}$$

Starting from the other value of $z_0 = \frac{1}{4}(\beta' + i\beta) = \frac{\beta}{4}$, one finds that for $\omega = \lambda z_0^{-1}$ and $\lambda \in R_+$

$$\frac{B_+}{B_-} = -\frac{\cos\left(\frac{\pi\nu}{2}+\omega z_0-\frac{i}{2}\ln(2\cos(\frac{j\pi}{2}))\right)}{\cos\left(-\frac{\pi\nu}{2}+\omega z_0-\frac{i}{2}\ln(2\cos(\frac{j\pi}{2}))\right)} \tag{A.50}$$

and for $\lambda \in R_-$

$$\frac{B_+}{B_-} = -e^{i\pi\nu} \tag{A.51}$$

A.4.1 Retarded propagators

The above results can be used to obtain the asymptotic expansion of the retarded propagator $G_R(\omega, l)$ along four directions in the complex ω plane. The retarded propagator for $\mathcal{O}$ in momentum space in the large ω limit is given by

$$G_R(\omega, l) = 2\nu\frac{\Gamma(1-\nu)}{\Gamma(1+\nu)}\left(\frac{\omega}{2}\right)^{2\nu}\frac{B_+}{B_-} \tag{A.52}$$

From A.48–A.51 we thus find that:

- 1. For $\omega = \lambda \overline{\mathcal{B}}^{-1}$, $\lambda \in R_-$ we have:

$$G_R = 2\nu \frac{\Gamma(-\nu)}{\Gamma(\nu)} \frac{\cos[-\frac{\pi\nu}{2} + \frac{\omega\overline{\mathcal{B}}}{4} - \frac{i}{2}\ln(2\cos(\frac{j\pi}{2}))]}{\cos[+\frac{\pi\nu}{2} + \frac{\omega\overline{\mathcal{B}}}{4} - \frac{i}{2}\ln(2\cos(\frac{j\pi}{2}))]} \left(\frac{-\omega}{2}\right)^{2\nu} \left(1 + O\left(\frac{1}{\omega}\right)\right) \quad \text{(A.53)}$$

- 2. For $\omega = \lambda \overline{\mathcal{B}}^{-1}$, $\lambda \in R_+$ we have:

$$G_R = 2\nu \frac{\Gamma(-\nu)}{\Gamma(\nu)} \left(\frac{\omega}{2}\right)^{2\nu} e^{-i\pi\nu} \left(1 + O\left(\frac{1}{\omega}\right)\right) \quad \text{(A.54)}$$

- 3. For $\omega = \lambda \mathcal{B}^{-1}$, $\lambda \in R_+$ we have:

$$G_R = 2\nu \frac{\Gamma(-\nu)}{\Gamma(\nu)} \frac{\cos[\frac{\pi\nu}{2} + \frac{\omega\mathcal{B}}{4} - \frac{i}{2}\ln(2\cos(\frac{j\pi}{2}))]}{\cos[-\frac{\pi\nu}{2} + \frac{\omega\mathcal{B}}{4} - \frac{i}{2}\ln(2\cos(\frac{j\pi}{2}))]} \left(\frac{\omega}{2}\right)^{2\nu} \left(1 + O\left(\frac{1}{\omega}\right)\right) \quad \text{(A.55)}$$

- 4. For $\omega = \lambda \mathcal{B}^{-1}$, $\lambda \in R_-$ we have:

$$G^R = 2\nu \frac{\Gamma(-\nu)}{\Gamma(\nu)} \left(\frac{-\omega}{2}\right)^{2\nu} e^{i\pi\nu} \left(1 + O\left(\frac{1}{\omega}\right)\right) \quad \text{(A.56)}$$

Note that the most singular term at $r \sim 0$ in the A.36 only appears through the shift $-\frac{i}{2}\ln(2\cos(\frac{j\pi}{2}))$. This factor diverges for $j \to 1$ as the corresponding term in the potential disappears . Another interesting case is $j = \frac{2}{3}$ for which in $d = 4$ the differential equation reduces to hypergeometric form for $l = 0$. In this case the exact form of $G_R(\omega)$ has been found in Appendix A3.

For $j = 0$ we find poles in $G_R(\omega)$ at:

$$\omega_n = \frac{4\pi}{\mathcal{B}}\left(\frac{1+\nu}{2} + n + \frac{i}{2}\log(2)\right), \quad \widetilde{\omega}_n = -\frac{4\pi}{\overline{\mathcal{B}}}\left(\frac{1+\nu}{2} + n - \frac{i}{2}\log(2)\right), \quad n = 0, 1, ...$$

It is important to notice that the asymptotic expression for G_R in A.54 can be obtained from that A.55 by an analytic continuation in the complex plane ω-plane through the real axis. This makes us believe that A.53 and A.55 can be trusted also to give the correct *subdominant pieces* in the expansion for large ω along the positive

real axis:

$$G_R(\omega) = 2\nu \frac{\Gamma(-\nu)}{\Gamma(\nu)} e^{-i\nu\pi} \left(\frac{\omega}{2}\right)^{2\nu} \cdot \\ \cdot \left[1 + 4i \cos\left(\frac{j\pi}{2}\right) \sin(\pi\nu) e^{2i\omega z_0} + ..\right] \left(1 + O\left(\frac{1}{\omega}\right)\right) \tag{A.57}$$

Note that the leading order terms reduce to the zero temperature result, which follows from conformal invariance. The coefficient of the subdominant part is controlled by coefficient j of the most singular term A.39 in the wave equation A.35 at the singularity. In particular, the subdominant term in A.57 goes away for $j = 1$, at which case A.39 vanishes. From A.57 we also find that

$$G_+ = -4\nu \frac{\Gamma(-\nu)}{\Gamma(\nu)} \left(\frac{\omega}{2}\right)^{2\nu} \sin(\pi\nu) \left[1 - 4\cos\left(\frac{j\pi}{2}\right) \cos\left(\nu\pi - \frac{\omega\tilde{\beta}}{2}\right) e^{-\frac{\omega\beta}{2}}\right] \left(1 + O\left(\frac{1}{\omega}\right)\right)$$

Similarly A.56 can be obtained from A.53 by analytic continuation through the negative real axis and we conclude that on the negative real axis (i.e. $\omega < 0$)

$$G_R(\omega) = 2\nu \frac{\Gamma(-\nu)}{\Gamma(\nu)} e^{i\nu\pi} \left(\frac{-\omega}{2}\right)^{2\nu} \left[1 - 4i \cos\left(\frac{j\pi}{2}\right) \sin(\pi\nu) e^{2i\omega\tilde{z}_0} + \cdots\right] \left(1 + O\left(\frac{1}{\omega}\right)\right)$$

$$G_+ = 4\nu \frac{\Gamma(-\nu)}{\Gamma(\nu)} \left(\frac{-\omega}{2}\right)^{2\nu} \sin(\pi\nu) e^{\omega\beta} \left[1 - 4\cos\left(\frac{j\pi}{2}\right) \cos\left(\nu\pi + \frac{\omega\tilde{\beta}}{2}\right) e^{\frac{\omega\beta}{2}}\right] \left(1 + O\left(\frac{1}{\omega}\right)\right)$$

We can also find the asymptotic expansion of G_R on the imaginary axis. For $\omega \in iR^-$ we get:

$$G_R(\omega) = 2\nu \frac{\Gamma(-\nu)}{\Gamma(\nu)} \left(\frac{i\omega}{2}\right)^{2\nu} \left(1 - 2i \sin(\pi\nu) \sinh\left(\frac{\beta\omega}{2}\right) \sec(\frac{j\pi}{2}) e^{-i\frac{\omega\tilde{\beta}}{2}} + ...\right) \left(1 + O\left(\frac{1}{\omega}\right)\right)$$

while for $\omega \in iR^+$:

$$G_R(\omega) = 2\nu \frac{\Gamma(-\nu)}{\Gamma(\nu)} \left(\frac{-i\omega}{2}\right)^{2\nu} \left(1 + O\left(\frac{1}{\omega}\right)\right)$$

For $\omega \in iR^-$ we also get:

$$G_+ = -2\nu \frac{\Gamma(-\nu)}{\Gamma(\nu)} \left(\frac{i\omega}{2}\right)^{2\nu} \sin(\pi\nu) \sec\left(\frac{\pi j}{2}\right) e^{-i\omega\frac{\beta}{2}}$$

A.5 A more sophisticated WKB analysis

A.5.1 general remarks

By performing the rescaling 3.24 equation 2.34 in the large ν limit reduces to:

$$\left(\frac{1}{\nu^2}\frac{d^2}{dz^2} - V(z) + u^2\right)\psi(z) = 0 \tag{A.58}$$

we want to find the form of $g(z)$ defined in 2.46 for $z \to \infty$. From there using 2.52 we will obtain an approximate expression for $G_+(u)$.

Define $\mathcal{Z}(z_0, z) = \int_{z_0}^{z} dz\kappa(z, u)$ where $\kappa(z, u) = \sqrt{V(z) - u^2}$

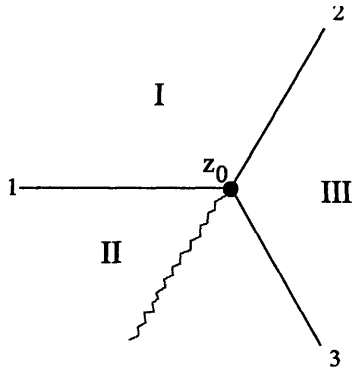

Figure A-2: Pattern of Stokes lines near a turning point

Close to a generic point z_0 the lines of constant imaginary part for $\mathcal{Z}(z_0, z)$ do not intersect. However whenever $V(z_0) = u^2$ there are three of these lines[2] converging towards z_0 at a $\frac{2\pi}{3}$ angle; these are called Stokes lines. On each of these $\mathcal{Z}(z_0, z) \in R$ and so the exponential factor $\kappa(z, u)^{-\frac{1}{2}} e^{\pm\nu\mathcal{Z}(z_0,z)}$ in the WKB approximation to the solution is real and either decreasing or increasing along the line. Both $\kappa(z, u)^{-\frac{1}{2}}$ and

[2]More than three lines is not a generic situation and is not considered

$\mathcal{Z}(z_0, z)$ are multi-valued functions around z_0 and we will define them by introducing a branch cut extending from z_0 in region II in A-2 . Suppose now $\mathcal{Z}(z_0, z) < 0$ along line 1; then in the WKB approximation of the solution decreasing along 1 only the term $\kappa(z,u)^{-\frac{1}{2}} e^{\nu \mathcal{Z}(z_0,z)}$ is present in regions I and II. We will find the WKB expansion of this solution in region III by applying the principle of exponential dominance stating that crossing a Stokes line the coefficient of the dominant term in the expansion does not change. The term $\kappa(z,u)^{-\frac{1}{2}} e^{\nu \mathcal{Z}(z_0,z)}$ is the dominant one on line 2 and so its coefficient is continuous and doesn't change while crossing it. However in region III we can also have a contribution proportional to $\kappa(z,u)^{-\frac{1}{2}} e^{-\nu \mathcal{Z}(z_0,z)}$ which will be the dominant one along line 3. In order to find its precise coefficient we analytically continue the expansion we have in region II up to line 3 but in doing so we cross the branch cut and so we get $-i\kappa(z,u)^{-\frac{1}{2}} e^{-\nu \mathcal{Z}(z_0,z)}$. Then in region III the asymptotic expansion is:

$$\psi(z) \sim \kappa(z,u)^{-\frac{1}{2}} (e^{\nu \mathcal{Z}(z_0,z)} - ie^{-\nu \mathcal{Z}(z_0,z)})$$

If instead the branch cut were in region I we would have obtained in analogous way:

$$\psi(z) \sim \kappa(z,u)^{-\frac{1}{2}} (e^{\nu \mathcal{Z}(z_0,z)} + ie^{-\nu \mathcal{Z}(z_0,z)})$$

Given a turning point z_0 its Stokes lines cannot intersect unless in another turning point which is not a generic situation and is excluded in what follows [3] and therefore divide the complex z plane into three regions. Two cases are possible:

a) The origin and $+\infty$ are in the same region then z_0 is called inactive

b)they are in different regions and z_0 is an active turning point.

For each active turning point imagine shading the regions in which the origin and $+\infty$ are; the intersection of all the shaded regions will be called active region in the following. Starting from the region containing the origin we can order the regions which are active by adjacency up to the one containing $+\infty$.

For every turning point there is a region which doesn't contain neither 0 or $+\infty$.

[3] these non generic cases are the ones that divide the parameter space in regions with topologically distinct patterns of Stokes lines

It is therefore possible to choose the branch cuts defining $\sqrt{V(z)-u^2}$ and $\mathcal{Z}$ in such a way that they do not cross into the active region.

Then in the active region we can globally define two wave-forms $\exp(\pm\nu\mathcal{Z}(z_0,z))$. For each wave-form the Stokes lines where it is dominant or subdominant are fixed by the sequence of active turning points as shown in figure.

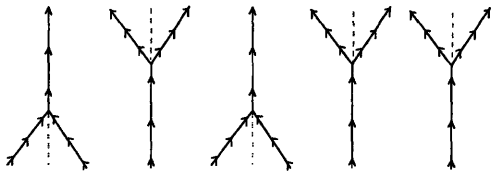

Figure A-3: schematic representation of the active region. The red dashed lines are branch cuts while the arrows are in the direction of decreasing real part for $\mathcal{Z}$

The WKB approximation to the desired solution is then given by choosing the appropriate coefficients of the two wave-forms in each region. When we cross one of the Stokes lines the coefficient in front of the wave-form which is dominant along that line does not change while the coefficient of the other wave changes according to the appropriate connection formula. Two cases are possible and are shown in figure (the arrows represent decreasing $\mathcal{Z}(z_0,z)$):

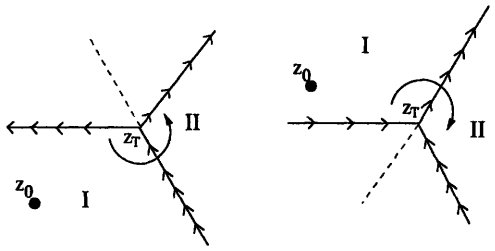

Figure A-4: Stokes line diagrams for the two cases of the connection formula at a turning point

Suppose we start with the wave $A\exp(\nu\mathcal{Z}(z_0,z))+B\exp(-\nu\mathcal{Z}(z_0,z))$ in region I then in the first case the first term is dominant while crossing the Stokes line and so its coefficient doesn't change. By applying the connection formula we get in region

II:

$$A\exp(\nu\mathcal{Z}(z_0,z)) + B\exp(-\nu\mathcal{Z}(z_0,z)) + iA\exp(\nu\mathcal{Z}(z_0,z_T) - \nu\mathcal{Z}(z_T,z))$$

while in the second case the dominant term is the second one and we obtain:

$$A\exp(\nu\mathcal{Z}(z_0,z)) - iB\exp(-\nu\mathcal{Z}(z_0,z_T) + \nu\mathcal{Z}(z_T,z)) + B\exp(-\nu\mathcal{Z}(z_0,z))$$

The application of the method just described to the specific case of the black hole background is in principle straightforward once the pattern of stokes lines corresponding to the values of k and u of interest is determined. Unfortunately the range of possibilities is quite extended and we will content ourselves to determine what are the turning points that give the dominant contribution to the result in various regimes and determine the position of quasi-normal modes.

Being $V(z(r))$ a single valued function of r it follows from the discussion in Appendix A8 of the function $r(z)$ that $V(z)$ will have branch points at those points z for which $r(z) = 0$. In the following we will use the determination for $r(z)$ described in Appendix A8 which has the following properties:

- 1 $Re(z) \to +\infty$ corresponds to $r(z)$ approaching the horizon. $z = 0$ corresponds to the boundary.
- 2 The only branch points present for $Re(z) > 0$ are located at $z = \frac{\beta}{4} + i\, n\frac{\beta}{2}$ where $n \in \mathbf{Z}$. For any branch point the branch cut extends on a line of constant imaginary part for z towards $Re(z) = -\infty$.
- 3 This determination is such that $V(z + i\frac{\beta}{2}) = V(z)$

A.5.2 k=0

We will now apply the method just described to the determination of the dominant contribution to $G_+(u)$ when $k = 0$ for different values of u. For u around the origin

[4] there is only one active turning point T (and its periodic images) which is the one considered in 3.30 for $u^2 \in R^+$. This is the turning point represented in 4-1 a). The pattern of Stokes lines is represented in figure for $Re(z) > 0$ and $Im(u) > 0$. The thick lines are the branch cuts extending from the singularity S at $z = \frac{\beta}{4} \pm \frac{2n+1}{4} i\beta \quad n \in \mathbf{Z}$ while the boundary at $z = 0$ is denoted by B.

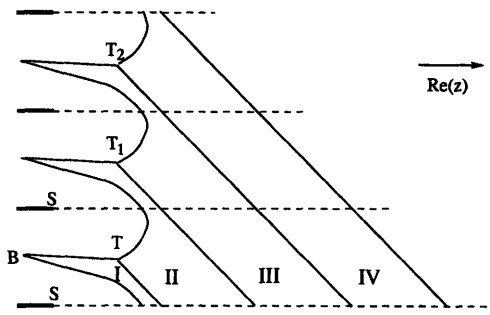

Figure A-5: Pattern of Stokes lines for $Re(z) > 0$ and $Im(u) > 0$

Requiring $\mathcal{Z}$ to be continuous in the active region fixes it up to a sign. In the following we will conventionally choose the determination of $\mathcal{Z}$ in the active region in the following way: For any two points $z_1 \quad z_2 = z_1 + i\frac{\beta}{2}$ the quantity $\mathcal{Z}(z_1, z_2)$ must be the same due to the periodicity of the function $V(z)$. By computing it for $Re(z_1) \to +\infty$ we obtain: $\mathcal{Z}(z_1, z_2) = \pm iu \int_0^{i\frac{\beta}{2}} dz$. We will choose the sign of $\mathcal{Z}$ such that $\mathcal{Z}(z_1, z_2) = -\frac{\beta}{2} u$

For z in zone I in figure the WKB wave-function corresponding to $g(z)$ is:

$$\begin{aligned} \psi &\sim A\kappa(z,u)^{-\frac{1}{2}} \exp(\nu \mathcal{Z}(z_T, z)) \\ A &= \lim_{\epsilon \to 0} \exp(\nu \mathcal{Z}(\epsilon, z_T)) \epsilon^{\nu} = \exp(\nu \mathcal{Z}^*(0, z_T)) \end{aligned} \tag{A.59}$$

with $\mathcal{Z}^*(0,z) = \lim_{\epsilon \to 0}(\mathcal{Z}(\epsilon, z) + \nu \log(\epsilon))$

Applying the rules given above we get for $z \in II \;\; III \;\; IV$.

[4] in particular $|u^2| < |f(r_*)|$ where $r_* = \left(-\frac{(d-2)\mu}{2}\right)^{\frac{1}{d}}$

$$\psi \sim A\kappa(z,u)^{-\frac{1}{2}}(\exp(\nu\mathcal{Z}(z_T,z)) + i\exp(-\nu\mathcal{Z}(z_T,z)))$$
$$\psi \sim A\kappa(z,u)^{-\frac{1}{2}}(\exp(\nu\mathcal{Z}(z_T,z)) + i\exp(-\nu\mathcal{Z}(z_T,z))[1+\exp(2\nu\mathcal{Z}(z_T,z_{T_1}))])$$
$$\psi \sim A\kappa(z,u)^{-\frac{1}{2}}(\exp(\nu\mathcal{Z}(z_T,z)) + i\exp(-\nu\mathcal{Z}(z_T,z))[1+\exp(2\nu\mathcal{Z}(z_T,z_{T_1})) + \exp(2\nu\mathcal{Z}(z_T,z_{T_2}))])$$

For $z \to +\infty$ we will get:

$$\psi \sim A\kappa(z,u)^{-\frac{1}{2}}(\exp(\nu\mathcal{Z}(z_T,z)) + i\exp(-\nu\mathcal{Z}(z_T,z))[\frac{1}{1-\exp(2\nu\mathcal{Z}(z_T,z_{T_1}))}])$$

then we can use the fact that as $z_{T_1} = z_T + i\frac{\beta}{2}$ the quantity $\exp(2\nu\mathcal{Z}(z_T,z_{T_1})) = e^{-\nu u\beta}$ to obtain

$$\psi \sim A\kappa(z,u)^{-\frac{1}{2}}(\exp(\nu\mathcal{Z}(z_T,z)) + i\frac{e^{\nu u\beta/2}}{2\sinh(\nu u\beta/2)}\exp(-\nu\mathcal{Z}(z_T,z))) \qquad \text{(A.60)}$$

We see then that the factor $\frac{e^{\nu u\beta/2}}{2\sinh(\nu u\beta/2)}$ arises naturally due to the periodic nature of the potential. For $z \to +\infty$ we have $\mathcal{Z}(z_T,z) \sim iuz$.

The function $g(z)$ can be written as a linear superposition of h_R, h_A defined in 2.46 .

$$g(u;z) = \frac{1}{2i\nu u}\left(-f(u)h_A(u;z) + f(-u)h_R(u;z)\right) \qquad \text{(A.61)}$$

It would seem that this expression is inconsistent with the form of the solution we found as the coefficients in front of $e^{i\nu uz}$ and $e^{-i\nu uz}$ are not related by $u \to -u$. However the form of the WKB approximation to $g(z)$ does not have to be continuous in u. In fact A.60 was found for $Im(u) > 0$ while for $Im(u) < 0$ the following expansion is valid

$$\psi \sim A\kappa(z,u)^{-\frac{1}{2}}(\exp(-\nu\mathcal{Z}(z_T,z)) - i\frac{e^{-\nu u\beta/2}}{2\sinh(\nu u\beta/2)}\exp(\nu\mathcal{Z}(z_T,z))) \qquad \text{(A.62)}$$

In function of $f(u)$ we then have the following expression for G_+:

$$G_+(u) = (2\nu)^2 \frac{e^{\beta\nu u}}{e^{\beta\nu u}-1} \frac{2\nu u}{f(u)f(-u)} \tag{A.63}$$

For $z \to \infty$ we have $\mathcal{Z}(z_T, z) \sim iuz$ so that by using the formula above we can write for $G_+(u)$:

$$G_+(u) = 2\nu e^{-2\nu \mathcal{Z}^*(0,z_T)}$$

The factor $\frac{e^{\nu u\beta/2}}{2\sinh(\nu u\beta/2)}$ in the result for the asymptotic behaviour of ψ for $z \to \infty$ simplifies in the expression for G_+.

Next we will consider how the expression we just found changes as u increases.

A.5.3 The k=0 case for large u

Increasing u the pattern of Stokes lines changes as a second turning point becomes active. For $|u| \to \infty$ with $Re(u) > 0$ and $Im(u) > 0$ we will denote with T the turning point for which $z_T \to 0$ and with K the turning point for which $z_K \to \frac{1}{4}(\beta + i\beta)$. For increasing $|u|$ then T approaches the boundary while K approaches the singularity. It is important to realize that if we increase u along the real axis from 0 the turning point considered in 3.30 and used in the previous computation valid for small u approaches the boundary and becomes T while if we increase u from 0 along the imaginary axis it approaches the singularity and becomes K as described in section 4.1.

For $|u|$ large and some value of $\arg(u)$ we have $Re(\mathcal{Z}(z_T, z_k)) = 0$ and the Stokes lines configuration is easiest to picture:

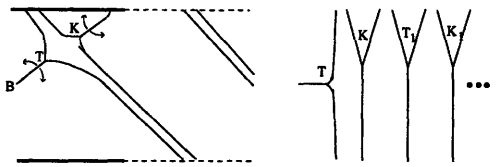

Figure A-6: Stokes lines configuration sketch for large $|u|$

Also pictured is a schematic representation of the active region. In this case too an infinite succession T_n and K_n of images of the turning points is active.

Given the configuration of turning points we have to apply the connection formula at $T\ K\ T_1\ K_1\ T_2\ K_2$ .. counterclockwise. Proceeding as before we will have for z in the active region between T and K

$$\psi(z) \sim \kappa(z,u)^{-\frac{1}{2}} e^{\nu \mathcal{Z}^*(0,z_T)} (e^{\nu \mathcal{Z}(z_T,z)} + ie^{-\nu \mathcal{Z}(z_T,z)})$$

Then by using the connection formula at K we get:

$$\psi(z) \sim \kappa(z,u)^{-\frac{1}{2}} e^{\nu \mathcal{Z}^*(0,z_T)} (e^{\nu \mathcal{Z}(z_T,z)} + ie^{-\nu \mathcal{Z}(z_T,z)}(1 + e^{2\nu \mathcal{Z}(z_T,z_K)}))$$

By repeating the steps for T_1 and K_1 we obtain:

$$\psi(z) \sim \kappa(z,u)^{-\frac{1}{2}} e^{\nu \mathcal{Z}^*(0,z_T)} (e^{\nu \mathcal{Z}(z_T,z)} + ie^{-\nu \mathcal{Z}(z_T,z)}(1 + e^{2\nu \mathcal{Z}(z_T,z_K)})(1 + e^{2\nu \mathcal{Z}(z_T,z_{T_1})}))$$

so that for $z \to +\infty$

$$\psi(z) \sim \kappa(z,u)^{-\frac{1}{2}} e^{\nu \mathcal{Z}^*(0,z_T)} \left(e^{\nu \mathcal{Z}(z_T,z)} + ie^{-\nu \mathcal{Z}(z_T,z)}(1 + e^{2\nu \mathcal{Z}(z_T,z_K)}) \frac{2e^{\nu u \beta/2}}{\sinh(\nu u \beta/2)} \right)$$

We can then use A.61 to obtain:

$$G_+ = 2\nu e^{-2\nu \mathcal{Z}^*(0,z_T)} \frac{1}{1 + e^{2\nu \mathcal{Z}(z_T,z_K)}}$$

Along the line in the u plane for which $\mathcal{Z}(z_T, z_K)$ is imaginary we have poles located at $\mathcal{Z}(z_T, z_K) = i(2n+1)\frac{\pi}{2\nu}$. The integral $\mathcal{Z}(z_T, z_K)$ can easily be evaluated explicitly For $d = 4$ and we obtain for the position of the poles:

$$u_n = \frac{4\pi}{\mathcal{B}} \left(\frac{1}{2} + n \right)$$

where $n \in N$.

When u is tilted toward the real axis T and K move in the direction of the red arrows $\exp(\mathcal{Z}(z_T, z_K)) << 1$ and $G_+ \sim 2\nu e^{-2\nu \mathcal{Z}^*(0,z_T)}$. [5]

[5]For u close to the real axis the Stokes lines configuration changes and some subdominant terms coming from the line of poles complex conjugate to the one just described appear however Z_T

For u tilted towards the imaginary axis T and K move in the direction of the blue arrow $\exp(\mathcal{Z}(z_T, z_K)) \gg 1$ and:

$$G_+ = 2\nu e^{-2\nu\mathcal{Z}^*(0,z_T)} \frac{1}{1+e^{2\nu\mathcal{Z}(z_T,z_K)}} \sim 2\nu e^{-2\nu\mathcal{Z}^*(0,z_K)}$$

In this case then for $|u|$ large the dominant contribution probes the geometry near the singularity.

A.5.4 $k \neq 0$

For $k \in R$ and small there are new solutions to $f(r)(1+\frac{k^2}{r}) = 0$ lying near the singularity but the turning points giving the dominant contribution to $G_+(u)$ are the same as for $k = 0$ except for the fact that their position will depend continuously on k. The approximate solutions for $G_+(u)$ are the same as before except that the integral defining $\mathcal{Z}(u)$ has to be evaluated at finite k.

However as described in section 3.3.2 for finite μ when k becomes greater than a critical value $k_c(\mu)$ the potential on the real z axis changes from being monotonically decreasing to the one depicted in 3-6 . There is a region between z_{min} and z_{max} for which the potential is an increasing function of z.

For $u_{min} < u < u_{max}$ there will be poles along the real axis as described in section 3.3.2. The pattern of turning points resulting in this situation is quite complicated and is not considered in detail here.

A.6 Explicit expressions of the integrals 3.42

In this appendix we will derive explicit expression for 3.42 in terms of elliptic integrals. In the $d = 4$ case this can be done for generic values of E and k. For $d = 3$ and $d = 7$ we are able to perform the integrations only for $k = 0$.

We will first present the results for $d = 4$ and then show how they simplify for $k = 0$. This limit is interesting because it can be compared directly to the expressions

continues to give the dominant contribution to G_+.

3.18. The fact that 3.18 coincide with the $k = 0$ limit of the integrals 3.42 is a check of the consistency of the semi-classical approximation to $G_+(\omega)$ described in section 3.2 and the approximation to $G_+(\omega)$ described in section 3.1.

We will then write expressions for 3.42 valid for $d = 3$ and $d = 7$ in the $k = 0$ case. Finally we collect some definitions and results on elliptic integrals that we use.

A.6.1 The $d = 4$ case

For $k^2 = -q^2 \neq 0$ the various integrals in 3.42 can be expressed in terms of elliptic integrals as follows.

First we change the integration variable in 3.42 to $y = r^2$. The turning point equation 3.40 becomes:

$$\begin{aligned} & y^2\left(f(r(y))\left(1-\frac{q^2}{y}\right)+E^2\right) = \\ & = y^3 + y^2(E^2 - q^2 + 1) - y(\mu + q^2) + \mu q^2 = (y - y_1)(y - y_3)(y - y_2) \end{aligned} \tag{A.64}$$

Also we introduce w_0 and w_1 such that

$$yf(r(y)) = y^2 + y - \mu = (y - w_0)(y - w_1) \tag{A.65}$$

Let y_1 be the solution corresponding to the turning point then the integrals 3.42 are rewritten as:

$$\begin{aligned} t(E,q) &= E\int_{y_1}^{\infty} \frac{y^{\frac{3}{2}}dy}{(y-w_0)(y-w_1)\sqrt{(y-y_1)(y-y_3)(y-y_2)}} \\ x(E,q) &= q\int_{y_1}^{\infty} \frac{dy}{\sqrt{y(y-y_1)(y-y_3)(y-y_2)}} \\ L(E,q) &= lim_{\Lambda\to\infty}\left(\int_{y_1}^{\Lambda^2} \frac{\sqrt{y}dy}{\sqrt{(y-y_1)(y-y_3)(y-y_2)}} - 2\log(\Lambda)\right) \end{aligned} \tag{A.66}$$

Introducing the following definitions:

$$a = \frac{y_3-y_2}{y_1-y_2} \quad \chi^2 = a\left(\frac{y-y_1}{y-y_3}\right) \quad c = \frac{y_3-w_0}{y_1-w_0}$$

$$\bar{c} = \frac{y_3 - w_1}{y_1 - w_1} \qquad s = \frac{y_3}{y_1 a} \qquad \phi = \arcsin(\sqrt{a}) \tag{A.67}$$

the t integral can be written as

$$t = B \int_0^{\sqrt{a}} \frac{(1 - s\chi^2)^{\frac{3}{2}} d\chi}{\sqrt{1 - \chi^2}} \left(\frac{c}{1 - \frac{c}{a}\chi^2} - \frac{\bar{c}}{1 - \frac{\bar{c}}{a}\chi^2} \right) \tag{A.68}$$

with

$$B = \frac{2E y_1^{\frac{3}{2}}}{(y_3 - y_2)^{\frac{1}{2}} (y_3 - y_1)(w_0 - w_1)} \tag{A.69}$$

A.68 can then be cast in the following form:

$$t = B \int_0^{\sqrt{a}} \frac{d\chi}{\sqrt{(1 - \chi^2)(1 - s\chi^2)}} \left(\frac{(c - sa)^2}{c(1 - \frac{c}{a}\chi^2)} - \frac{(\bar{c} - sa)^2}{\bar{c}(1 - \frac{\bar{c}}{a}\chi^2)} + (sa)^2 \frac{c - \bar{c}}{c\bar{c}} \right)$$

This can be expressed directly in terms of elliptical integrals $F[\phi, m]$ and $\Pi[n, \phi, m]$ (defined in appendix A.6.4):

$$\begin{aligned} t = {} & \frac{2E(y_3 - y_1)}{(w_0 - w_1)\sqrt{y_1(y_3 - y_2)}(y_3 - w_0)(y_3 - w_1)} \left(\frac{(y_3 - w_1)w_0^2}{y_1 - w_0} \Pi \left[\frac{c}{a}, \phi, s \right] + \right. \\ & \left. - \frac{(y_3 - w_0)w_1^2}{y_1 - w_1} \Pi \left[\frac{\bar{c}}{a}, \phi, s \right] + (w_0 - w_1) \frac{y_3^2}{(y_3 - y_1)} F[\phi, s] \right) \end{aligned} \tag{A.70}$$

The same substitutions applied to the L integral yield:

$$\begin{aligned} L(E, q) &= \lim_{\Lambda \to \infty} \left(\int_{y_1}^{\Lambda^2} \frac{\sqrt{y} dy}{\sqrt{(y - y_1)(y - y_3)(y - y_2)}} - 2\log(\Lambda) \right) \\ &= \lim_{\Lambda \to \infty} 2\left(\sqrt{\frac{y_1}{y_3 - y_2}} (sa\, F\left[\tilde{\phi}, s\right] + (1 - sa)\Pi\left[\frac{1}{a}, \tilde{\phi}, s\right]) - \log(\Lambda) \right) \end{aligned} \tag{A.71}$$

where $\tilde{\phi} = \arcsin\left(\sqrt{a}\frac{\Lambda^2 - y_1}{\Lambda^2 - y_3}\right)$.

For x we get:

$$x(E, q) = q \frac{2}{\sqrt{y_1(y_3 - y_2)}} F[\phi, s] \tag{A.72}$$

The elliptic integrals that appear in the previous expressions have branch points when one of the following occurs:

$\sin^2(\phi) = a = \frac{1}{s}$ that is for $y_1 = y_3$.

$\sin(\phi) \to \infty$ corresponding to $a \to \infty$ that is for $y_1 = y_2$.

Branch cuts for the various integrals then start at those values of E and q for which the turning point coincides with another solution of the turning point equation 3.40 [6].

A.6.2 $d = 4$ and $k = 0$

In the $k = 0$ limit one of the solutions to the turning point equation A.65 is at $y = 0$. This solution is not the turning point as it does not change with E therefore we can choose it to be y_2. Then the quantity s defined in A.67 is equal to 1 in this limit and the previous expressions A.70 and A.72 can be written in terms of logarithms using the formulas in the last section of this appendix. We obtain:

$$\begin{aligned} t = \frac{2E}{(\omega_0-\omega_1)}\left(\frac{\omega_0}{\sqrt{(y_0-\omega_0)(y_1-\omega_0)}}\log\left(\frac{1+\sqrt{c}}{1-\sqrt{c}}\right)\right) + \\ -\frac{2E}{(\omega_0-\omega_1)}\left(\frac{\omega_1}{\sqrt{(y_0-\omega_1)(y_1-\omega_1)}}\log\left(\frac{1+\sqrt{c}}{1-\sqrt{c}}\right)\right) \end{aligned} \tag{A.73}$$

By writing A.65 as $y^2 + y(E^2 - \omega_0 - \omega_1) + \omega_0\omega_1$ this expression can be cast as:

$$\begin{aligned} t \;=\; & \frac{\sqrt{\omega_0}}{\omega_0-\omega_1}\log\left(\frac{(E-\sqrt{\omega_0}-\sqrt{\omega_1})(E-\sqrt{\omega_0}+\sqrt{\omega_1})}{(E-\sqrt{\omega_0}-\sqrt{\omega_1})(E-\sqrt{\omega_0}+\sqrt{\omega_1})}\right) + \\ & -\frac{\sqrt{\omega_1}}{\omega_0-\omega_1}\log\left(\frac{(E+\sqrt{\omega_0}+\sqrt{\omega_1})(E-\sqrt{\omega_0}+\sqrt{\omega_1})}{(E-\sqrt{\omega_0}-\sqrt{\omega_1})(E+\sqrt{\omega_0}-\sqrt{\omega_1})}\right) \end{aligned} \tag{A.74}$$

[6] As we have seen in appendix A5 at these values there can be a topology change in the active region and a new line of poles can form. When the mass parameter ν is taken to ∞ these poles merge to give a natural prescription for the position of the branch cuts of $Z(u,k)$ as described in section 3.3.

Then using 2.14 we can express the complexified temperature in terms of ω_0 and ω_1 as $\mathcal{B} = -2\pi i(\sqrt{\omega_1} - \sqrt{\omega_0})^{-1}$ and obtain[7] :

$$t(u = iE) = \frac{\beta}{4\pi} \log\left(\frac{A_+\tilde{A}_-}{A_-\tilde{A}_+}\right) - i\frac{\beta}{4\pi} \log\left(\frac{A_+\tilde{A}_+}{A_-\tilde{A}_-}\right) - \frac{i}{2}\beta \tag{A.75}$$

where

$$A_\pm = \frac{\sqrt{2}\pi}{|\mathcal{B}|} \pm \frac{u}{\sqrt{2}} e^{i\theta_\mathcal{B}}, \qquad \tilde{A}_\pm = \frac{\sqrt{2}\pi}{|\mathcal{B}|} \pm \frac{u}{\sqrt{2}} e^{-i\theta_\mathcal{B}},$$

and $\theta_\mathcal{B}$ is the phase of $\mathcal{B}$.

In the same way in the limit $y_2 = 0$ we get for $L(E, 0)$

$$L = \log(y_1 - y_3) \tag{A.76}$$

which following the same steps can be transformed to read:

$$L(u = iE) = -\frac{1}{2} \log(A_+\tilde{A}_+A_-\tilde{A}_-) \tag{A.77}$$

The branch cuts in A.75 and A.77 are straight lines extending radially from $\pm\frac{2\pi}{\mathcal{B}}$ and $\pm\frac{2\pi}{\bar{\mathcal{B}}}$ to ∞ as follows from the discussion of section 3.3. A.75 and A.77 coincide with 3.18 ; therefore the approximation described in sec 3.1 for gives in the limit 3.15 the same results as the semiclassical approximation developed in sec 3.2 when $k = 0$.

A.6.3 $d = 3,\ d = 6$

For $d = 3,\ 6$ and $k = 0$ it is also possible to evaluate 3.42 in terms of elliptic integrals following a similar procedure.

For $d = 3$ we will define $y = r$ and the three solutions to $f(y) = 0$ will be denoted with $w_0,\ w_1,\ w_2$ while the three solutions to the turning point equation $y(f(y) + E^2) = 0$ will be denoted with $y_1,\ y_2,\ y_3$. In a similar way for $d = 6$ we will define $y = r^2$ and the three solutions to $f(r(y)) = 0$ will be denoted $w_0,\ w_1,\ w_2$ while the three solutions to $y^2(f(y) + E^2) = 0$ will be denoted $y_1,\ y_2,\ y_3$. In both

[7] the constant is fixed by requiring $\lim_{u\to+\infty} t(u) = 0$ with the branch cuts extending radially to ∞ and the usual determination for the logarithms

cases y_1 will correspond to the turning point. Then the results for the t and L integral are:

for d=3

$$
\begin{aligned}
t \quad &= \frac{4E(y_3-y_1)}{(w_0-w_1)(w_0-w_2)(w_1-w_2)\sqrt{y_1(y_3-y_2)}}\cdot \\
&\cdot\left(\frac{(w_1-w_2)w_0^2}{(y_1-w_0)(y_3-w_0)}\Pi\left[\frac{c}{a},\phi,s\right]-\frac{(w_0-w_2)w_1^2}{(y_1-w_1)(y_3-w_1)}\Pi\left[\frac{\overline{c}}{a},\phi,s\right]+\right. \qquad \text{(A.78)}\\
&\left.+\frac{(w_0-w_1)w_2^2}{(y_1-w_2)(y_3-w_2)}\Pi\left[\frac{\widetilde{c}}{a},\phi,s\right]+\frac{y_3^2(w_0-w_1)(w_0-w_2)(w_1-w_2)}{(y_3-y_1)(y_3-w_0)(y_3-w_1)(y_3-w_2)}F\left[\phi,s\right]\right)
\end{aligned}
$$

where $\widetilde{c}=\frac{y_3-w_2}{y_1-w_2}$ and all the other quantities are as defined in A.67 .

$$
\begin{aligned}
L(E,q) &= \lim_{\Lambda\to\infty}\left(2\int_{y_1}^{\Lambda}\frac{\sqrt{y}dy}{\sqrt{(y-y_1)(y-y_3)(y-y_2)}}-2\log(\Lambda)\right)\\
&= \lim_{\Lambda\to\infty}4\left(\sqrt{\frac{y_1}{y_3-y_2}}\Big(sa\;F\left[\widetilde{\phi},s\right]+(1-sa)\Pi\left[\tfrac{1}{a},\widetilde{\phi},s\right]\Big)-\tfrac{1}{2}\log(\Lambda)\right) \qquad \text{(A.79)}
\end{aligned}
$$

where $\widetilde{\phi}=\arcsin\left(\sqrt{a}\frac{\Lambda-y_1}{\Lambda-y_3}\right)$

for d=6

$$
\begin{aligned}
t &= \frac{2E(y_3-y_1)}{(w_0-w_1)(w_0-w_2)(w_1-w_2)\sqrt{y_1(y_3-y_2)}}\cdot \\
&\cdot\left(\frac{(w_1-w_2)w_0^3}{(y_1-w_0)(y_3-w_0)}\Pi\left[\frac{c}{a},\phi,s\right]-\frac{(w_0-w_2)w_1^3}{(y_1-w_1)(y_3-w_1)}\Pi\left[\frac{\overline{c}}{a},\phi,s\right]+\right. \qquad \text{(A.80)}\\
&\left.+\frac{(w_0-w_1)w_2^3}{(y_1-w_2)(y_3-w_2)}\Pi\left[\frac{\widetilde{c}}{a},\phi,s\right]+\frac{y_3^3(w_0-w_1)(w_0-w_2)(w_1-w_2)}{(y_3-y_1)(y_3-w_0)(y_3-w_1)(y_3-w_2)}F\left[\phi,s\right]\right)
\end{aligned}
$$

the expression for L is the same as in A.79 but $\widetilde{\phi}=\arcsin\left(\sqrt{a}\frac{\Lambda^2-y_1}{\Lambda^2-y_3}\right)$

A.6.4 conventions for elliptic integrals

We define the following integrals

$$
\begin{aligned}
\Pi[n,\phi,m] &= \int_0^{\sin(\phi)}\frac{dt}{(1-nt^2)\sqrt{(1-t^2)(1-mt^2)}}\\
F[\phi,m] &= \Pi[0,\phi,m]=\int_0^{\sin(\phi)}\frac{dt}{\sqrt{(1-t^2)(1-mt^2)}}
\end{aligned}
$$

$$
\begin{aligned}
K[m] &= F[\frac{\pi}{2}, m] = \int_0^1 \frac{dt}{\sqrt{(1-t^2)(1-mt^2)}} \\
E[m] &= \int_0^1 \frac{\sqrt{1-mt^2}}{\sqrt{1-t^2}} dt
\end{aligned}
\tag{A.81}
$$

The functions $\Pi[n, \phi, m]$ and $F[\phi, m]$ for fixed n, m have branch points located at: $\sin(\phi) = \pm\frac{1}{\sqrt{m}}$ and $\phi = \infty$. Conversely for fixed ϕ, n they have branch points at $m = \frac{1}{\sin^2(\phi)}$ and $m = \infty$. It then follows that $K[m]$ has branch points located at $m = 1$ $m = \infty$

The following formulas are used to obtain the explicit series expansion of $K[m]$ for $m \sim -1$:

$$
\begin{aligned}
\frac{d}{dm} K[m] &= \frac{E[m] - (1-m)K[m]}{2m(1-m)} \\
\frac{d}{dm} E[m] &= \frac{E[m] - K[m]}{2m}
\end{aligned}
\tag{A.82}
$$

from which one obtains:

$$
K[m] = K[-1] + \frac{1}{4}(2K[-1] - E[-1])(m+1) + \frac{1}{16}(5K[-1] - 3E[-1])(m+1)^2 + \ldots \tag{A.83}
$$

We also use the following formulas [8] to obtain A.73 and A.76 :

$$
\begin{aligned}
\Pi(n, \arcsin(\sqrt{a}), 1) &= \frac{1}{2(n-1)} \left(\sqrt{n} \log\left(\frac{1+\sqrt{na}}{1-\sqrt{na}} \right) - 2\log\left(\frac{1+\sqrt{a}}{\sqrt{1-a}} \right) \right) \\
F(\arcsin(\sqrt{a}), 1) &= \log\left(\frac{1+\sqrt{a}}{\sqrt{1-a}} \right)
\end{aligned}
\tag{A.84}
$$

A.7 Asymptotic behaviour of $Z(E, q)$

In this appendix we study the asymptotic behaviour of $Z(E, q)$ for $E \to \infty$ along the real and imaginary axis for $d = 4$. First we consider $q = 0$ and then $q \neq 0$ with q fixed. I this last case the asymptotic expansion along the imaginary E axis

[8] which can be found for example in www.functions.wolfram.com

is radically different from that along the real axis which is invalid for $q \sim O(E^{-1})$. For $q \leq O(E^{-1})$ a different expansion along the real E axis is presented. Finally we consider the case $E \sim q \gg 1$ for the reduced metric 2.6.

A.7.1 q=0

We will first consider what is the asymptotic behaviour of $t(E,q)$, $L(e,q)$ and $Z(E,q)$ for $d=4$ and $q=0$ in the two limits $E \to \pm\infty$ and $u = iE \to \pm\infty$. We have to expand the explicit expressions A.75 and A.77. The branch cuts in the logarithms extend radially to ∞. With this choice of branches the following holds for $u \to \pm\infty$.

$$\begin{aligned} t(u) &= it_0 - \frac{2i}{u} + i\sum_{i=1}^{\infty} 2n \frac{a_n(\mu)}{u^{2n+1}} \\ L(u) &= -2\log\left(\pm\frac{u}{2}\right) - \sum_{n=1}^{\infty}(2n+1)\frac{a_n(\mu)}{u^{2n}} \\ Z(u) &= -ut_0 + 2\log\left(\pm\frac{u}{2}\right) + 2 + \sum_{n=1}^{\infty}\frac{a_n(\mu)}{u^{2n}} \end{aligned} \tag{A.85}$$

where the $a_n(\mu)$ are polynomials in μ and:

$$t_0 = \begin{cases} 0 & \mathrm{Re}u \to +\infty \\ \\ \beta & \mathrm{Re}u \to -\infty \end{cases} \tag{A.86}$$

For $E \to \pm\infty$ the expansion is instead:

$$\begin{aligned} t(E) &= t_0 - \frac{2}{E} + \sum_{i=1}^{\infty} 2n(-1)^n \frac{a_n(\mu)}{E^{2n+1}} \\ L(E) &= -2\log\left(\frac{E}{2}\right) + \sum_{n=1}^{\infty}(2n+1)(-1)^n\frac{a_n(\mu)}{E^{2n}} \\ Z(E) &= -Et_0 + 2\log\left(\pm\frac{E}{2}\right) + 2 + \sum_{n=1}^{\infty}(-1)^n\frac{a_n(\mu)}{E^{2n}} \end{aligned} \tag{A.87}$$

where

$$t_0 = \begin{cases} \frac{\beta}{2} & \mathrm{Re}E \to +\infty \\ \\ -\frac{\beta}{2} & \mathrm{Re}E \to -\infty \end{cases} \tag{A.88}$$

The expansion for $E \to \infty$ and $u \to \infty$ are related by setting $E = -iu$ except from terms coming from the choice of determination of the logarithms in A.75 and A.77. As we will see for $q \neq 0$ the situations is very different and the expansion along the imaginary and real u axis are qualitatively different.

A.7.2 $q \neq 0$ case

Next we will expand the expressions we have obtained in appendix A6 for 3.42 when $k = iq \in R$ nonzero and $E \to \pm\infty$ or $u \to \pm\infty$ with k held fixed. To do so we need first to expand the solutions to the turning point equation A.65 which is given by:

$$y^2 \left(f(r(y)) \left(1 + \frac{k^2}{y} \right) + E^2 \right) = 0 \tag{A.89}$$

One of the solutions is of order $O(E^2)$ while the other two solutions are of order $O(E^{-1})$. By denoting with y_1 the large solution we can parameterize them as:

$$y_1 = -(E^2 + k^2 + 1 + 2d) \quad y_3 = d + e \quad y_2 = d - e \tag{A.90}$$

where both e and d are small in the limit $|E| \to \infty$. d and e have the following expansions:

$$\begin{aligned} d &= \sum_{n=1} \left(\frac{1}{E} \right)^{2n} P_n(k, \mu) \\ e &= \sum_{n=0} \mu k^2 \left(\frac{1}{Ek\sqrt{\mu}} \right)^{2n+1} Q_n(k, \mu) \end{aligned} \tag{A.91}$$

where P_n Q_n are polynomials in k^2 and μ. P_n is at most $O(k^{2n})$ while Q_n can be

$O(k^{4n})$ [9].

Notice the following:

- 1 The radius of convergence of the expansions is determined by the merging of one or more solutions y_i. For example the expansion for e breaks down for small k; this is due to the fact that for $q^2 = -k^2 =\sim \frac{\mu}{4E^2}$ the two small solutions coincide and $e \sim 0$. The radius of convergence of the series is determined by the position of this singularity.

- 2 The series expansion of e^2 is non singular in the $k \sim 0$ limit as it can be expressed in terms of d using A.93

- 3 For $k \sim E$ all the terms in the series expansions for e and d are potentially of

[9]This can be obtained as follows. First by plugging the parametrization A.90 in the turning point equation A.89 we get the following equation for d:

$$8\,d^3 + d^2\left(8 + 8\,k^2 + 8\,E^2\right) + d\left(2 + 6\,k^2 + 2\,k^4 + 4\,E^2 + 4\,k^2\,E^2 + 2\,E^4 - 2\,\mu\right) - \mu - E^2\,\mu + k^2 + k^4 + k^2\,E^2 = 0$$

This equation has only one solution which is small in the limit of large E and for it $d \sim E^{-2}$. By writing $d = gE^{-2}$ the equation for d can be cast as

$$E^2\left(2\,g + k^2 - \mu\right) + 4\,g + k^2 - \mu + 4\,g\,k^2 + k^4 + \frac{2\,g + 8\,g^2 + 6\,g\,k^2 + 2\,g\,k^4 - 2\,g\,\mu}{E^2} + \frac{8\,g^2 + 8\,g^2\,k^2}{E^4} + \frac{8\,g^3}{E^6} = 0$$

from which it is apparent that $d = gE^{-2}$ will have the expansion:

$$d = \sum_{n=1} P_n(k^2, \mu) E^{-2n} \tag{A.92}$$

where $P_n(k^2, \mu)$ are polynomials in k^2 and μ of degree at most k^{2n}. The first term of the series is $P_1(k^2, \mu) = \frac{1}{2}(\mu - k^2)$.

By matching the terms of order y in $(y - y_1)(y - y_2)(y - y_3)$ and in A.89 we get the following equation for e:

$$e^2 = -2\,d - 3\,d^2 - k^2 - 2\,d\,k^2 - 2\,d\,E^2 + \mu \tag{A.93}$$

from which upon using the expansion A.92 follows:

$$e^2 = \sum_{n=1} F_n(k^2, \mu) E^{-2n} \tag{A.94}$$

where $F_n(k^2, \mu)$ are polynomials in μ and k^2 up to order k^{2n}. As the first term in the expansion is given by $F_1(k^2, \mu) = \mu k^2$ by taking a square root we get for e:

$$e = \frac{\sqrt{\mu}\,k}{E} \sum_{n=0} \left(\frac{1}{kE}\right)^{2n} Q_n(k, \mu) \tag{A.95}$$

with $Q_n(k, \mu)$ polynomials in k^2 and μ of order at most k^{4n}

the same order. This also is a reflection of the merging of two of the solutions for $k = \pm iE \pm 1$.

Having determined the expansion of the solutions to the turning point equation A.89 for $|E| \to \infty$ and fixed $k \neq 0$ we can proceed to find the expansion for the functions $t(E,k)$ $Z(E,k)$ $x(E,k)$

First let's consider the case $u \to \pm\infty$. From the discussion in section 4.1 the turning point is the large positive solution that is $y_1 \sim u^2$ in our parametrization. We want to expand the expression A.72 for $x(E,k)$. For this we first consider the quantities a and s defined in A.67 which can be expanded as follows in function of e and d.

$$\begin{aligned} a &= \frac{1}{u^2}\sum_{n=0} P_n(e,d,k^2)u^{-2n} \\ s &= \frac{d+e}{2e} + \frac{1}{e}\sum_{n=1} K_n(e,d,k^2)u^{-2n} \end{aligned} \tag{A.96}$$

where P_n and K_n are polynomials in the indicated variables of order at most k^{2n}. Before substituting the expansions for e and d it is useful to make a further observation.

The elliptic integral $F[\sin^{-1}(\sqrt{a}), s]$ has the following expansion valid for small a:

$$F[\sin^{-1}\sqrt{a}, s] = \sqrt{a}\sum_{n=0} c_n(s)a^n \tag{A.97}$$

where $c_n(s)$ are polynomials in s of order at most s^n. Then As k^2, e, $d \ll u^2$ we can expand the expression for $x(u,k)$ as follows:

$$\vec{x} = \frac{-2i\vec{k}}{\sqrt{y_1(y_3-y_2)}}F[\sin^{-1}(\sqrt{a}), s] = -2i\vec{k}\sqrt{\frac{a}{y_1(y_3-y_2)}}\sum_{n=0} c_n(s)a^n = -\frac{i\vec{k}}{u^2}\sum_{n=0}\frac{1}{u^{2n}}D_n(e,d,k^2)$$

where $D_n(e,d,k^2)$ is a polynomial in the three variables.

At this point we observe that exchanging the two solutions y_2 and y_3 (that is e and $-e$) and leaving the turning point unaltered cannot change the result so the $D_n(e,d,k^2)$ have to be even in e. Therefore the expansion is non singular in the $k \to 0$

limit and using the previous results A.91 for d and e we get the following:

$$\vec{x} = -ik\left(\sum_{n=1}\left(\frac{1}{u}\right)^{2n} M_n^{(1)}(k)\right) \tag{A.98}$$

where $M_n^{(1)}(k)$ are polynomials in k^2 and μ of order at most k^{2n}

We could use a similar method to expand $t(u,k)$ and $Z(u,k)$ too but it is simpler to take advantage of the relations 3.43 existing between the various integrals. This method leaves undetermined a contribution to $Z(u,k)$ independent of k which can be fixed using the form of the expansion valid at $k=0$ obtaining:

$$\begin{aligned} t &= i\sum_{n=1}(2nk^2)\left(\frac{1}{u}\right)^{2n+1} M_n(k) - i\partial_u Z(u,0) \\ Z &= \sum_{n=1} k^2\left(\frac{1}{u}\right)^{2n} M_n(k) + Z(u,0) \\ Z(u,0) &= -ut_0 + 2\log\left(\pm\frac{u}{2}\right) + 2 + \sum_{n=1}^{\infty}\frac{a_n(\mu)}{u^{2n}} \end{aligned} \tag{A.99}$$

where the expansion for $Z(u,0)$ is the same as in A.86 and the $M_n(k)$ are also polynomials in k^2 and μ of order at most k^{2n}.

As expected none of these expansions is singular in the limit $k^2 \sim 0$. This is because for $u \to \pm\infty$ the turning point y_1 is very far from the two close solutions y_2 and y_3.

The situation is very different in the $E \in R$ case for which the turning point in the integrals 3.42 approaches $r=0$ as $E \to \pm\infty$. We then parameterize y_1 y_3 y_2 as:

$$y_1 = d+e \quad y_3 = d-e \quad y_2 = -E^2 - k^2 - 1 - 2d$$

where y_1 is the turning point. In this case the solution y_3 is very close to the turning point and can coincide with it for $k \sim O(E^{-1})$. We therefore expect the asymptotic expansion we will obtain to be singular in the $k=0$ limit.

Notice that for $k \in R$ we can deform the integration contour for the x integral A.67 which originally runs from y_1 to $+\infty$ to run from y_1 to $-\infty$ and rewrite it as

follows:

$$\begin{aligned}
&\int_{y_1}^{\infty} \frac{dy}{\sqrt{y(y-y_1)(y-y_3)(y-y_2)}} = \\
&= \int_{y_1}^{y_2} \frac{dy}{\sqrt{y(y-y_1)(y-y_3)(y-y_2)}} + \int_{y_2}^{-\infty} \frac{dy}{\sqrt{y(y-y_1)(y-y_3)(y-y_2)}} = \\
&= \frac{2}{\sqrt{y_1(y_3-y_2)}} F[\frac{\pi}{2}, s] - \frac{2}{\sqrt{y_2(y_3-y_1)}} F[\psi, s'] \qquad \text{(A.100)}
\end{aligned}$$

where

$s' = \frac{y_3(y_1-y_2)}{y_2(y_1-y_3)} \quad \sin^2(\psi) = \frac{y_1-y_3}{y_1-y_2}$

The second integral is qualitatively the same as the one occurring for $u^2 \gg k^2 > 0$ because y_2 which plays the role of the turning point goes to $-\infty$ while the other two solutions approach 0. Its expansion is similar to A.98 and is not singular in the $k \sim 0$ limit.

To obtain an expansion for the first integral we notice that for $E \to \infty$ using the expansions A.91 the parameter $s = \frac{y_3(y_1-y_2)}{y_1(y_3-y_2)}$ approaches -1. Around $s = -1$ the elliptic integral $K[s] = F\left[\frac{\pi}{2}, s\right]$ admits a Taylor expansion in $(s+1)$ (see A.83):

$$K[s] = \sum_{n=0} a_n (1+s)^n \qquad \text{(A.101)}$$

By considering the structure of A.91 the following expansion follows after some algebra[10]:

$$\frac{2}{\sqrt{y_1(y_3-y_2)}} K(s) = \sum_{n=0} \left(\frac{1}{k\sqrt{\mu E}}\right)^{n+\frac{1}{2}} T_n^{(1)}(k) \qquad \text{(A.103)}$$

where $T_n^{(1)}(k)$ is a polynomial in k^2 and μ of order at most k^{2n}.

[10]First it is useful to express the integral in terms of the solutions y_i using A.101 :

$$\frac{2}{\sqrt{y_1(y_3-y_2)}} K[s] = 2 \sum_{n=0} a_n \left(y_1(y_3-y_2)\right)^{-n-\frac{1}{2}} \left(2y_1y_3 - y_2(y_1+y_3)\right)^n \qquad \text{(A.102)}$$

The factor $(2y_1y_3 - y_2(y_1+y_3))$ is easily seen to depend only on e^2 and therefore has an expansion in powers of E^{-2}. This is not the case for $(y_1(y_3-y_2))$ which instead will have an expansion like the one for e in A.91 . In particular $(y_1(y_3-y_2)) \sim \sqrt{\mu}kE + O((kE)^{-1})$ from which we get that the expansion of A.102 will be of the form indicated.

As expected this series reflects the presence of the branch point approximately located at $q^2 = -k^2 = \sim \frac{\mu}{2E^2}$.

Summing the nonsingular contribution at $k = 0$ from the second integral in A.100 and using the same method as for $u \to \infty$ we get for the expansions of $t(E,k)$ and $Z(E,k)$:

$$\begin{aligned}
x(E,k) &= -i\vec{k}\left(\sum_{n=0}\left(\frac{1}{k\sqrt{\mu}E}\right)^{n+\frac{1}{2}} T_n^{(1)}(k) + \sum_{n=1}\left(\frac{1}{E}\right)^{2n} L_n^{(1)}(k)\right) \\
t(E,k) &= -\sum_{n=0}(n+\frac{1}{2})k^2\left(\frac{1}{kE\sqrt{\mu}}\right)^{n+\frac{3}{2}} T_n(k) - \sum_{n=1}(2nk^2)\left(\frac{1}{E}\right)^{2n+1} L_n(k) - \partial_E Z(E,0) \\
Z(E,k) &= \sum_{n=0} k^2\left(\frac{1}{\sqrt{\mu}kE}\right)^{n+\frac{1}{2}} T_n(k) + \sum_{n=1} k^2\left(\frac{1}{E}\right)^{2n} L_n(k) + Z(E,0) \\
Z(E,0) &= -Et_0 + 2\log\left(\pm\frac{E}{2}\right) + 2 - \sum_{n=1}^{\infty}(-1)^n \frac{a_n(\mu)}{E^{2n}}
\end{aligned} \tag{A.104}$$

where the expansion for $Z(E,0)$ is the same as in A.88 while L_n and T_n are polynomials in k and μ of order at most k^{2n}.

In the regime $|kE| \ll \sqrt{\mu}$ and $E^2 \gg 1$ the previous expansions are invalid. Instead we introduce the parameter $\epsilon\mu = -k^2E^2$ and expand e and d for $E \to \infty$ and $\epsilon \sim 0$. The expansion for d can be obtained by substituting $k^2 = -\epsilon\mu E^{-2}$ in A.91 which is non-singular as $k \to 0$. For e we can use A.93 to find that the double expansion for e^2 starts as $\mu^2(\frac{1}{4}+\epsilon)E^{-4} + O(E^{-6})$ from which we get:

$$e = \frac{1}{E^2}\sum_{n=0,m=0} b_{n,m}(\mu)\epsilon^n E^{-2m}$$

where the $b_{n,m}(\mu)$ are polynomials in μ.

For $k = 0$ one of the solutions to A.89 is at $y = 0$. As we chose y_1 to be the turning point and y_2 to be large in the limit $E \to \infty$ we therefore must have $y_3 = d - e = 0$. As a consequence $d - e \to 0$ as $\epsilon \to 0$ and this implies that:

$$s = \frac{(d-e)(E^2+k^2+1+3d+e)}{(d+e)(E^2+k^2+1+3d-e)} \sim O(\epsilon)$$

Therefore we can expand $K[s]$ around $s = 0$:

$$K[s] \sim \sum_{n=0} b_n s^n$$

By substitution we get:

$$\vec{x} = \frac{-2i\vec{k}}{\sqrt{y_1(y_3 - y_2)}} K(s) = -i\vec{k} \sum_{n=0,m=0} h(\mu)_{n,m} \frac{\epsilon^n}{E^{2m}} \tag{A.105}$$

with $h(\mu)$ polynomials in μ. Then also $Z(E, k)$ will have a similar expansion:

$$Z(E, \epsilon) \;\; = -Et_0 + 2\log\left(\pm\tfrac{E}{2}\right) + 2 + \textstyle\sum_{n=0,m=1}^{\infty} \frac{\epsilon^n}{E^{2m}} k_{m,n}(\mu) \tag{A.106}$$

with $k(\mu)$ polynomials in μ. Notice tat these expansions are only valid for k at most of order $O\left(E^{-1}\right)$. For any finite value of k A.104 have to be used instead.

A.7.3 The light-cone limit

We consider in the $\mu \to \infty$ case 2.6 in $d = 4$ the regime $u^2 \sim k^2 \gg 1$ with both u and k real. The computation follows closely the steps leading to A.99 and A.104 .

Define the following quantity $g = (u^2/k^2 - 1)$. The turning point equation A.65 now reads:

$$y^3 - gk^2y^2 - y - k^2 = 0 \tag{A.107}$$

The turning point y_1 is always real and $y_1 > 1$. For $g > 0$ we can parameterize $y_1 = k^2 g - 2d \quad y_3 = d + e \quad y_2 = d - e$ while for $g < 0$ the parametrization will be $y_3 = k^2 g - 2d \quad y_1 = d + e \quad y_2 = d - e$

The quantities d and e have the following expansion :

$$\begin{aligned} d \;\; &= \tfrac{1}{k^2 g^2} \textstyle\sum_{n=0} a_n(g) \frac{1}{g^{3n} k^{4n}} \\ e \;\; &= \tfrac{1}{\sqrt{-g}} \textstyle\sum_{n=0} b_n(g) \frac{1}{g^{3n} k^{4n}} \end{aligned} \tag{A.108}$$

where $a_n(g)$ and $b_n(g)$ are polynomials in g.

This series expansion diverges for $g^3k^4 = \hat{g} = O(1)$. This is due to the fact that in this regime A.107 can be approximated with $\hat{y}^3 - \hat{g}\hat{y}^2 - 1 = 0$ where $\hat{y} = yk^{\frac{2}{3}}$ and this last equation has coincidental solutions [11] for $\hat{g} = -3 \cdot 4^{\frac{1}{3}}$. Therefore for $\hat{g}$ of order one all three solutions are of order $k^{\frac{2}{3}}$ and for $k \to \infty$ one can approximate them with the solutions to $\hat{y}^3 - \hat{g}\hat{y}^2 - 1 = 0$ times $k^{\frac{2}{3}}$. The resulting expressions for $x(k,\hat{g})$ $Z(k,\hat{g})$ $t(k,\hat{g})$ are not transparent therefore we will consider in turns the limits $g \gg k^{-\frac{4}{3}}$ and $-1 < g \ll -k^{-\frac{4}{3}}$.

In the first case looking at the expansions for d and e we see that the situation is essentially similar to the previous computation for finite $k^2 > 0$ and $u^2 > 0$. In fact by using A.108 we see that also in this case $a \sim O(\frac{1}{u^2})$ while s is finite as in A.96.

Then we can argue that in the expansion of

$$\vec{x} = \frac{-2i\vec{k}}{\sqrt{y_1(y_3 - y_2)}} F[\phi, s] = -2i\vec{k}\sqrt{\frac{a}{y_1(y_3 - y_2)}} \sum c_n(s) a^n$$

only even terms in e are allowed obtaining:

$$\begin{aligned} ix &= \frac{1}{gk} \sum_{n=0} P_n^{(1)}(g) \frac{1}{g^{3n}k^{4n}} \\ -it &= \frac{\sqrt{1+g}}{gk} \sum_{n=0} P_n^{(2)}(g) \frac{1}{g^{3n}k^{4n}} \\ Z &= \log(u^2 - k^2) + C + \frac{1}{g^3k^4} \sum_{n=0} P_n(g) \frac{1}{g^{3n}k^{4n}} \end{aligned} \tag{A.109}$$

where the $P^{(i)}(g)$ are polynomials in g and $C = 2 - \log(4)$.

The expression for Z shows a logarithmic behaviour in $u^2 - k^2$ however its regime of validity is restricted to $u^2 - k^2 \gg k^{\frac{2}{3}}$ that is $g \gg k^{-\frac{4}{3}}$.

For negative values of g instead we can parameterize the solutions as:

$$y_2 = k^2 g - 2d \quad y_1 = d + e \quad y_3 = d - e$$

With the d and e expansions still given by A.108 . The turning point solution y_1

[11] for real k the two merging solutions are not the turning point y_1

is now closer and closer to 1 as $g \to -1$. In this case we can proceed as in A.100 and change the contour of integration obtaining after manipulations which track precisely A.100 - A.104 the following expansions:

$$\begin{aligned} ix &= (-g)^{-\frac{1}{4}} \sum_{m=0} L_m^{(1)}(g) \frac{1}{g^{\frac{3n}{2}} k^{2n}} + \frac{1}{gk} \sum_{n=0} Q_n^{(1)}(g) \frac{1}{g^{3n} k^{4n}} \qquad \text{(A.110)} \\ -it &= t(g) + (-g)^{-\frac{1}{4}} \sum_{m=1} L_m^{(2)}(g) \frac{1}{g^{\frac{3n}{2}} k^{2n}} + \frac{\sqrt{1+g}}{gk} \sum_{n=0} Q_n^{(2)}(g) \frac{1}{g^{3n} k^{4n}} \\ Z &= kz(g) + \frac{1}{(-g)^{\frac{3}{4}} k} \sum_{m=0} L_m(g) \frac{1}{g^{\frac{3}{2}n} k^{2n}} + \log(k^2 - u^2) + \frac{1}{g^3 k^4} \sum_{n=0} Q_n(g) \frac{1}{g^{3n} k^{4n}} \end{aligned}$$

where the $L(g)$ and $Q(g)$ are polynomials in g and the function $z(g)$ has the following explicit form: $\frac{\pi}{2}\sqrt{1+g} - 2K[-1]_2F_1(-\frac{1}{2}, \frac{1}{4}, \frac{1}{2}, 1+g)$ while $t(g) = 2\sqrt{1+g}z'(g)$; this expansion too is not valid for $g \sim k^{-\frac{4}{3}}$.

For $g \sim k^{-\frac{4}{3}}$ all the y_i scale as $k^{2/3}$ and $Z \sim O(k^0)$ interpolating between the expansions above.

The fact that the logarithmic divergence as $k = u$ present in A.109 and A.110 is resolved as $g \sim k^{-\frac{4}{3}}$ is due to the fact that in the $\mu \to \infty$ limit the branch points 3.57 for $Z(u,k)$ remain at a finite distance from the real axis. Conversely at finite μ for $k \sim u$ large the branch cuts stretch along the real axis as described in section 3.3.2.

A.8 Tortoise coordinate

In this appendix the analytic structure of the function $r(z)$ will be described in some detail and we will present its determination used in Appendices A.4 and A.5.

First recall the definition of the tortoise coordinate.

$$z(r) = \int_r^\infty dr' \frac{1}{f(r')} \qquad \text{(A.111)}$$

where $f(r) = r^2 + 1 - \frac{\mu}{r^{d-2}}$.

The solutions of $f(r) = 0$ will be denoted in the following by $r_i \quad i = 0, 1, .., d-1$ in particular r_0 is the positive real solution corresponding to the horizon. Also the residues at r_i in the integral for $z(r)$ will be denoted as $Res(r_i) = \frac{\beta_i}{4\pi}$. Then $\beta_0 = \beta$

the inverse temperature of the black hole.

In order to obtain a definite value of $z(r)$ we have to specify a particular contour connecting ∞ to r. Suppose that one particular contour $\mathcal{C}$ is chosen and the value $z_{\mathcal{C}}(r)$ is obtained. All the possible values of z corresponding to the same point will be $z(r) = z_{\mathcal{C}}(r) + 2i\sum_{i=0}^{d-1}\alpha_i\beta_i$ where $\alpha_i \in \mathbf{Z}$ and will form a lattice in the complex z plane. Some choices of the α_i determine the same point as, for example, $\alpha_i = 1$ for all i is equivalent to $\alpha_i = 0$ due to the fact that the sum of the residues must be zero as $f(r) \sim r^2$ for $r \sim \infty$, moreover in the case that d is even for each r_i also $-r_i$ is a solution of $f(r) = 0$ and the sum of the corresponding residues is zero. This lattice is simple in the case of $d = 3, 4, 6$ for which one has a triangular, rectangular or hexagonal lattice respectively. In the other cases the lattice points will be generically dense in the complex z plane. We can give a unique prescription for $z(r)$ by imposing that the contour $\mathcal{C}$ cannot cross a set of lines starting from the r_i. For example we can take these lines as propagating from 0 to the r_i radially but this is only one of many possible choices [12]. These lines will then be branch cuts for the function $z(r)$.

Some properties of the function $z(r)$ which will be useful in the following are:

- 1 The behaviour for $r \to \infty$ is $z(r) \sim \frac{1}{r}$
- 2 The behaviour for $r \sim r_i$ is $z(r) \sim -\frac{\beta_i}{4\pi}\log(r - r_i)$.
- 3 The behaviour for $r \sim 0$ is $z \sim \frac{r^{d-1}}{(d-1)\mu} + z(0)$ where $z(0)$ is any one of its possible values. Viceversa $r \sim ((d-1)\mu(z - z(0)))^{\frac{1}{d-1}}$.

From the last item in the list above we see that the function $r(z)$ is not single valued. The following is the description of the particular determination of this function that is used in the appendices A.4 and A.5. Notice that for $r \sim r_0$ the function $r(z) = r_0 + \exp(\frac{4\pi z}{\beta})$ is periodic with period $i\frac{\beta}{2}$. In fact the lines of constant real part for $z(r)$ around r_0 are topologically S_1 around r_0. This is valid only for $Re(z)$ greater than $\frac{\beta}{4}$. At this value of $Re(z)$ the line passes at $r = 0$ for $z = \frac{\beta}{4} + i\frac{\beta}{2}(n + \frac{1}{2})$ $n \in \mathbf{Z}$. These points are then branch points for the function $r(z)$. We will choose the branch

[12] note that this choice works due to the fact that the sum of the residues must be 0

cuts propagating from them to have constant imaginary part and to go towards $Re(z) = -\infty$. By following this prescription for all branch points we find a determination of $r(z)$ such that $r(z + i\frac{\beta}{2}) = r(z)$. With this choice of determination for $Re(z) > 0$ the only branch points are those described $z = \frac{\beta}{4} + i\frac{\beta}{2}(n + \frac{1}{2}) \quad n \in \mathbf{Z}$.

Suppose to approach the horizon from the boundary on the positive real r axis then this corresponds to moving on the real z axis from 0 to $+\infty$. Going around r_0 clockwise of an angle π in the r plane corresponds to shifting the imaginary part of z by $\frac{\beta}{4}$. Then going from r_0 to $r = 0$ on the real axis corresponds to moving along a line of constant imaginary part from $z = \infty$ to $z = \frac{\beta + i\beta}{4}$. We then see that by denoting with C the contour just described connecting $r = \infty$ to $r = 0$ we obtain $\frac{\beta}{4} = \int_C \frac{dr}{f(r)}$.

Appendix B

Appendix B

B.1 Self-energy in the real time formalism

In this appendix we first review some basic properties of real-time correlation functions. We then prove that the spectral density functions of fundamental fields in 5.1 have a discrete spectrum after the resummation of the self-energy diagrams à la Dyson.

B.1.1 Analytic properties of various real-time functions

Various real-time thermal Wightman function for an operator $\mathcal{O}$ are defined by

$$\begin{aligned} G_+(t) &= \frac{1}{Z}\mathrm{tr}\left(e^{-\beta H}\mathcal{O}(t)\mathcal{O}(0)\right) - C \\ G_-(t) &= \frac{1}{Z}\mathrm{tr}\left(e^{-\beta H}\mathcal{O}(0)\mathcal{O}(t)\right) - C \\ G_F(t) &= \theta(t)G_+(t) + \theta(-t)G_-(t), \\ G_R(t) &= i\theta(t)\frac{1}{Z}\mathrm{tr}\left(e^{-\beta H}[\mathcal{O}(t),\mathcal{O}(0)]\right), \\ G_A(t) &= -i\theta(-t)\frac{1}{Z}\mathrm{tr}\left(e^{-\beta H}[\mathcal{O}(t),\mathcal{O}(0)]\right) \end{aligned} \tag{B.1}$$

where Z is the partition function and C is a constant to be specified below. It is also convenient to introduce

$$G_{12}(t) = G_+(t - i\beta/2) \tag{B.2}$$

which can be obtained from $G_+(t)$ by an analytic continuation.

By inserting complete sets of states in B.1, $G_+(t)$ can be written as

$$G_+(t) = \frac{1}{Z}\sum_{i\neq j} e^{-iE_j t} e^{iE_i(t+i\beta)}\,\rho_{ij} \tag{B.3}$$

where i, j sum over the physical states of the theory and $\rho_{ij} = |\,\langle i|\mathcal{O}(0)|j\rangle\,|^2$. Comparing B.3 and B.1, C is chosen to be

$$C = \frac{1}{Z}\sum_i e^{-E_i\beta}\,\rho_{ii} \tag{B.4}$$

Note that C is chosen so that the Fourier transform of $G_+(t)$ does not have a "contact" term proportional to $\delta(\omega)$. Assuming the convergence of the sums is controlled by the exponentials, it follows from B.3 that $G_+(t)$ is analytic in t within the range $-\beta < \mathrm{Im}\, t < 0$. Similarly $G_-(t)$ is analytic for $0 < \mathrm{Im}\, t < \beta$ and $G_{12}(t)$ for $-\frac{\beta}{2} < \mathrm{Im}t < \frac{\beta}{2}$.

Introducing the spectral density function

$$\rho(\omega) \;= (1 - e^{-\beta\omega})\,\textstyle\sum_{i,j}(2\pi)\delta(\omega - E_i + E_j)e^{-\beta E_j}\rho_{ij} \tag{B.5}$$

then the Fourier transforms of B.1 can be written as

$$\begin{aligned}
G_+(\omega) &= \frac{1}{1 - e^{-\beta\omega}}\rho(\omega) \\
G_{12}(\omega) &= e^{-\frac{1}{2}\beta\omega}G_+(\omega) = e^{\frac{1}{2}\beta\omega}G_-(\omega) = \frac{1}{2\sinh\frac{\beta\omega}{2}}\rho(\omega) \\
G_R(\omega) &= -\int_{-\infty}^{\infty}\frac{d\omega'}{2\pi}\frac{\rho(\omega')}{\omega - \omega' + i\epsilon} \\
G_A(\omega) &= -\int_{-\infty}^{\infty}\frac{d\omega'}{2\pi}\frac{\rho(\omega')}{\omega - \omega' - i\epsilon} \\
G_F(\omega) &= G_R(\omega) + iG_-(\omega)
\end{aligned} \tag{B.6}$$

From B.6 we also have

$$\rho(\omega) = -i(G_R(\omega) - G_A(\omega)) \tag{B.7}$$

We also note that the Euclidean correlation function in momentum space can be obtained from

$$G_E(\omega_l) = \begin{cases} G_R(i\omega_l) & l \geq 0 \\ \\ G_A(i\omega_l) & l < 0 \end{cases}, \qquad \omega_l = \frac{2\pi l}{\beta}, \quad l \in \mathbf{Z} \tag{B.8}$$

Some further remarks:

- 1. From B.5–B.6,

$$\rho(-\omega) = -\rho(\omega), \qquad G_{12}(-\omega) = G_{12}(\omega), \qquad G_R(-\omega) = G_A(\omega)\ . \tag{B.9}$$

- 2. For a theory with a discrete spectrum, from B.5, the spectral function $\rho(\omega)$ and $G_+(\omega)$ are given by a sum of discrete delta functions supported on the real axis, while $G_R(\omega)$ is given by a discrete sum of poles along the real axis.

B.1.2 Self-energy in real-time formalism

In this section we consider real-time correlation functions of fundamental fields M_α in perturbation theory using the real-time formalism. We denote various quantities in B.1 with $\mathcal{O} = M_\alpha$ by $D_+^{(\alpha)}, D_F^{(\alpha)}$ etc and will suppress superscript α from now on. We prove that the corresponding spectral density functions have a discrete spectrum after the resummation of the self-energy diagrams à la Dyson. For simplicity, we will consider the high temperature limit so that we can ignore the singlet projection (see 5.20).

In the real time formalism [74] the degrees of freedom of the theory get doubled (see also [19]). For each original field (type 1) in 5.1 one introduces an equivalent field

(type 2)[1] whose interaction vertices differ by a sign from the ones for fields of type 1. Vertices therefore do not mix the two different kind of fields but propagators do and are written as a 2×2 matrix. For example, in frequency space the propagator for M_α (in the interacting theory) can be written as $D_{ab}(\omega), a, b = 1, 2$ with each component given by

$$\begin{aligned} D_{11}(\omega) &= D_F(\omega), & D_{22}(\omega) &= D_{11}^*(-\omega) \\ D_{12}(\omega) &= \frac{e^{\frac{\beta}{2}\omega}}{e^{\beta\omega}-1}\rho(\omega), & D_{21}(\omega) &= D_{12}(\omega) \end{aligned} \tag{B.10}$$

D_{ab} can be diagonalized as

$$D_{ab} = U \begin{pmatrix} D_g(\omega) & 0 \\ 0 & D_g^*(\omega) \end{pmatrix} U \tag{B.11}$$

with

$$U = \begin{pmatrix} \cosh\gamma & \sinh\gamma \\ \sinh\gamma & \cosh\gamma \end{pmatrix}, \quad \cosh\gamma = \frac{e^{\frac{\beta}{2}|\omega|}}{\sqrt{e^{\beta|\omega|}-1}}, \quad \sinh\gamma = \frac{1}{\sqrt{e^{\beta|\omega|}-1}} \tag{B.12}$$

and

$$D_g(\omega) = i\int \frac{d\omega'}{2\pi}\frac{\rho(\omega')}{\omega-\omega'+i\epsilon\omega} = \begin{cases} -iD_R(\omega) & \omega > 0 \\ \\ -iD_A(\omega) & \omega < 0 \end{cases} \tag{B.13}$$

The last expression in B.13 implies that when analytically continued from the positive real axis, $D_g(\omega)$ cannot have singularities in the upper half ω-plane. Similarly when analytically continued from the negative real axis, $D_g(\omega)$ cannot have singularities in the lower half ω-plane. Note that $D_g(\omega)$ can have a discontinuity at $Im(\omega) = 0$. If $D_g(\omega)$ does turn out to be analytic on the real axis, then it can have singularities only on the real axis in the limit $\epsilon \to 0$, which in turn implies that D_R, D_A and D_F can have singularities only on the real axis in the limit $\epsilon \to 0$.

[1] In a path integral derivation these correspond to the fields whose time argument is $t - i\sigma$ and we will take $\sigma = \frac{\beta}{2}$.

We will now show that $D_g(\omega)$ obtained using the Dyson equation from any finite order computation of the self-energy is a rational function with singularities only on the real axis. This implies that the spectral function ρ consists of a sum of finite number of delta functions supported on the real axis.

Note that the Dyson equation can be written as

$$\frac{1}{D_g(\omega)} = \frac{1}{D_g^{(0)}(\omega)} - i\tilde{\Pi}(\omega) \tag{B.14}$$

where

$$D_g^{(0)} = \frac{i}{\omega^2 - m^2 + i\epsilon} \tag{B.15}$$

is the free theory expression and $\tilde{\Pi}(\omega)$ can be computed from the perturbation theory as follows: (i) Compute 2×2 matrix $\Pi_{ab}(\omega)$ from the sum of amputated 1PI diagrams for the propagator in real time formalism; (ii) Diagonalizing $\Pi_{ab}(\omega)$ using B.12, i.e.

$$\Pi_{ab} = U \begin{pmatrix} \tilde{\Pi}(\omega) & 0 \\ 0 & \tilde{\Pi}^*(\omega) \end{pmatrix} U \ . \tag{B.16}$$

That Π_{ab} can be diagonalized using U is a consequence B.11.

Now expanding D_g and $\tilde{\Pi}$ in power series of λ

$$\begin{aligned} D_g &= D_g^{(0)} + \lambda D_g^{(1)} + \lambda^2 D_g^{(2)} + \cdots \\ \tilde{\Pi} &= \lambda\tilde{\Pi}^{(1)} + \lambda^2\tilde{\Pi}^{(2)} + \cdots \end{aligned} \tag{B.17}$$

from equation B.14 we have

$$D_g^{(1)} = D_g^{(0)}(i\tilde{\Pi}^{(1)})D_g^{(0)}, \quad D_g^{(2)} = D_g^{(0)}(i\tilde{\Pi}^{(2)})D_g^{(0)} + D_g^{(0)}(i\tilde{\Pi}^{(1)})D_g^{(0)}(i\tilde{\Pi}^{(1)})D_g^{(0)}, \ldots \tag{B.18}$$

¿From our discussion in section 5.2 (applied to fundamental fields), at any finite order in perturbation theory $\rho(\omega)$ consists of sums of terms of the form 5.23. Plugging such a $\rho(\omega)$ into B.13 one finds that $D_g^{(n)}(\omega)$ is a rational function and is analytic on the

real axis at each order in the perturbative expansion (i.e. there is no discontinuity at $Im(\omega) = 0$). Using B.18 we find that $\widetilde{\Pi}^{(n)}(\omega)$ must also be a rational function and analytic on real axis. This in turn implies that the resummed $D_g(\omega)$ found from B.14 is a rational function and analytic on real axis. We conclude that the singularities of D_g must lie on the real axis and there are only a finite number of them at any finite order in the computation of the self-energy Π. From B.13 the spectral density function must be a finite sum of delta functions supported on the real axis.

B.2 Energy spectrum and eigenvectors of sparse random matrices

In this appendix we summarize features of eigenvalues and eigenvectors of a random sparse matrix found in [81, 69, 82]. Consider an $M \times M$ real symmetric matrix A whose elements A_{ij} for $i \geq j$ are independent identically distributed random variables with even probability distribution $f(A_{ij})$. Let $f(x)$ be of the following form:

$$f(x) = (1 - \alpha)\delta(x) + \alpha h(x) \tag{B.19}$$

where $0 < \alpha < 1$ and $h(x)$ is even and not delta-function like at $x = 0$. Let the variance of $h(x)$ be v^2. The parameter α measures the sparsity of the matrix: for each row or column of the matrix there will be on average $\alpha M = K$ elements which are different from zero. K is called the connectivity of the matrix. When $K < 1$ it is possible for eigenvectors to be localized in a subspace with dimension smaller than M. For $K > 1$ in the large M limit no such localization occurs and the matrix has to be diagonalized in the full M dimensional space.

When $K \gg 1$, the density of states reduces to Wigner's semicircular law in an expansion in K^{-1}:

$$\rho(E) = \frac{1}{2\pi\Gamma^2}\sqrt{4\Gamma^2 - E^2}\left(1 + O(K^{-1})\right) \tag{B.20}$$

Where E is the eigenvalue value and Γ is given by:

$$\Gamma^2 = Kv^2\left(1 + O(K^{-1})\right) \tag{B.21}$$

Notice that Kv^2 is the average value of

$$\Gamma_i^2 = \sum_{j \neq i} |A_{ij}|^2 \tag{B.22}$$

over the rows or columns of the sparse matrix. The first correction to $\rho(E)$ gives a change in the edge location, however there also are nonperturbative tails to the distribution which for $E \gg \Gamma$ assume the form:

$$\rho(E) \sim \left(\frac{E^2}{eK}\right)^{-E^2} \tag{B.23}$$

Their effect is to make the spectrum unbounded.

Denote by T the orthogonal change of basis matrix which brings A to diagonal form for $K \gg 1$. T has a random uniform distribution over the group of orthogonal $M \times M$ matrices. Therefore the eigenvectors of A are a random orthonormal basis of the total space which means that apart from correlations[2] which are negligible in the large M limit their elements are independently distributed gaussian random variables with mean 0 and variance $\frac{1}{M}$. In particular the eigenvectors are completely delocalized. Therefore for large K the situation is similar to that for the Gaussian Orthogonal Ensemble (GOE).

B.3 Single anharmonic oscillator

It is clear that the argument presented in section 5.3 applies to the real time correlation functions of a single anharmonic oscillator at finite temperature[3](with changes

[2]which are due to normalization conditions.

[3]This section is motivated from a discussion with Steve Shenker.

of combinatorial factors)

$$S = \int dt \left(\frac{1}{2}\dot{x}^2 - \frac{1}{2}x^2 - \frac{1}{4!}\lambda x^4 \right) . \tag{B.24}$$

For example one can conclude that the perturbation theory for

$$D_+(t) = \langle x(t)x(0) \rangle_\beta \tag{B.25}$$

should diverge at a time scale 5.55 for $T \gg \omega_0$ (we set $\omega_0 = 1$ in B.24). Here we give an alternative derivation of this. Inserting complete sets of states in B.25 we find that

$$D_+(t) = Z^{-1} \sum_{n,m} | \langle n|x|m \rangle |^2 e^{-\beta E_n - it(E_m - E_n)} \tag{B.26}$$

where $Z = \sum_n e^{-\beta E_n}$ and $|n\rangle$ are interacting theory eigenstates. If we are interested only in contributions of the form $(\lambda t)^n$ we get:

$$D_+(t) = Z_0^{-1} \sum_{n,m} | \langle n|x|m \rangle_0 |^2 e^{-\beta E_n^{(0)} - it(E_m^{(0)} - E_n^{(0)}) - it\lambda(E_m^{(1)} - E_n^{(1)})} + \cdots \tag{B.27}$$

where quantities with index 0 are computed in the free theory and $\lambda E^{(1)}$ are the energy shifts at first order in perturbation theory. Equation B.27 can be evaluated as

$$D_+(t) = \frac{1}{2} Z_0^{-1} \sum_{n=0}^{\infty} (n+1)[e^{-\beta(n+\frac{1}{2}) - it(1+\frac{\lambda}{8}(n+1))} + e^{-\beta(n+\frac{3}{2}) + it(1+\frac{\lambda}{8}(n+1))}] + \cdots \tag{B.28}$$

which can be summed to give

$$D_+(t) = \frac{(e^\beta - 1)e^{\beta - it(1-\frac{\lambda}{8})}}{2(e^{\beta + \frac{it\lambda}{8}} - 1)^2} + \frac{(e^\beta - 1)e^{it(1-\frac{\lambda}{8})}}{2(e^{\beta - \frac{it\lambda}{8}} - 1)^2} + \cdots \tag{B.29}$$

In B.29 there are double poles at

$$t = \pm i \frac{8\beta}{\lambda} + k \frac{16\pi}{\lambda}, \qquad k \in Z . \tag{B.30}$$

If one resums the diagrams discussed in section 5.3, one would then get simple poles and the positions of the poles are further away from the real axis than those of B.29 indicating that there are some positive contributions not captured by the class of Feynman diagrams. Some remarks:

- 1. Note that the reason for the behavior B.28–B.30 can be attributed to the fact that the first order energy shift[4]

$$\lambda(E_{n+1}^{(1)} - E_n^{(1)}) \propto \lambda n \tag{B.31}$$

- 2. The above argument shows that the divergence of perturbation theory at $t \sim \frac{1}{\lambda T}$ has nothing to do with the standard argument of the breakdown of perturbation theory by taking $\lambda \to -\lambda$. Indeed the behavior here is due to a single class of diagrams not due to the $n!$ growth of the number of diagrams.

- 3. The way the perturbation theory breaks down for a matrix quantum mechanics in the high energy sector appears to be very different from the above discussion for a single oscillator. More explicitly, let us write B.27 for the matrix case as

$$D_+(t) = Z_0^{-1} \sum_n e^{-\beta E_n^{(0)}} \sum_m |\langle n|M|m\rangle_0|^2 e^{-it(E_m^{(0)} - E_n^{(0)}) - it\lambda(E_m^{(1)} - E_n^{(1)})} + \cdots \tag{B.32}$$

  As we discussed in the main text, the sum over m in the above equation will involve an exponentially large number of states with free theory energies ranging over of order $O(N)$. A naive estimate of $E_m^{(1)} - E_n^{(1)}$ also gives order $O(N)$. Unfortunately the story appears to be rather complicated and we have not able to extract a divergent time scale $1/\lambda T$ from B.32.

[4]Note the following behavior also eventually breaks down for large enough n due to level crossing.

B.4 Estimate of various quantities

We now estimate 5.69–5.72 after averaging them over states of similar energies. We will be interested in how these quantities scale with N in the large N limit. An important property that we will assume below for these averaged quantities is that they are slow-varying functions of ϵ or E. In the large N limit, we can then estimate them using the corresponding thermal averages, which can in turn be expressed in terms of various correlation functions at finite temperature. For example, the thermal average of Σ_i is

$$\widehat{\Sigma}(\beta) = \frac{1}{Z}\sum_i e^{-\beta E_i}\Sigma_i = \frac{1}{Z}\int dE\, e^{-\beta E}\Omega(E)\,\Sigma(E) \tag{B.33}$$

where $\Sigma(E)$ is the microcanonical average and $\Omega(E) = e^{S(E)}$ the density of states. Since $\Sigma(E)$ is a slow-varying function of E, we can perform a saddle point approximation of the last expression, yielding

$$\Sigma(E) \approx \widehat{\Sigma}(\beta_E)\left(1 + O(1/N^2)\right) \tag{B.34}$$

with β_E determined by $\frac{\partial S(E)}{\partial E} = \beta_E$. Using the last equality of 5.72 we can write $\widehat{\Sigma}(\beta)$ as

$$\begin{aligned}\widehat{\Sigma}(\beta) &= \frac{1}{Z}\sum_{i,j,i\neq j} e^{-\beta E_i}|\,\langle i|V|j\rangle\,|^2 \\ &= \langle V(0)V(0)\rangle_\beta\end{aligned} \tag{B.35}$$

where $\langle V(0)V(0)\rangle_\beta$ denotes the connected Wightman function as defined by B.3. From the standard large N scaling argument B.35 is of order $O(N^2)$ (recall that we include a factor of N in the definition of V). Thus unless B.35 is zero at leading order we conclude that $\Sigma(E)$ can be written in a form

$$\Sigma(E) = N^2 h(\lambda, E/N^2) \tag{B.36}$$

where $h(\lambda, \mu)$ is a function independent of N. An exactly parallel argument can be applied to $\sigma(\epsilon)$ in which case B.35 is replaced by expectation values in free theory and thus we find that

$$\sigma(\epsilon) = N^2 \widetilde{h}(\lambda, \epsilon/N^2) \tag{B.37}$$

for some function $\widetilde{h}$.

As another example, let us look at the thermal average of 5.71,

$$\frac{1}{Z} \sum_i e^{-\beta E_i} \overline{\epsilon}_i = \frac{1}{Z} \int dE \, e^{-\beta E} \Omega(E) \, \overline{\epsilon}(E) \approx \overline{\epsilon}(E_\beta) \tag{B.38}$$

Using the last equality of 5.71, the left hand side of B.38 can in turn be written as

$$E_\beta - \langle V \rangle_\beta \tag{B.39}$$

where $\langle V \rangle_\beta$ is the thermal one-point function of V in the interacting theory and scales with N as $O(N^2)$. Thus we can write

$$\overline{\epsilon}(E) = N^2 g(\lambda, E/N^2) \tag{B.40}$$

for some function h. An exactly parallel argument yields

$$\overline{E}(\epsilon) = N^2 \widetilde{g}(\lambda, \epsilon/N^2) \; . \tag{B.41}$$

To summarize, we find that the averaged values of $\Gamma(\epsilon)$ and $\Delta(E)$ are both of order $O(N)$ in the 't Hooft limit for any nonzero λ. Thus in the large N limit, both the correlation length between interacting theory energy levels and the energy range that the free theory states are mixed under perturbation go to infinity.

B.5 Some useful relations

In this appendix we derive some important relations which will be used in Appendix B6 to derive the matrix elements of an operator $\mathcal{O}$ between generic states in the high energy sector.

B.5.1 Density of states

The conservation of states implies that the density of states $\Omega(E)$ of the full theory and $\Omega_0(\epsilon)$ of the free theory should be related by

$$\Omega(E) = \Omega_0(\bar{\epsilon}(E))\frac{d\bar{\epsilon}(E)}{dE} \tag{B.42}$$

which implies

$$\frac{1}{\Omega(E)}\frac{d\Omega(E)}{dE} = \frac{d\bar{\epsilon}(E)}{dE}\frac{1}{\Omega_0(\bar{\epsilon}(E))}\frac{d\Omega_0}{d\epsilon}\Big|_{\bar{\epsilon}(E)} + \frac{\frac{d^2\bar{\epsilon}(E)}{dE^2}}{\frac{d\bar{\epsilon}(E)}{dE}}$$

In the large N limit the second term in the above equation should be of order $O(1/N^2)$. Thus we find that

$$\beta(E) = \beta_0(\bar{\epsilon}(E))\frac{d\bar{\epsilon}(E)}{dE} \tag{B.43}$$

with

$$\beta(E) = \frac{1}{\Omega(E)}\frac{d\Omega(E)}{dE}, \qquad \beta_0(\epsilon) = \frac{1}{\Omega_0(\epsilon)}\frac{d\Omega_0}{d\epsilon}\ . \tag{B.44}$$

We also expect that

$$\bar{\epsilon}(\overline{E}(\epsilon)) \approx \epsilon \tag{B.45}$$

Note that all the above relations are valid only to leading order in N.

B.5.2 Properties of $\chi_E(\epsilon)$ and $\rho_\epsilon(E)$

Consider the microcanonical average of 5.66 and 5.67, which we denote as $\rho_\epsilon(E)$ and $\chi_E(\epsilon)$ respectively. From 5.66 and 5.67 one should have

$$\rho_\epsilon(E) = \frac{\Omega(E)}{\Omega_0(\epsilon)}\chi_E(\epsilon) \; . \tag{B.46}$$

From 5.68 we should also have

$$\int d\epsilon \, \chi_E(\epsilon) = 1 \tag{B.47}$$

and

$$\int dE \, \rho_\epsilon(E) = \frac{1}{\Omega_0(\epsilon)} \int dE \, \Omega(E) \, \chi_E(\epsilon) = 1 \; . \tag{B.48}$$

Given that

$$\overline{\epsilon}(E) = \int d\epsilon \, \epsilon \, \chi_E(\epsilon), \qquad \Sigma(E) = \Delta^2(E) = \int d\epsilon \, (\epsilon - \overline{\epsilon}(E))^2 \chi_E(\epsilon) \tag{B.49}$$

we can write $\chi_E(\epsilon)$ as

$$\chi_E(\epsilon) = f_E(\epsilon - \overline{\epsilon}(E)) \tag{B.50}$$

with f_E a function which has a spread of $\Delta(E) \sim O(N)$. Since we expect $f_E(\omega)$ to fall off quickly to zero in the large N limit outside the range $(-\frac{1}{2}\Delta(E), \frac{1}{2}\Delta(E))$, equations B.47 and B.48 lead to

$$\int_{-\infty}^{\infty} d\omega \, f_E(\omega) = 1 \tag{B.51}$$

and

$$\int_{-\infty}^{\infty} dE \, \frac{\Omega(E)}{\Omega_0(\epsilon)} f_E(\epsilon - \overline{\epsilon}(E)) = 1 \tag{B.52}$$

Changing the integration variable of B.52 to $\epsilon' = \overline{\epsilon}(E)$ and using B.45, we find that

$$\int d\epsilon' \frac{\Omega_0(\epsilon')}{\Omega_0(\epsilon)} f_{\overline{E}(\epsilon')}(\epsilon - \epsilon') = \int_{-\infty}^{\infty} d\omega \, f_{\overline{E}(\epsilon)}(\omega) \frac{\Omega_0(\epsilon - \omega)}{\Omega_0(\epsilon)} = 1 \tag{B.53}$$

where in the second expression we have replaced $f_{\overline{E}(\epsilon')}$ by $f_{\overline{E}(\epsilon)}$. This is because, as a function of $\epsilon - \epsilon'$, the spread of f is of order $O(N)$, while $\overline{E}(\epsilon') \approx \overline{E}(\epsilon) + O(\frac{\epsilon' - \epsilon}{N^2}) \approx \overline{E}(\epsilon)$. The second expression of B.53 can now be written as

$$\int_{-\infty}^{\infty} d\omega f_E(\omega) e^{-\beta_0(\overline{\epsilon}(E))\omega} = 1 \tag{B.54}$$

Equations B.51 and B.54 can be written in a more symmetric manner as

$$\int_{-\infty}^{\infty} d\omega \, e^{\frac{1}{2}\beta(E)\omega} \, g_E(\omega) = \int_{-\infty}^{\infty} d\omega \, e^{-\frac{1}{2}\beta(E)\omega} \, g_E(\omega) = 1 \tag{B.55}$$

where we have introduced a function

$$g_E(\omega) = e^{-\frac{1}{2}\beta(E)\omega} \frac{d\overline{\epsilon}(E)}{dE} f_E\left(\frac{d\overline{\epsilon}(E)}{dE}\omega\right) . \tag{B.56}$$

Equations B.55 imply that $g_E(\omega)$ should fall off faster than $e^{-\frac{1}{2}\beta(E)|\omega|}$ as $\omega \to \pm\infty$.

B.5.3 A relation between matrix elements and correlation functions in free theory

In this subsection we derive in free theory a relation between the matrix elements of an operator $\mathcal{O}$ between states in the high energy sector and correlation functions. For simplicity we consider theories with a single fundamental frequency ω_0, like $\mathcal{N} = 4$ SYM or 5.3.

The Lehmann spectral decomposition for frequency space Wightman function $G_+^{(0)}(\omega)$ of some operator $\mathcal{O}$ in free theory can be written as

$$G_+^{(0)}(\omega) = \frac{1}{Z_0} \sum_{a,b} e^{-\beta\epsilon_a} \rho_{ab} \, \delta(\omega - \epsilon_b + \epsilon_a) \tag{B.57}$$

where $\rho_{ab} = |\langle a|\mathcal{O}(0)|b\rangle|^2$. Due to energy conservation, $\mathcal{O}$ can only connect levels whose energy differences lie between $-\Delta\omega_0$ and $\Delta\omega_0$, where Δ is the dimension of $\mathcal{O}$, i.e. ρ_{ab} can only be non-vanishing for $|\epsilon_a - \epsilon_b| \leq \Delta\omega_0$. We can thus rewrite B.57 as

$$G_+^{(0)}(\omega) = \frac{1}{Z_0} \sum_{k=-\Delta}^{\Delta} G_k \delta(\omega - k\omega_0) \tag{B.58}$$

with

$$\begin{aligned} G_k &= \frac{1}{Z_0} \sum_a e^{-\beta\epsilon_a} \sum_{\epsilon_b = \epsilon_a + k\omega_0} \rho_{ab} \\ &= \frac{1}{Z_0} \sum_a e^{-\beta\epsilon_a} \rho_k(a) \end{aligned} \tag{B.59}$$

where $\sum_{\epsilon_b=\epsilon}$ denotes that one sums over $|b\rangle$ whose energy is given by $\epsilon_b = \epsilon$. Note here we have assumed that the free theory energy levels are equally spaced as in $\mathcal{N} = 4$ SYM theory on S^3. We also introduced

$$\rho_k(a) = \sum_{\epsilon_b = \epsilon_a + k\omega_0} \rho_{ab} \tag{B.60}$$

We now separate the sum a in B.59 in terms of energies and degeneracies, i.e.

$$\sum_a = \sum_\epsilon \sum_{\epsilon_a = \epsilon}$$

We thus find that

$$G_k = \tfrac{1}{Z_0} \textstyle\sum_\epsilon \mathcal{N}(\epsilon) e^{-\beta\epsilon} \overline{\rho}_k(\epsilon) \tag{B.61}$$

where we have introduced the micro-canonical average of $\rho_k(b)$for energy ϵ

$$\overline{\rho}_k(\epsilon) = \frac{1}{\mathcal{N}(\epsilon)} \sum_{a \in \epsilon} \rho_k(a) = \frac{1}{\mathcal{N}(\epsilon)} \sum_{\epsilon_a = \epsilon} \sum_{\epsilon_b = \epsilon + k\omega_0} \rho_{ab} \,. \tag{B.62}$$

We expect that the microcanonical average $\overline{\rho}_k(\epsilon)$ should be a slow varying function of ϵ, i.e. it can be written in a form $N^\alpha f(\epsilon/N^2)$ for some constant α. In the large N

limit since $\mathcal{N}(\epsilon)e^{-\beta\epsilon}$ is sharply peaked at ϵ_β specified by, one can perform a saddle point approximation in B.61 to get

$$G_k = \overline{\rho}_k(\epsilon_\beta) + \cdots \tag{B.63}$$

From B.57 we thus find that

$$G_+(\omega) = \sum_k \overline{\rho}_k(\epsilon_\beta)\delta(\omega - k\omega_0) \tag{B.64}$$

In the large N limit since the connected part of $G_+(\omega)$ scales with N as $O(N^0)$, thus we find from B.64 that

$$\overline{\rho}_k(\epsilon_\beta) \sim O(N^0). \tag{B.65}$$

B.6 Derivation of matrix elements

In this appendix we give a derivation of 5.75. The main object of interests to us is

$$\begin{aligned} \rho_{ij} &= \sum_{a,b} |c_{ia}|^2 |c_{jb}|^2 \rho_{ab} \\ &= \sum_a |c_{ia}|^2 \sum_k \sum_{\epsilon_b = \epsilon_a + k\omega_0} |c_{jb}|^2 \rho_{ab} \end{aligned} \tag{B.66}$$

Due to the sparse and random nature of ρ_{ab}, one cannot naively approximate the sums over a and b in by integrals. Instead one must be careful with the discreteness nature of the sum. Note that

$$\sum_{\epsilon_b = \epsilon_a + k\omega_0} |c_{jb}|^2 \rho_{ab} \approx \overline{c}_j(\epsilon_a + k) \sum_{\epsilon_b = \epsilon_a + k\omega_0} \rho_{ab} = \overline{c}_j(\epsilon_a + k)\rho_k(a)$$

which can be justified as follows. Inside a given energy shell, ρ_{ab} can be treated as a random sparse matrix. Thus one can treat the summand as a random sampling of $|c_{jb}|^2$. Since the number of sampling points goes to infinity (as a power in N) in the large N limit, we can approximate $|c_{jb}|^2$ by its average value of the energy shell. We

now have

$$\begin{aligned}\rho_{ij} &= \sum_k \sum_a |c_{ia}|^2 \overline{c}_j(\epsilon_a + k)\rho_k(a) \\ &= \sum_k \sum_\epsilon \overline{c}_j(\epsilon + k) \sum_{\epsilon_a = \epsilon} |c_{ia}|^2 \rho_k(a) \\ &= \sum_k \sum_\epsilon \overline{c}_j(\epsilon + k)\mathcal{N}(\epsilon)\overline{c}_i(\epsilon)\overline{\rho}_k(\epsilon) \end{aligned} \tag{B.67}$$

In the second line above we separated the sum over all states a into the sum over the energy and the sum over states in each energy shell. In the third line we replaced the sum in an energy shell by its average values. The replacement is all right since $|c_{ia}|^2$ and $\rho_k(a)$ are completely independent variables, so the average of their product should factorize.

Now given that all quantities in the last line of B.67 are averaged quantities, we approximate the sum over ϵ by an integral. Averaging i, j over states of the same energy and using 5.67, we find

$$\begin{aligned}\rho_{E_1E_2} &= \sum_k \int \frac{d\epsilon}{\Omega_0(\epsilon + k)} \chi_{E_2}(\epsilon + k)\chi_{E_1}(\epsilon)\,\overline{\rho}_k(\epsilon) \\ &= \sum_k \int \frac{d\epsilon}{\Omega_0(\epsilon + k)} f_{E_2}(\epsilon + k - \overline{\epsilon}_2) f_{E_1}(\epsilon - \overline{\epsilon}_1)\,\overline{\rho}_k(\epsilon) \\ &= \sum_k \int \frac{dp}{\Omega_0(\overline{\epsilon}_{12} + p + k)} f_{E_2}(p + k + \frac{1}{2}\Delta_{12}) f_{E_1}(p - \frac{1}{2}\Delta_{12})\,\overline{\rho}_k(p + \overline{\epsilon}_{12}) \end{aligned} \tag{B.68}$$

with

$$\overline{\epsilon}_{1,2} = \overline{\epsilon}(E_{1,2}), \qquad \overline{\epsilon}_{12} = \frac{1}{2}(\overline{\epsilon}(E_1) + \overline{\epsilon}(E_2)) = \overline{\epsilon}(E), \qquad \Delta_{12} = \overline{\epsilon}(E_1) - \overline{\epsilon}(E_2) = \left.\frac{d\overline{\epsilon}(E)}{dE}\right|_E \omega$$

where

$$E = \frac{E_1 + E_2}{2}, \qquad \omega = E_1 - E_2$$

Equation B.68 can be further simplified as

$$\begin{aligned}\rho_{E_1E_2} &= \frac{1}{\Omega(E)} \sum_k G_{12}(k) \int_{-\infty}^{\infty} dp\, g_E(p + k' + \frac{1}{2}\omega)\, g_E(p - \frac{1}{2}\omega) \\ &= \frac{1}{\Omega(E)} A(\omega; E) \end{aligned} \tag{B.69}$$

with

$$G_{12}(k) = e^{-\frac{1}{2}\beta_0(\bar{\epsilon}_{12})k}\overline{\rho}_k(\bar{\epsilon}_{12}), \qquad k' = \frac{1}{\frac{d\bar{\epsilon}(E)}{dE}}k \tag{B.70}$$

and $g_E(\omega)$ was defined in B.56. Note that from equation B.64, G_{12} are essentially the Fourier components of free theory correlation functions. $A(\omega; E)$ should be a smooth function of ω since the integral in B.69 appears to be well defined for all ω. It is easy to check that

$$A(-\omega; E) = A(\omega; E) \tag{B.71}$$

since $G_{12}(k) = G_{12}(-k)$. Further as $\omega \to \infty$, we find that

$$A(\omega; E) \propto e^{-\frac{1}{2}\beta(E)|\omega|} \ . \tag{B.72}$$

Now let us examine possible singularities of $A(\omega, E)$ on the real axis. We start with the definition B.50 of f_E. Since $\chi_E(\epsilon)$ is the average of 5.67 over states of similar energies, $f_E(\omega)$ must be a real positive function of $\omega \in R$. Then the function $g_E(\omega)$ introduced in B.56 should also be real and positive as $\bar{\epsilon}(E)$ is a monotonous function of E. The positivity and normalization conditions B.55 imply that $g_E(\omega)$ can at most have integrable singularities of the form[5]

$$g_E(\omega) \approx \frac{K_i}{|\omega - \omega_i|^{\alpha_i}}, \qquad \omega \to \omega_i, \quad \alpha_i < 1 \tag{B.73}$$

Note that the closer α_i is to one the smaller is K_i from the normalization requirement. Now let us look at the definition B.69 of $A(\omega; E)$,

$$A(\omega; E) \ = \sum_k G_{12}(k)s(\omega + k) \tag{B.74}$$

[5]Such integrable singularities can only arise if c_{ia} have accumulation points in the large N limit. While it appears unlikely that this can happen, we do not have a rigorous proof at the moment.

where

$$s(\omega) = \int_{-\infty}^{\infty} dx\, g_E(x + \frac{1}{2}\omega)\, g_E(x - \frac{1}{2}\omega)\ . \tag{B.75}$$

Note that the finite sum over k in B.74 cannot introduce singularities in ω therefore we focus on $s(\omega)$. As $g_E(\omega)$ falls off faster than $e^{-\frac{1}{2}\beta(E)|\omega|}$ as $\omega \to \pm\infty$, the integral in B.75 is convergent for $x \to \pm\infty$. Thus we only need to worry about possible divergences arising from the middle of the integration range. Integrating B.75 we find that

$$\int_{-\infty}^{\infty} d\omega s(\omega) = \int_{-\infty}^{\infty} dx g_E(x) \int_{-\infty}^{\infty} dy g_E(y) \tag{B.76}$$

which is finite by B.55 . Therefore the only singularities allowed for $s(\omega)$ are of integrable kind $\frac{K}{|\omega-\omega_s|^\alpha}$ with $\alpha < 1$. We can find the locations of ω_s in terms of (integrable) singularities of $g_E(\omega)$ as follows. Since $g_E(x - \frac{1}{2}\omega)$ and $g_E(x + \frac{1}{2}\omega)$ are both integrable the only possible divergences of B.75 are at values of ω for which the integrable singularities of two function sit on top of each other. This happens for $\omega = \omega_i - \omega_j$ where the ω_i are the locations of the singularities for $g_E(\omega)$. For $\omega = \omega_i - \omega_j + \epsilon$ with ϵ small the integral B.75 near $x \approx \frac{1}{2}(\omega_i + \omega_j)$ can be written as $K_i K_j \int_{-\delta}^{\delta} dy \frac{1}{|y-\frac{1}{2}\epsilon|^{\alpha_j}|y+\frac{1}{2}\epsilon|^{\alpha_i}}$ where δ is some multiple of ϵ. By rescaling we see that it behaves as $\epsilon^{1-\alpha_i-\alpha_j}$. Therefore the integral $s(\omega)$ can at most have a singularity of the form $\frac{K_i K_j}{|\omega-\omega_i+\omega_j|^\alpha}$ with $\alpha = \alpha_i + \alpha_j - 1 < 1$.

Thus we conclude that on the real axis $A(\omega; E)$ can have at most integrable singularities of the form

$$A(\omega; E) \propto \frac{1}{|\omega - \omega_s|^{\alpha_s}}, \qquad \alpha_s < 1\ . \tag{B.77}$$

Bibliography

[1] Ofer Aharony, Joseph Marsano, Shiraz Minwalla, Kyriakos Papadodimas, and Mark Van Raamsdonk. The hagedorn / deconfinement phase transition in weakly coupled large N gauge theories. *Adv. Theor. Math. Phys.*, 8:603–696, 2004.

[2] Ofer Aharony, Joseph Marsano, Shiraz Minwalla, Kyriakos Papadodimas, and Mark Van Raamsdonk. A first order deconfinement transition in large N Yang-Mills theory on a small S^3. *Phys. Rev.*, D71:125018, 2005.

[3] Vijay Balasubramanian, Per Kraus, and Albion E. Lawrence. Bulk vs. boundary dynamics in anti-de Sitter spacetime. *Phys. Rev.*, D59:046003, 1999.

[4] Vijay Balasubramanian, Per Kraus, Albion E. Lawrence, and Sandip P. Trivedi. Holographic probes of anti-de Sitter space-times. *Phys. Rev.*, D59:104021, 1999.

[5] Vijay Balasubramanian, Per Kraus, and Masaki Shigemori. Massless black holes and black rings as effective geometries of the D1-D5 system. *Class. Quant. Grav.*, 22:4803–4838, 2005.

[6] Vijay Balasubramanian, Donald Marolf, and Moshe Rozali. Information recovery from black holes. *Gen. Rel. Grav.*, 38:1529–1536, 2006.

[7] Maximo Banados, Claudio Teitelboim, and Jorge Zanelli. The black hole in three-dimensional space-time. *Phys. Rev. Lett.*, 69:1849–1851, 1992.

[8] T. Banks and W. Fischler. Space-like singularities and thermalization. 2006.

[9] Tom Banks, Michael R. Douglas, Gary T. Horowitz, and Emil J. Martinec. AdS dynamics from conformal field theory. 1998.

[10] J. L. F. Barbon and E. Rabinovici. Very long time scales and black hole thermal equilibrium. *JHEP*, 11:047, 2003.

[11] J. L. F. Barbon and E. Rabinovici. Long time scales and eternal black holes. *Fortsch. Phys.*, 52:642–649, 2004.

[12] J. L. F. Barbon and E. Rabinovici. Topology change and unitarity in quantum black hole dynamics. 2005.

[13] N. Beisert, C. Kristjansen, and M. Staudacher. The dilatation operator of $\mathcal{N} = 4$ super Yang-Mills theory. *Nucl. Phys.*, B664:131–184, 2003.

[14] Niklas Beisert and Matthias Staudacher. Long-range PSU(2, 2|4) bethe ansaetze for gauge theory and strings. *Nucl. Phys.*, B727:1–62, 2005.

[15] Jacob D. Bekenstein. Black holes and entropy. *Phys. Rev.*, D7:2333–2346, 1973.

[16] Jacob D. Bekenstein. Generalized second law of thermodynamics in black hole physics. *Phys. Rev.*, D9:3292–3300, 1974.

[17] Jacob D. Bekenstein. A universal upper bound on the entropy to energy ratio for bounded systems. *Phys. Rev.*, D23:287, 1981.

[18] V. A. Belinskii, E. M. Lifshitz, and I. M. Khalatnikov. On a general cosmological solution of the Einstein equations with a time singularity. *Zh. Eksp. Teor. Fiz.*, 62:1606–1613, 1972.

[19] M. Le Bellac. *Thermal field theory.* Cambridge, New York: Cambridge University Press, 1996.

[20] Iosif Bena, Joseph Polchinski, and Radu Roiban. Hidden symmetries of the AdS(5) $\times$ S^5 superstring. *Phys. Rev.*, D69:046002, 2004.

[21] M. V. Berry. Infinitely many stokes smoothings in the gamma function. *Proc. Roy. Soc. Lond.*, A434:465, 1991.

[22] N. D. Birrell and P. C. W. Davies. Quantum fields in curved space. Cambridge, Uk: Univ. Pr. (1982) 340p.

[23] J. C. Breckenridge, Robert C. Myers, A. W. Peet, and C. Vafa. D-branes and spinning black holes. *Phys. Lett.*, B391:93–98, 1997.

[24] Mauro Brigante, Guido Festuccia, and Hong Liu. Inheritance principle and non-renormalization theorems at finite temperature. *Phys. Lett.*, B638:538–545, 2006.

[25] Vitor Cardoso, Jose Natario, and Ricardo Schiappa. Asymptotic quasinormal frequencies for black holes in non- asymptotically flat spacetimes. *J. Math. Phys.*, 45:4698–4713, 2004.

[26] Lance J. Dixon, Jeffrey A. Harvey, C. Vafa, and Edward Witten. Strings on orbifolds. *Nucl. Phys.*, B261:678–686, 1985.

[27] Guido Festuccia and Hong Liu. Excursions beyond the horizon: Black hole singularities in Yang-Mills theories. I. *JHEP*, 04:044, 2006.

[28] Lukasz Fidkowski, Veronika Hubeny, Matthew Kleban, and Stephen Shenker. The black hole singularity in AdS/CFT. *JHEP*, 02:014, 2004.

[29] Ben Freivogel, Steven B. Giddings, and Matthew Lippert. Toward a theory of precursors. *Phys. Rev.*, D66:106002, 2002.

[30] Kazuyuki Furuuchi. From free fields to AdS: Thermal case. *Phys. Rev.*, D72:066009, 2005.

[31] Y. V. Fyodorov, O. A. Chubykalo, F. M Izrailev, and G. Casati. Wigner random banded matrices with sparse structure: Local spectral density of states. *Phys. Rev. Lett.*, 76(10):1603–1606, Mar 1996.

[32] Yi-hong Gao and Miao Li. Large N strong/weak coupling phase transition and the correspondence principle. *Nucl. Phys.*, B551:229–241, 1999.

[33] R. Geroch and G. Horowitz. Global structure of spacetimes. In *Hawking, S.W., Israel, W.: General Relativity*, (1979).

[34] Steven B. Giddings. The boundary S-matrix and the AdS to CFT dictionary. *Phys. Rev. Lett.*, 83:2707–2710, 1999.

[35] Michael B. Green, J. H. Schwarz, and Edward Witten. Superstring theory. vol. 1: Introduction, vol. 2: Loop amplitudes, anomalies and phenomenology. Cambridge, Uk: Univ. Pr. (1987) (Cambridge Monographs On Mathematical Physics).

[36] Brian R. Greene, David R. Morrison, and Andrew Strominger. Black hole condensation and the unification of string vacua. *Nucl. Phys.*, B451:109–120, 1995.

[37] David J. Gross and Andre Neveu. Dynamical symmetry breaking in asymptotically free field theories. *Phys. Rev.*, D10:3235, 1974.

[38] David J. Gross, Robert D. Pisarski, and Laurence G. Yaffe. QCD and instantons at finite temperature. *Rev. Mod. Phys.*, 53:43, 1981.

[39] S. S. Gubser, Igor R. Klebanov, and Alexander M. Polyakov. Gauge theory correlators from non-critical string theory. *Phys. Lett.*, B428:105–114, 1998.

[40] J. B. Hartle and S. W. Hawking. Path integral derivation of black hole radiance. *Phys. Rev.*, D13:2188–2203, 1976.

[41] Sean A. Hartnoll and S. Prem Kumar. AdS black holes and thermal Yang-Mills correlators. *JHEP*, 12:036, 2005.

[42] S. W. Hawking. Particle creation by black holes. *Commun. Math. Phys.*, 43:199–220, 1975.

[43] S. W. Hawking. Black holes and thermodynamics. *Phys. Rev.*, D13:191–197, 1976.

[44] S. W. Hawking. Breakdown of predictability in gravitational collapse. *Phys. Rev.*, D14:2460–2473, 1976.

[45] S. W. Hawking and Don N. Page. Thermodynamics of black holes in anti-de Sitter space. *Commun. Math. Phys.*, 87:577, 1983.

[46] S. W. Hawking and R. Penrose. The singularities of gravitational collapse and cosmology. *Proc. Roy. Soc. Lond.*, A314:529–548, 1970.

[47] Stephen Hawking. The occurrence of singularities in cosmology. III. causality and singularities. *Proc. Roy. Soc. Lond.*, A300:187–201, 1967.

[48] C. P. Herzog and D. T. Son. Schwinger-Keldysh propagators from AdS/CFT correspondence. *JHEP*, 03:046, 2003.

[49] Gary T. Horowitz and Juan M. Maldacena. The black hole final state. *JHEP*, 02:008, 2004.

[50] Gary T. Horowitz and Joseph Polchinski. A correspondence principle for black holes and strings. *Phys. Rev.*, D55:6189–6197, 1997.

[51] Veronika E. Hubeny. Precursors see inside black holes. *Int. J. Mod. Phys.*, D12:1693–1698, 2003.

[52] Veronika E Hubeny, Hong Liu, and Mukund Rangamani. Bulk-cone singularities & signatures of horizon formation in AdS/CFT. *JHEP*, 01:009, 2007.

[53] W. Israel. Thermo field dynamics of black holes. *Phys. Lett.*, A57:107–110, 1976.

[54] Clifford V. Johnson, Amanda W. Peet, and Joseph Polchinski. Gauge theory and the excision of repulson singularities. *Phys. Rev.*, D61:086001, 2000.

[55] V. A. Kazakov, A. Marshakov, J. A. Minahan, and K. Zarembo. Classical / quantum integrability in AdS/CFT. *JHEP*, 05:024, 2004.

[56] Nak-woo Kim, Thomas Klose, and Jan Plefka. Plane-wave matrix theory from $\mathcal{N} = 4$ super Yang-Mills on $R \times S^3$. *Nucl. Phys.*, B671:359–382, 2003.

[57] M. Kleban, M. Porrati, and R. Rabadan. Poincare recurrences and topological diversity. *JHEP*, 10:030, 2004.

[58] Igor R. Klebanov and Edward Witten. AdS/CFT correspondence and symmetry breaking. *Nucl. Phys.*, B556:89–114, 1999.

[59] B. Lautrup. On high order estimates in QED. *Phys. Lett.*, B69:109–111, 1977.

[60] Albion Lawrence and Amit Sever. Holography and renormalization in lorentzian signature. *JHEP*, 10:013, 2006.

[61] Miao Li. Evidence for large N phase transition in $\mathcal{N} = 4$ super Yang- Mills theory at finite temperature. *JHEP*, 03:004, 1999.

[62] David A. Lowe and Larus Thorlacius. Comments on the black hole information problem. *Phys. Rev.*, D73:104027, 2006.

[63] Juan M. Maldacena. The large N limit of superconformal field theories and supergravity. *Adv. Theor. Math. Phys.*, 2:231–252, 1998.

[64] Juan M. Maldacena. Eternal black holes in anti-de-Sitter. *JHEP*, 04:021, 2003.

[65] Juan M. Maldacena and Leonard Susskind. D-branes and fat black holes. *Nucl. Phys.*, B475:679–690, 1996.

[66] Donald Marolf. States and boundary terms: Subtleties of lorentzian AdS/CFT. *JHEP*, 05:042, 2005.

[67] Samir D. Mathur. The fuzzball proposal for black holes: An elementary review. *Fortsch. Phys.*, 53:793–827, 2005.

[68] J. A. Minahan and K. Zarembo. The bethe-ansatz for $\mathcal{N} = 4$ super Yang-Mills. *JHEP*, 03:013, 2003.

[69] A D Mirlin and Y V Fyodorov. Universality of level correlation function of sparse random matrices. *Journal of Physics A: Mathematical and General*, 24(10):2273–2286, 1991.

[70] Suphot Musiri, Scott Ness, and George Siopsis. Perturbative calculation of quasi-normal modes of AdS Schwarzschild black holes. *Phys. Rev.*, D73:064001, 2006.

[71] Jose Natario and Ricardo Schiappa. On the classification of asymptotic quasinormal frequencies for d-dimensional black holes and quantum gravity. *Adv. Theor. Math. Phys.*, 8:1001–1131, 2004.

[72] R. G. Newton. Scattering theory of waves and particles. McGraw-Hill Education (January 1967), Chapter 12.

[73] R. G. Newton. Scattering theory of waves and particles. McGraw-Hill Education (January 1967).

[74] A. J. Niemi and G. W. Semenoff. Finite temperature quantum field theory in Minkowski space. *Ann. Phys.*, 152:105, 1984.

[75] Alvaro Nunez and Andrei O. Starinets. AdS/CFT correspondence, quasinormal modes, and thermal correlators in $\mathcal{N} = 4$ SYM. *Phys. Rev.*, D67:124013, 2003.

[76] R. Penrose. Singularities and time asymmetry. In *Hawking, S.W., Israel, W.: General Relativity*, 581- 638.

[77] Roger Penrose. Gravitational collapse and space-time singularities. *Phys. Rev. Lett.*, 14:57–59, 1965.

[78] Asher Peres. Ergodicity and mixing in quantum theory. I. *Phys. Rev. A*, 30(1):504–508, Jul 1984.

[79] J. Polchinski. String theory. vol. 1: An introduction to the bosonic string, vol. 2: Superstring theory and beyond. Cambridge, UK: Univ. Pr. (1998).

[80] Joseph Polchinski, Leonard Susskind, and Nicolaos Toumbas. Negative energy, superluminosity and holography. *Phys. Rev.*, D60:084006, 1999.

[81] G. J. Rodgers and A. J. Bray. Density of states of a sparse random matrix. *Phys. Rev. B*, 37(7):3557–3562, Mar 1988.

[82] Guilhem Semerjian and Leticia F Cugliandolo. Sparse random matrices: the eigenvalue spectrum revisited. *Journal of Physics A: Mathematical and General*, 35(23):4837–4851, 2002.

[83] George Siopsis. Large mass expansion of quasi-normal modes in $AdS_(5)$. *Phys. Lett.*, B590:105–113, 2004.

[84] Dam T. Son and Andrei O. Starinets. Minkowski-space correlators in AdS/CFT correspondence: Recipe and applications. *JHEP*, 09:042, 2002.

[85] Mark Srednicki. The approach to thermal equilibrium in quantized chaotic systems. *Journal of Physics A: Mathematical and General*, 32(7):1163–1175, 1999.

[86] Matthias Staudacher. The factorized S-matrix of CFT/AdS. *JHEP*, 05:054, 2005.

[87] Andrew Strominger and Cumrun Vafa. Microscopic origin of the Bekenstein-Hawking entropy. *Phys. Lett.*, B379:99–104, 1996.

[88] Bo Sundborg. The Hagedorn transition, deconfinement and $\mathcal{N} = 4$ SYM theory. *Nucl. Phys.*, B573:349–363, 2000.

[89] Leonard Susskind, Larus Thorlacius, and John Uglum. The stretched horizon and black hole complementarity. *Phys. Rev.*, D48:3743–3761, 1993.

[90] Leonard Susskind and Edward Witten. The holographic bound in anti-de Sitter space. 1998.

[91] Gerard 't Hooft. *in The Whys of subnuclear physics, Proc. Int. School, Erice, Italy, 1977.* Plenum, New York.

[92] Gerard 't Hooft. Counting planar diagrams with various restrictions. *Nucl. Phys.*, B538:389–410, 1999.

[93] Charles B. Thorn. Infinite N(c) QCD at finite temperature: Is there an ultimate temperature? *Phys. Lett.*, B99:458, 1981.

[94] A. Avez V.I. Arnold. *Ergodic problems of classical mechanics.* Redwood City, Calif. : Addison-Wesley, the Advanced Book Program, 1989.

[95] E. Wigner. Characteristics vectors of bordered matrices with infinite dimensions. *Ann.Math.*, 65:203, 1957.

[96] Edward Witten. Anti-de Sitter space and holography. *Adv. Theor. Math. Phys.*, 2:253–291, 1998.

[97] Edward Witten. Anti-de Sitter space, thermal phase transition, and confinement in gauge theories. *Adv. Theor. Math. Phys.*, 2:505–532, 1998.

[98] Laurence G. Yaffe. Large N limits as classical mechanics. *Rev. Mod. Phys.*, 54:407, 1982.